Dear Editor,

please find attached a point-by-point response to the reports of both reviewers, the revised manuscript and a version of the manuscript with all the changes between the new and the old version marked.

Following the objections and recommendations of both reviewers, we have heavily modified the original manuscript. First of all, we have changed the structure of our paper, focusing on Section 2 on a more in-depth explanation and evaluation of the freezing mechanisms in ULAQ-CCM and then discussing all the SG-induced changes in Section 3. Furthermore, we have added a description and the appropriated references for CCSM-CAM4, from which we took the SSTs for our simulations. Considering we relied on Simone Tilmes for all matters related to CCSM-CAM4, we have added her to our list of co-authors.

Both reviewers criticized our lack of heterogeneous freezing scheme. Following this, we have performed again all our simulations considering also this mechanism. All figures and results have been updated accordingly. Non-linear interaction between heterogeneous and homogeneous freezing mechanisms reduces the amount of homogeneous freezing in some areas, thus affecting the net impact of sulfate geoengineering on the UT ice radiative forcing. Because of this, all the tables, abstract and discussion have been updated to reflect the changes in radiative forcing differences with respect to our original simulations.
All other comments by the reviewers have been addressed in the responses, and the manuscript changed accordingly when necessary.

Lastly, considering the feedback we received from both reviewers, we have decided to have the manuscript undergo a full technical editing. For this reason, we also attach the certificate we received from the service we used.

We would like to thank again you and the reviewers for the precious feedbacks on our manuscript.

Respectfully yours,

Daniele Visioni on behalf of all authors

LANGUAGE EDITING CERTIFICATE

This document certifies that the manuscript listed below was edited for proper English language, grammar, punctuation, spelling, and overall style by one or more of the highly qualified native English speaking editors at Wiley Editing Services.

Manuscript title:
Upper tropospheric ice sensitivity to sulfate geoengineering

Authors:
Daniele Visioni, Giovanni Pitari, Glauco di Genova, Simone Tilmes

Date Issued:
May 29, 2018

Certificate Verification Key:
D5F9-4D01-BC90-E362-AD89

This certificate may be verified at https://secure.wileyeditingservices.com/certificate. This document certifies that the manuscript listed above was edited for proper English language, grammar, punctuation, spelling, and overall style. Neither the research content nor the authors' intentions were altered in any way during the editing process. Documents receiving this certification should be English-ready for publication; however, the author has the ability to accept or reject our suggestions and changes. If you have any questions or concerns about this document or certification, please contact help@wileyeditingservices.com.

CERTIFIED Wiley Editing Services

Response to reviewer # 1

Reviewer comments are in bold. Author responses are in blue.

This is an interesting and timely study of how geoengineering in the form of stratospheric aerosol injection (SAI) would impact ice clouds in the upper troposphere (UT). Few papers have been published on this poorly understood aspect of SAI, so in that sense the paper is a welcome contribution to the geoengineering discussion.

We would like to thank the reviewer for his insightful comments and suggestions. We will try to address all of them below.

Overall comment:

However, the paper is in its current form very unclear when it comes to the representation of central processes in the ULAQ model, poorly structured, and full of incorrect/poor grammar. It need a serious overhaul in all these respects. I further question the validity of the results presented, in light of the coarse resolution of the model, as well as its overly simplistic treatment of UT ice nucleation. I challenge the authors to justify why their results can be trusted despite these shortcomings. Below I've listed some additional major concerns I had about the paper, and thereafter some minor comments (typos, questions for clarification, etc.). I would like to see all of these concerns addressed before I will consider the paper suitable for publication in ACP.

(a) A better, clearer and more complete presentation of the main processes governing ice particle formation in the ULAQ-CCM has been made in the revised manuscript.
(b) An improvement in the manuscript structure has been made, following also a specific recommendation from the reviewer (see below).
(c) Following the suggestion of both reviewers, an English technical editing of the manuscript has been done.
(d) The ULAQ-CCM version adopted in this study uses a T21 horizontal resolution, which may be (in general) defined as a rather coarse horizontal resolution. On the other hand, it has been demonstrated in many previous published works that this is a fully acceptable resolution for studies focusing on stratospheric dynamics and transport, as well as on strat-trop exchange (e.g., Pitari et al., 2016a; Pitari et al., 2016b; Visioni et al., 2018). It is obviously possible to use higher horizontal resolutions, but this is not a strict physical requirement. Many model inter-comparison campaigns prove this (see for example SPARC-CCMVal-2 or the ongoing SPARC-CCMI: Morgenstern et al., 2017; Morgenstern et al., 2018; see also other referenced papers in the manuscript, where the ULAQ model scores well compared to other models with higher horizontal resolution). This is even more true in the case of UT ice formation, which is largely driven by sub-grid vertical motions in global composition models; the latter may explicitly predict only the large-scale dynamics and need to parameterize mesoscale vertical motions, even with higher horizontal resolutions. On the other hand, we believe that the use of a high vertical resolution is necessary to properly catch the time-latitude-longitude varying altitude of the tropopause and then the upper limit for UT ice formation. A proper vertical resolution is indeed adopted in the ULAQ model (568 m in pressure altitude). In this way, the different aerosol behavior above and below the tropopause is also well caught in the ULAQ-CCM.
(e) Cirrus ice formation in the ULAQ-CCM results from both homogeneous and heterogeneous freezing mechanisms and their competition. However, in our first draft of the manuscript we had decided to turn off the heterogeneous freezing mechanism, in order to focus on the SG

aerosol induced perturbation to ice formation from homogeneous freezing only. We acknowledge the specific point raised by the reviewer. The reduced updraft will affect ice formation from homogeneous freezing in a different way if ice particles may also form via heterogeneous freezing. This latter process, in fact, requires normally lower supersaturation conditions, both on mineral dust and black carbon particles. For this reason, we have performed again all our simulations with both mechanisms turned on, allowing their non-linear interaction. Results are substantially affected, with a resulting smaller indirect RF due to upper tropospheric ice changes induced by sulfate geoengineering. Looking at the revised results of our numerical experiments, we are really indebted with both reviewers for raising this specific scientific point, helping us in a more correct assessment of the ice perturbation due to SG aerosol and its indirect radiative forcing. In the manuscript, we now give a compact description of how ice particles are formed on both channels (HET-HOM), highlighting the major source of uncertainty in the parameterization of the heterogeneous freezing. A more robust scientific knowledge is present for the homogeneous freezing mechanism. In this case the numerical code adopted in the ULAQ model in the one well documented in the literature by Kärcher and Lohmann (2002) and Lohmann and Kärcher (2002), plus other subsequent studies, among which the most relevant for our present purposes is Kuebbeler et al. (2012).

Major comments:

1) With respect to the paper structure, I found it strange that in Section 2 ("ULAQ-CCM and setup of numerical experiments") some model results in response to SG are presented (in Fig. 3-6), but not until sections 2.1 and 2.2. are descriptions of the model treatment of stratospheric aerosols and ice clouds described. I suggest moving the presentation and discussion of model results until AFTER you've described the model, and to only put content in the various sections that is consistent with the section titles.

In the revised version of the manuscript we have shown all the model results after the sections where we describe the model, as suggested.

2) There is no discussion of the effect of additional SO_4 available for homogeneous nucleation in the SG cases, as evident in Fig. 7a. Why is the effect of what appears to be a tripling of SO_4 particles that can nucleate ice seemingly negligible? Please explain?

The increase of SO_4 in the upper troposphere due to the sulfate injection has a negligible effect on the rates of homogeneous freezing, as shown in Cirisan et al. (2013) (mainly because the number density of background SO_4 aerosols in the UT is already much greater than the number density of ice crystals). Furthermore, liquid supercooled sulfuric acid aerosols are inefficient IN for heterogeneous freezing; solid aerosol particles, mainly mineral dust and black carbon, may act as IN with different ice active fraction depending on aging processes and environmental conditions (e.g. Hendricks et al., 2011). For these reasons, changes in the UT population of sulfate aerosols are not expected to play a direct role in the changes in ice particle formation processes. It is actually the thermo-dynamical perturbation induced by lower stratospheric SG sulfate aerosols that may significantly impact the rate of ice formation via homogeneous freezing. This is indeed the central point of our study. In the revised manuscript, we have addressed this issue in a more in-depth way.

Minor comments:

Abstract: "Goal of. . ." should be changed to "The goal of.."

Changed.

Abstract: Don't understand what "coupled to" means in this context.

In previous experiments looking at sulfate geoengineering changes on UT ice, surface temperatures were kept fixed and only the LS warming was considered. In our case, in the experiment G4 both the surface cooling and the LS warming contribute to the modifications of the atmosphere dynamics.

Page 2, line 4, End sentence after "documented.

Done.

Page 2, line 9: Add "optimal" before "magnitude and location".

Added.

Page 2, line 23: Add reference for the claim that homogeneous nucleation normally dominates cirrus formation. "Supersaturation ratio" should be "saturation ratio".

Most of the literature considering geoengineering experiments (in particular, cirrus seeding) point out that most of the freezing is due to homogeneous processes, and that when including heterogeneous freezing processes, the differences are small. See for instance Gasparini et al. (2015), Gasparini et al. (2017), Storevlmo et al. (2014). We have added in the text these references and discuss better the relative weight of the two freezing mechanisms. Beyond geoengineering experiments, see also Kärcher and Lohmann (2002) for the specific point of homogeneous freezing normally dominating over the heterogeneous freezing of cirrus ice formation. Uncertainties in the latter case are discussed in Hendricks et al. (2011).

Page 2, line 31: "anyway" is not suitable here. "However" could be an alternative.

Corrected.

Page 2, line 32: cloud optical properties are also important here.

Added.

Page 4, line 1: This statement is confusing: sulphuric acid droplets are not ice nuclei. Please clarify. Furthermore, this statement is not very interesting unless you explain WHY there was no effect on RF.

As specified above in the response to the second major point, sulphuric acid liquid supercooled droplets are very inefficent ice nuclei. For the sake of increasing clarity, we have modified our sentence in the following way: "An upper tropospheric increase of sulfate aerosol number concentration is expected in SG conditions, due to gravitational sedimentation and large-scale transport of the particles below the tropopause from the LS. However, sulphuric acid liquid supercooled droplets are very inefficent ice nuclei (IN) for heterogeneous freezing. At the same time, the background number concentration of UT aerosols acting as nuclei for homogeneous frezing is already much higher with respect to the ice particle number density. For this reason, a negligible increase of the active IN population would be found in the UT, and the same would hold true for the positive RF associated to a possible increase of ice particles from this effect, as Cirisan et al. (2013) conclude in their study."

Page 4: Vertical velocity is important for cirrus formation not primarily because it transport water vapour to the UT, but because it controls the adiabatic cooling rate and thus supersaturation, for a given water vapour content.

We have changed the sentence accordingly.

Page 4, line 14-17: Catastrophic grammar.

Grammar adjusted.

Figure 1: This figure is confusing and not well explained. I don't find it particularly helpful at this stage of the paper, but it could be good as a final figure summarizing the findings in the paper.

This figure has been moved to the final part of the manuscript, as well as Figure 2.

Page 5, line 5: Ash dust is not the same.

Corrected.

Page 6, line 1: Sassen et al. (2008) is a paper on cirrus coverage seen by CALIPSO, so I don't see how that could possibly address UT ice changes.

Yes, it was a mistake. The reference we were intending to put was Sassen et al. (1995), where possible changes in cirrus are discussed in relation to the Pinatubo eruption. We have now corrected this in the revised manuscript.

Page 6/Table 1: The horizontal resolution is extremely coarse - how can we have confidence in changes driven by dynamics in this context?

As explained above in the response to the overall comment of the reviewer, the ULAQ-CCM version adopted in this study uses a T21 horizontal resolution, which may be (in general) defined as a rather coarse horizontal resolution. On the other hand, it has been demonstrated in many previous published works that this is a fully acceptable resolution for studies focusing on stratospheric dynamics and transport, as well as on strat-trop exchange. Many model inter-comparison campaigns prove this (see for example SPARC-CCMVal-2 or the ongoing SPARC-CCMI). In addition, UT ice formation is largely driven by sub-grid vertical transport processes in global composition models; the latter may explicitly predict only the large-scale dynamics and need to parameterize mesoscale vertical motions, even with higher horizontal resolutions.

Page 7, line 4: Clumsy and confusing statement. Suggest writing: ...a negative anomaly in the Arctic region that is approximately 1 K larger than that of high southern latitudes.

We have rephrased it as the reviewer suggested.

Page 7, line 7: What do you mean by "increasing atmospheric stabilisation"? Do you mean "increasing atmospheric stability?

Yes, we have corrected this.

Page 7, line 16-18: The Antarctic warming is not statistically significant, so I don't see the point in discussing it.

Although the reviewer remark is correct, we would like to keep this short discussion as a justification for the large variability of SST changes at high latitudes. A slight modification has been made by writing: "Although not statistically significant, the SG induced warming…"

Page 8, line 2: Is the vertical velocity change mainly caused by changes to TKE, or also due to large-scale (resolved) velocity changes. If TKE is very important here, I would like to see vertical profiles of TKE for both simulations.

In the revised manuscript, we have explicitly included the Lohmann and Kärcher (2002) formulation for the vertical velocity (Eq. 5). In a first approximation, w in the UT is close to $TKE^{0.5}$ and the vertical velocity perturbation is dominated by changes of this latter term, so that we believe that inclusion of a new figure in the revised manuscript does not add much. We attach here the vertical profiles of w in G4 and Base experiments (Fig. R1_1), as well as the vertical profile of w changes [G4-Base], comparing the results with and without the large-scale contribution to w. It is clear that TKE changes greatly control the SG perturbation of UT updraft. The TKE vertical profile asked by the reviewer is implicit in panel (b) of the Fig. R1_1, due the w_{TKE} formulation.

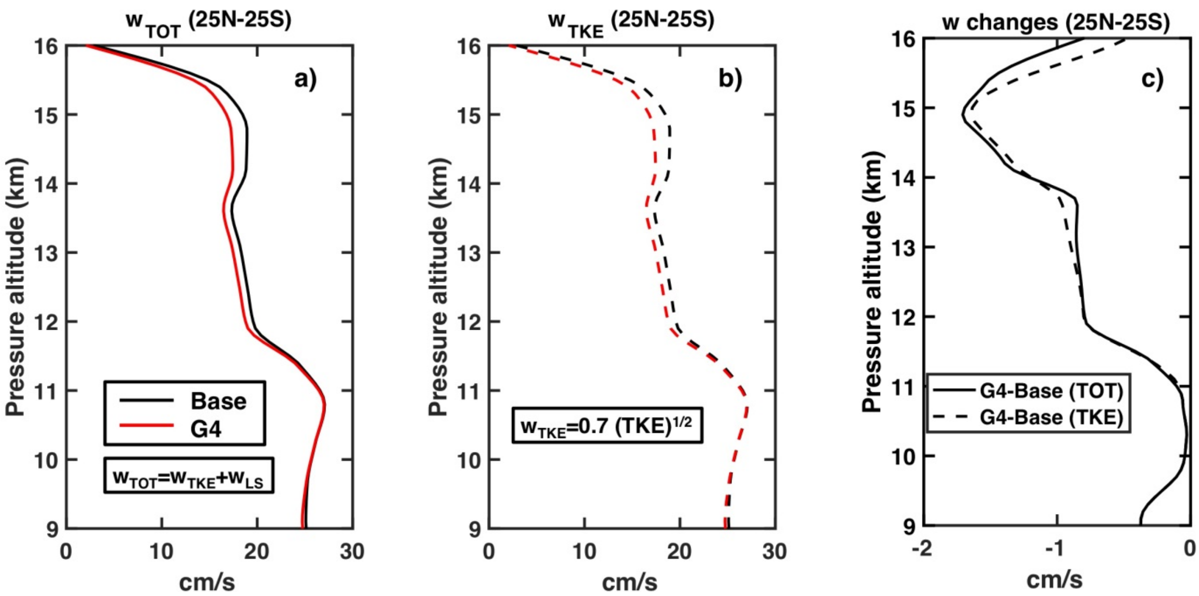

Fig. R1_1. Average upper tropospheric tropical profiles of the vertical velocity w (cm/s) in G4 and Base experiments (years 2030-39). (a) Total vertical velocity calculated as $w_{TOT}=w_{TKE}+w_{LS}$ (where w_{TKE} indicates the mesoscale component calculated as a function of TKE and w_{LS} indicates the large-scale model-resolved component). (b) Vertical velocity component w_{TKE} alone, calculated as $w_{TKE}=0.7\times(TKE)^{1/2}$ (see Lohmann and Kärcher, 2002; see also Eq. 5 in the revised manuscript). As expected, w_{TKE} dominates in w_{TOT} (c) Vertical velocity changes G4-Base for w_{TOT} (solid line) and w_{TKE} only (dashed line) (of the order of 5% in the tropical UT). Very little changes are produced in the large-scale component under SG conditions.

Page 9, lines 19-20: Discuss here the uncertainty associated with cloud ice in MERRA, which uses highly uncertain cloud parameterisations and incorporates very few ice cloud

observations in its reanalysis. It would be better to use CALIPSO/CloudSat retrievals of ice cloud properties.

In the revised manuscript, we have added some discussion on the uncertainties of the datasets we have used for comparison with our results. We have decided to use a reanalyses dataset such as MERRA-2 also considering the large uncertainties in the satellite retrieval datasets (see for instance Zhang et al., 2010; Duncan and Eriksson, 2018) and their availability.

Page 10, line 3: Given how central UT vertical velocities are to this paper, you need to be clearer about how the calculation of vertical velocity is done, i.e. include equation for vertical velocity as a function of TKE, and clearly state if you put any upper/lower bounds in it.

In the revised manuscript, we have explicitly included the Lohmann and Kärcher (2002) formulation for the vertical velocity (Eq. 5) (see also Fig. R1_1 above). No imposed bounds to w are considered and its time-spatial variability is clearly shown in Figure 6 of the original manuscript.

Page 10, line 4: What justifies the assumption that cirrus clouds form only via homogeneous nucleation? That seems to be in stark contrast to papers that report that cirrus clouds appear to form mainly through heterogeneous nucleation (e.g., Cziczo et al., 2013).

Please refer to our reply above, regarding the homogeneous - heterogeneous freezing mechanisms, in response to the reviewer overall comment. In the revised manuscript, we discuss the major source of uncertainties and add a caveat regarding the presence of different opinions available in the literature, like the ones the reviewer suggested.
As specified above, we have taken the reviewer criticism under serious consideration and decided to redo our numerical simulations with both freezing mechanisms turned on, allowing their non-linear interaction. Results are substantially affected, with a resulting smaller indirect RF due to upper tropospheric ice changes induced by sulfate geoengineering. Looking at the revised results of our numerical experiments, we are really indebted with both reviewers for raising this specific scientific point, helping us in a more correct assessment of the ice perturbation due to SG aerosol and its indirect radiative forcing.

Page 13, line 15: Remove "from".

Removed.

Page 16, line 13-14: This is inaccurate - homogeneous nucleation sets in at approximately 238K, but NOT through "water vapour freezing", but rather through the spontaneous freezing of small solution droplets.

Corrected accordingly.

Page 16, line 18-19: This is an outdated view (and references that back this claim are not provided) - the current understanding is that a majority of cirrus clouds form via heterogeneous nucleation.

Please see above. Heterogeneous nucleation would dominate only if the locally available IN (mostly BC and mineral dust) would have a high ice active fraction (>~10%). These values, however, although being measured in laboratory studies for mineral dust close to the homogeneous freezing threshold (Field et al., 2006; Möhler et al., 2006; Welti et al., 2009), are most probably

highly overestimated in the real atmosphere, due to rapid aging of dust particles (as well as BC) through sulfate coating (Hendricks et al., 2011). We acknowledge (and added in the revised manuscript) the counterpoint that studies such as Cziczo et al. (2013) show that the heterogeneous freezing may dominate over the homogeneous, in the formation of UT ice particles. However, we believe there is plenty of literature showing through both modeling and in-chamber experiments the huge uncertainties relative to our understanding of UT ice formation through heterogeneous freezing, in particular regarding the available aerosol population that is actually able to form ice in the upper troposphere (ice active fraction).
For instance, regarding black carbon, laboratory measurements demonstrate that the ice active fraction (f) ranges between 0.1% and 1% (Koehler et al., 2009), which means that only a very small fraction of the available black carbon particles in the UT can act as IN. Considering the rapid BC aging in the real atmosphere (due to sulfate coating), f~0.1% may be probably considered as un upper limit for the ice active fraction, although a clear picture has not yet emerged for the factors which actually control f for a given type of atmospheric IN (Hendricks et al., 2011), thus producing a significant level of uncertainty in the present knowledge of UT ice formation via heterogeneous freezing. For mineral dust the uncertainty is even higher, with f ranging between 0.1% and 10%, although it might be even lower (Minikin et al., 2003; Cziczo et al., 2009).
Those measurements are the only one that, as modelers, we can take into account when considering which fraction is to be used in our simulations (in our experiments we chose f=0.25% for BC and 1% for mineral dust, following the best recommendations of Hendricks et al., 2011, see Eq. 1 in the revised manuscript).

Fig. 8: Again, I do not think of MERRA as the most appropriate data set for validation of the simulated UT ice.

See response above.

Page 16, line 21 (and throughout the manuscript): The standard terminology is "ice mass mixing ratio", not "ice mass fraction" which can be misleading.

Following the suggestion, we have changed it everywhere in the manuscript.

Page 16, line 8 - 15: The description of how UT ice clouds form is extremely unclear. How is cloud cover determined? What probability distribution for supersaturation is used, and how does it relate to TKE. A lot of essential information is left out here.

We disagree on this point. We have clearly stated our simplified probabilistic approach adopted for supersaturation, with a normal (Gaussian) distribution for the UT relative humidity: "For the ice supersaturation ratio, we adopt a simplified probabilistic approach, starting from the knowledge of climatological frequencies of the UT relative humidity (RH_{ICE}), from which a mean value and a standard deviation can be calculated, assuming a normal distribution". We are aware that this represents an important model simplification, and in fact we started our discussion with the above clear statement.

Page 18, line 4: "each thick" is not correct English.

Corrected.

Page 18, line 8: What do you mean by "we are only considering sub-visible clouds"?

The sentence has been modified as follows: "This should not surprise, in principle, due to the fact that vertical velocities calculated as a function of TKE do not normally exceed 30 cm/s, so that events leading to thick cirrus formation are not considered."

Fig. 10: Is the ice crystal number density calculated only when there is a cloud (i.e. an in-cloud average), or is this an average over both cloudy and cloud-free grid-boxes? The former quantity is certainly of most interest and more directly comparable to field measurements.

We always refer to averages weighted with the probability to have cirrus formation (~P_{HOM}). The reviewer is right in saying that an in-cloud average would be more directly comparable to field measurements. That's why we used our P_{HOM} to make this type of comparison in a meaningful way. In the original manuscript, we wrote: "Using these P_{HOM} values, it is possible to scale a n_i value measured in the mid-latitude airborne campaign of Ström et al. (1997) during a young cirrus formation, in order to derive an average climatological value to be considered consistent with our modeling approach. They measured a mid-latitude ice concentration value n=0.3 cm^{-3} in a young cirrus cloud at T=220 K and p=320 hPa. If we scale this result with our corresponding P_{HOM}=12±3%, a "climatological-mean" value n=0.025±0.005 cm^{-3} is obtained, close to our model predicted value of 0.031± 0.008 cm^{-3}."

Page 18, line 10-11: Neglecting heterogeneous ice nucleation would lead to an overestimate of ice crystal number, because you are not able to represent the competition between heterogeneous and homogeneous nucleation that will in some cases lead to a suppression of homogeneous nucleation and therefore a reduction in ice crystal number density. In other words, that cannot explain the disagreement with MERRA+MODIS seen in Fig. 9.

The reviewer is perfectly right. As explained above in detail, our new results confirm this. Again we thank both reviewers for raising this point and providing us a strong scientific argument to redo our numerical experiments. The following sentence has been deleted: "In addition, ice formation from heterogeneous freezing on active IN, as mineral dust particles for example, is not taken into account in our modelling approach."

Page 26, line 7-9: How can you be confident about the radiative effect when the model consistently produces ice clouds that are optically too thin? This could bias especially the LW cooling effect of cloud thinning.

Our confidence comes from comparing our results to previous findings (as in Kuebbeler et al., 2012, Gasparini et al., 2017). In addition, the reviewer point is rather unclear, in the sense that the ice OD for G4, G4K and Base simulations is not small in absolute values. We may then calculate the ice radiative effects both on SW and LW, once appropriate Mie scattering parameters have been derived, using a correct wavelength-dependent refractive index (Warren 1984; Warren and Brandt, 2008; Curtis et al., 2005) and the calculated particle size distribution. Results of our radiative transfer code have been successfully compared with those of Schumann et al. (2012) under similar conditions. We have added in the paper the appropriate references.

General comment: Friberg et al. (2015) seem to qualitatively support your findings based on analysis of cirrus cloud reflectance changes after volcanic eruptions, so that would be a good paper to cite.

We have read the paper suggested by the reviewer and had the occasion to speak with the lead author. In the revised manuscript, we now briefly discuss their conclusions and have added the appropriate reference.

References:

Cirisan, A., Spichtinger, P., Luo, B. P., Weisenstein, D. K., Wernli, H., Lohmann, U., and Peter, T.: Microphysical and radiative changes in cirrus clouds by geoengineering the stratosphere, Journal of Geophysical Research: Atmospheres, 118, 4533–4548, doi:10.1002/jgrd.50388, http://dx.doi.org/10.1002/jgrd.50388, 2013.

Curtis, D. B., Rajaram, B., Toon, O. B., and Tolbert, M. A.: Measurement of the temperature-dependent optical constants of water ice in the 15–200 μm range, Appl. Opt., 44, 4102–4118, doi:10.1364/AO.44.004102, http://ao.osa.org/abstract.cfm?URI=ao-44-19-4102, 2005.

Cziczo, D. J., Froyd, K. D., Gallavardin, S. J., Moehler, O., Benz, S., Saathoff, H., and Murphy, D. M.: Deactivation of ice nuclei due to atmospherically relevant surface coatings, Environmental Research Letters, 4, 044 013, http://stacks.iop.org/1748-9326/4/i=4/a=044013, 2009.

Cziczo, D. J., Froyd, K. D., Hoose, C., Jensen, E. J., Diao, M., Zondlo, M. A., Smith, J. B., Twohy, C. H., and Murphy, D. M.: Clarifying the Dominant Sources and Mechanisms of Cirrus Cloud Formation, Science, 340, 1320–1324, doi:10.1126/science.1234145, http://science.sciencemag.org/content/340/6138/1320, 2013.

Duncan, D. I. and Eriksson, P.: An update on global atmospheric ice estimates from satellite observations and reanalyses, Atmos. Chem. Phys. Discuss., https://doi.org/10.5194/acp-2018-275, in review, 2018.

Field, P. R., Möhler, O., Connolly, P., Krämer, M., Cotton, R., Heymsfield, A. J., Saathoff, H., and Schnaiter, M.: Some ice nucleation characteristics of Asian and Saharan desert dust, Atmos. Chem. Phys., 6, 2991-3006, https://doi.org/10.5194/acp-6-2991-2006, 2006.

Friberg J., B. G. Martinsson, M. K. Sporre, S. M. Andersson, C. A. M. Brenninkmeijer, M. Hermann, P. F. J. van Velthoven, and A. Zahn (2015), Influence of volcanic eruptions on midlatitude upper tropospheric aerosol and consequences for cirrus clouds, Earth and Space Science, 2, 285–300, doi: 10.1002/2015EA000110.

Gasparini, B. and Lohmann, U.: Why cirrus cloud seeding cannot substantially cool the planet, Journal of Geophysical Research: Atmospheres, 121, 4877–4893, doi:10.1002/2015JD024666, https://agupubs.onlinelibrary.wiley.com/doi/abs/10.1002/2015JD024666, 2016.

Gasparini, B., Munch, S., Poncet, L., Feldmann, M., and Lohmann, U.: Is increasing ice crystal sedimentation velocity in geoengineering simulations a good proxy for cirrus cloud seeding?, Atmospheric Chemistry and Physics, 17, 4871–4885, doi:10.5194/acp-17-4871-2017, https://www.atmos-chem-phys.net/17/4871/2017/, 2017.

Hendricks, J., Kärcher, B., and Lohmann, U.: Effects of ice nuclei on cirrus clouds in a global climate model, Journal of Geophysical Research: Atmospheres, 116, doi:10.1029/2010JD015302, http://dx.doi.org/10.1029/2010JD015302, d18206, 2011.

Kärcher, B. and Lohmann, U.: A parameterization of cirrus cloud formation: Homogeneous freezing of supercooled aerosols, Journal of Geophysical Research: Atmospheres, 107, doi:10.1029/2001JD000470, http://dx.doi.org/10.1029/2001JD000470, 2002.

Koehler, K. A., P. J. DeMott, S. M. Kreidenweis, O. B. Popovicheva, M. D. Petters, C. M. Carrico, E. D. Kireeva, T. D. Khokhlova, and N. K. Shonija (2009), Cloud condensation nuclei and ice nucleation activity of hydrophobic and hydrophilic soot particles, Phys.Chem.Chem.Phys., 11, 7906–7920.

Kuebbeler, M., Lohmann, U., and Feichter, J.: Effects of stratospheric sulfate aerosol geo-engineering on cirrus clouds, Geophysical Research Letters, 39, doi:10.1029/2012GL053797, http://dx.doi.org/10.1029/2012GL053797, l23803, 2012.

Lohmann, U. and Kärcher, B.: First interactive simulations of cirrus clouds formed by homogeneous freezing in the ECHAM general circulation model, Journal of Geophysical Research: Atmospheres, 107, AAC 8–1–AAC 8–13, doi:10.1029/2001JD000767, http: //dx.doi.org/10.1029/2001JD000767, 2002.

Minikin, A., A. Petzold, J. Ström, R. Krejci, M. Seifert, P. van Velthoven, H. Schlager, and U. Schumann (2003), Aircraft observations of the upper tropospheric fine particle aerosol in the Northern and Southern Hemispheres at midlatitudes, *Geophys. Res. Lett.*, 30, 1503, doi: 10.1029/2002GL016458, 10.

Möhler, O., Field, P. R., Connolly, P., Benz, S., Saathoff, H., Schnaiter, M., Wagner, R., Cotton, R., Krämer, M., Mangold, A., and Heymsfield, A. J.: Efficiency of the deposition mode ice nucleation on mineral dust particles, Atmos. Chem. Phys., 6, 3007-3021, https://doi.org/10.5194/acp-6-3007-2006, 2006.

Morgenstern, O., Hegglin, M. I., Rozanov, E., O'Connor, F. M., Abraham, N. L., Akiyoshi, H., Archibald, A. T., Bekki, S., Butchart, N., Chipperfield, M. P., Deushi, M., Dhomse, S. S., Garcia, R. R., Hardiman, S. C., Horowitz, L. W., Jockel, P., Josse, B., Kinnison, D., Lin, M., Mancini, E., Manyin, M. E., Marchand, M., Marecal, V., Michou, M., Oman, L. D., Pitari, G., Plummer, D. A., Revell, L. E., Saint-Martin, D., Schofield, R., Stenke, A., Stone, K., Sudo, K., Tanaka, T. Y., Tilmes, S., Yamashita, Y., Yoshida, K., and Zeng, G.: Review of the global models used within phase 1 of the Chemistry–Climate Model Initiative (CCMI), Geoscientific Model Development, 10, 639–671, doi:10.5194/gmd-10-639-2017, https://www.geosci-model-dev.net/10/639/2017/, 2017.

Morgenstern, O., Stone, K. A., Schofield, R., Akiyoshi, H., Yamashita, Y., Kinnison, D. E., Garcia, R. R., Sudo, K., Plummer, D. A., Scinocca, J., Oman, L. D., Manyin, M. E., Zeng, G., Rozanov, E., Stenke, A., Revell, L. E., Pitari, G., Mancini, E., Di Genova, G., Visioni, D., Dhomse, S. S., and Chipperfield, M. P.: Ozone sensitivity to varying greenhouse gases and ozone-depleting substances in CCMI-1 simulations, Atmos. Chem. Phys., 18, 1091-1114, https://doi.org/10.5194/acp-18-1091-2018, 2018.

Sassen, K., D. O. Starr, G. G. Mace, M. R. Poellot, S. H. Melfi, W. L. Eberhard, J. D. Spinhirne, E. W. Eloranta, D. E. Hagen and J. Hallett, The 5-6 December 1991 FIRE II jet stream cirrus case study: Possible influences of volcanic aerosols. d. Atmos. Sci., 52, 97-123, 1995.

Schumann, U., Mayer, B., Graf, K., and Mannstein, H.: A Parametric Radiative Forcing Model for Contrail Cirrus, Journal of Applied Meteorology and Climatology, 51, 1391–1406, doi:10.1175/JAMC-D-11-0242.1, https://doi.org/10.1175/JAMC-D-11-0242.1, 2012.

Storelvmo, T. and Herger, N.: Cirrus cloud susceptibility to the injection of ice nuclei in the upper troposphere, Journal of Geo- physical Research: Atmospheres, 119, 2375–2389, doi:10.1002/2013JD020816, https://agupubs.onlinelibrary.wiley.com/doi/abs/10.1002/2013JD020816, 2014.

Strom, J., Strauss, B., Anderson, T., Schrader, F., Heintzenberg, J., and Wendling, P.: In Situ Observations of the Microphysical Properties of Young Cirrus Clouds, Journal of the Atmospheric Sciences, 54, 2542–2553, doi:10.1175/1520-0469(1997)054<2542:ISOOTM>2.0.CO;2, http://dx.doi.org/10.1175/1520-0469(1997)054<2542:ISOOTM>2.0.CO;2, 1997.

Warren, S. G.: Optical constants of ice from the ultraviolet to the microwave, Appl. Opt., 23, 1206–1225, doi:10.1364/AO.23.001206, http://ao.osa.org/abstract.cfm?URI=ao-23-8-1206, 1984.

Warren, S. G. and Brandt, R. E.: Optical constants of ice from the ultraviolet to the microwave: A revised compilation, Journal of Geophysical Research: Atmos., 113, doi:10.1029/2007JD009744, https://agupubs.onlinelibrary.wiley.com/doi/abs/10.1029/2007JD009744, 2008.

Welti, A., Lüönd, F., Stetzer, O., and Lohmann, U.: Influence of particle size on the ice nucleating ability of mineral dusts, Atmos. Chem. Phys., 9, 6705-6715, https://doi.org/10.5194/acp-9-6705-2009, 2009.

Zhang, Z., S. Platnick, P. Yang, A. K. Heidinger, and J. M. Comstock, Effects of ice particle size vertical inhomogeneity on the passive remote sensing of ice clouds, J. Geophys. Res., 115, D17203, doi:10.1029/2010JD013835, 2010.

Response to reviewer # 2

Reviewer comments are in bold. Author responses are in blue.

This manuscript analyzes geo-engineering simulations of sulfur injection in the ULAQ CCM. The paper is generally well written. It suffers from some minor grammar mistakes, but the scientific points are made. I am not sure how valid they are however.

We thank the reviewer for his in-depth review and for his comments. We will try to respond to all the points raised, and to show that our work is scientifically robust.

Overall comment:

I think the methodology may be deeply flawed, since I am not certain that applying another model SSTs, from a model with no ice nucleation and poor upper tropospheric cirrus clouds, is a sufficiently useful method to look at perturbations. I think the resulting dynamical response could just be a model bias when the SSTs from another model is applied, and I fear that this would simply confuse the literature with another dubious single model study. This study needs some major revisions to address these points, and it may not actually be acceptable for ACP given the possible methodological flaws.

We disagree on this point. At the same time, it is rather clear from the first sentence and from other remarks below, that we were not able to make the scientific structure of our work sufficiently clear to the reader. We have tried to do it much better in the revised version and in the present reply to the reviewer.

(a) Our study takes inspiration from a previous one (Kuebbeler et al, 2012), where SSTs were kept unchanged in the sulfate geoengineering perturbed G4 case (5 Tg-SO_2/yr injection in the tropical lower stratosphere), with respect to the control simulation without geoengineering aerosols. In that case, dynamical changes produced by the lower stratospheric aerosol heating become drivers of a significant indirect effect of sulfate geoengineering (SG) on ice particle formation in the upper troposphere via homogeneous freezing. The increasing atmospheric static stability, due to the lower stratospheric aerosol-induced warming, produces a reduction in synoptic scale vertical motions with a resulting decrease in ice particle formation.

(b) An important question (raised in the same paper of Kuebbeler et al., 2012) may obviously be to what extent the surface cooling produced by the increased planetary albedo in G4 conditions (i.e., the DIRECT effect of geoengineering aerosol, for which SG is actually designed) may contribute to dynamical changes together with the lower stratospheric aerosol heating.

(c) In order to tackle this last scientific question, different approaches are possible. The ideal procedure would be to use an ocean-atmosphere coupled model, with chemistry-aerosol-ice clouds on-line, fully interactive with radiation and dynamics and with a vertical extension covering both troposphere and stratosphere. Possibly in a multi-model configuration, to assess inter-model differences (i.e. MIP approach). At the moment, however, this is rather difficult to achieve, since all the above requirements are not easy to be found and adapted to a SG configuration. This would be what the reviewer calls (below) a more "definitive" study.

(d) An alternative approach would be to use an atmospheric climate-chemistry coupled model (CCM) with sulfur chemistry and sulfate aerosol microphysics on-line (Pitari et al., 2014; Visioni et al., 2018), in-depth process evaluation (Visioni et al., 2017b), ice cloud formation scheme and its evaluation (as attempted in the present work). This is exactly what we have done with the ULAQ-CCM. On the other hand, it is well known that CCMs need an external specification of SSTs (due to their intrinsic formulation). This has been extensively made in previous international model campaigns, on-going since 2006 (i.e., SPARC-CCMVal-1, SPARC-CCMVal-2, SPAR-CCMI-1). What is needed for this purpose is the output of an atmosphere-ocean coupled model run with and without SG, under a given RCP scenario. The desired SG effect on SST is indeed the DIRECT aerosol effect (i.e., surface cooling due to the increasing planetary albedo), and CCSM-CAM4 does it well. Indirect effects on both chemistry and upper tropospheric ice are secondary effects not needed at this stage, contrary to what the reviewer claims. In fact, having an external SST change sensitive also to SG aerosol INDIRECT perturbations (chemistry and ice), would actually create an inconsistency in the nudging procedure. We rely of the fact that the SG aerosol radiative perturbation is the dominant one (see Visioni et al., 2017a) and we use the resulting changes on SST predicted by CCSM-CAM4 as the first-approximation dynamical driver for a CCM designed for the same SG perturbation (i.e., 8 Tg-SO_2/yr), but also including indirect effects on ice clouds (present work) and chemistry (see Visioni et al., 2017b). We will try to address this point in the revised version of the manuscript.

(e) We strongly believe that our "single model work", which is scientifically respectable as the "single model work" of Kuebbeler et al (2012), may be considered a good step forward, in the sense that the use of an externally specified SST sensitive to the direct SG aerosol radiative perturbation makes the CCM ice response more realistic than keeping SSTs fixed with respect to the baseline reference case.

(f) At the same time, we hope that in future a "more definitive" study will be conducted with on-line predicted SSTs, function of direct and indirect radiative changes produced by stratospheric SG aerosols.

General Comments:

1. I know the authors' first language is not English, and English is not an easy or kind language for the article and plural mistakes they are making, but I would suggest an edit by a native English speaker.

Following the suggestion of both reviewers, an English technical editing of the manuscript has been done.

2. As noted below, I am uncomfortable with some of the validation references. They should probably focus on papers, rather than other notes or presentations.

We are not sure what the reviewer is referring to. We have however reviewed the references used in the paper regarding the validation data we used. The only technical report in the original manuscript is Chou et al. (2001) regarding the longwave radiative transfer code; a journal paper was also cited for the shortwave radiative transfer code (Randles et al., 2013). Bosilovich et al. (2017) describes the MERRA-2 data and is a peer reviewed paper. If the reviewer asks for additional references regarding observational data, we have added two more, i.e. Gelaro et al. (2017) and Duncan and Eriksson (2018).

3. Most significantly: how does imposing SSTs from another model with an uncertain response tell us anything about the real atmosphere. You are just shocking one model with another, and you get a response. Why does the no feedback response matter, and how is it relevant? It is stated that some other models get a similar response, but I am not convinced. How would you even know if the model was self-consistent?

As explained in the response to the overall general comment, this is the normal way CCMs are used for baseline and sensitivity experiments (to RCP scenarios, solar fluxes, short lived species ground fluxes and many other components of the climate systems, along with their connection with chemistry) [see above points (d-e)]. Our results are consistent with those of Kuebbeler et al. (2012) for the upper tropospheric ice sensitivity to stratospheric SG aerosols, in the sense that the lower stratospheric aerosol longwave and solar heating rates are the major driver for circulation changes, but we go a step forward considering also the potential significance of the tropospheric cooling induced by the stratospheric aerosols [see above points (d-f)].
The reviewer often uses the argument of "self-consistency", but this does not apply in CCM experiments, because SSTs are an input parameter in this type of model. I think we have clearly explained in response to the overall comment, that we use SSTs from the CCSM-CAM4 ocean-atmosphere model for having a reliable input on "baseline" surface temperatures in a future RCP scenario and a "reliable" input for the SG aerosol perturbation to these temperatures. The latter is the "dominant direct" climate effect of SG. Indirect effects (i.e. chemistry and upper tropospheric ice) are treated consistently in the UAQ-CCM formulation, assuming SST changes produced by the SG stratospheric aerosols as a good first approximation. The CCSM-CAM4 SG stratospheric aerosol distribution used in the geoengineering simulation has been detailed in Tilmes et al. (2015).

Incomplete sentence "The goal of the present study..."

Corrected.

Relative to the clear sky net...

Changed.

How is this study different than previous work?

The only other study regarding the thermo-dynamical effects of sulfate geoengineering on cirrus cloud was that of Kuebbeler et al. (2012). In their case, however, sea surface temperatures where kept fixed. In our study, as the authors of the aforementioned paper asked in their conclusions, we try to analyze the difference between a sulfate injection with (G4) and without (G4K) the changes in sea surface temperatures due to the injected sulfate. We believe that, by showing the differences between G4 and G4K results in our model, we can gain further knowledge regarding this particular side effect.

How much of these results are due to just individual model climatologies? Seems like the effects depend on how much homo v. heterogeneous ice a model has, and what a large-scale model does to create and maintain cirrus. Why would your study be any more definitive?

We don't believe our study to be definitive in any way. We show, when comparing our G4K results with those from Kuebbeler et al. (2012), that the results from the two models are comparable in that scenario, and that further differences appear when considering changes in sea surface temperatures produced by the SG aerosol perturbation. We believe that by analyzing the differences caused by only that factor (SST changes due to the SG aerosol direct effect) we can constrain one of the possible factors that might influence the dynamical response to sulfate geoengineering. This approach was also used in a previous study related to methane changes (Visioni et al., 2017b), where we compared our results (in simulations with and without changing SSTs) against results from GEOSCCM.

The goal....

Corrected.

by including...

Changed.

ULAQ model description and a reference are needed. Does the description appear later? It does. Add see below.

Following also the precious suggestions of reviewer 1, in the revised manuscript we have modified the structure of the paper in order to have the model description before anything else.

CCSM-CAM4 needs a description and the acronym spelled out. At least a reference for the simulations. Is there more model description later? Applying the cooling from another model seems problematic: presumably CCSM4 has some of the same feedbacks, operating in different ways?

In the revised manuscript we have described CCSM-CAM4 and tried to better explain our modeling approach in the use of this model SSTs. Again, please refer to our response to the overall comment.

I don't like that you have created a very arbitrary perturbation that changes vertical motion and transport in a coarse resolution GCM. The result is that I believe your perturbation is very model specific and artificial. I support attempting to understand processes in a model but this whole paper seems very dependent on a single model formulation. I'm not convinced you can or should separate all the affects this way.

As previously explained, the methodology of using externally provided SSTs as input parameter in CCM experiments is intrinsic in the CCM formulation itself. This has been done in all CCMVal-1, CCMVal-2 and CCMI-1 experiments, and more recently for the ISA-MIP Project (Timmreck et al., 2018; https://www.geosci-model-dev-discuss.net/gmd-2017-308/). As for using perturbed SSTs in case of a geoengineering scenario, we can point out to previous works where our dynamical perturbations have been compared to other models (Pitari et al., 2014; Visioni et al., 2017b).
The resulting dynamical changes are not arbitrary, but consistent with the SG aerosol dynamical drivers, i.e. perturbation of lower stratospheric heating rates and SSTs. A clear discussion is made in the manuscript on how the resulting changes in vertical motion are produced and how they are sensitive to these aerosol drivers. The results are obviously valid in the limitation of "a single model formulation" (as in the case of Kuebbeler et al., 2012, by the way), but may certainly represent a step forward and could be a valuable reference point in the literature for future multi-model experiments, possibly with ocean-atmosphere coupled models.

I think you need to describe relevant features of the cloud and transport scheme of ULAQ, and the basic features of CCSM4 here. What ice nucleation mechanisms are included and how does the cloud scheme create cirrus clouds? What radiation scheme is used? How do the volcanic emissions evolve? For CCSM4: how do its volcanic emissions evolve and how is that related.

As already specified above, a new paragraph on the CCSM-CAM4 model has been included in the revised manuscript. A full description of the ULAQ-CCM is available in the Morgenstern et al. (2017) paper, which summarizes the major features of all global-scale model participating in the SPARC-CCMI model initiative. Details on the radiation scheme are also available in this latter

paper, as well as in Pitari et al. (2014). Evolution of volcanic clouds in the ULAQ-CCM has been fully discussed in Pitari et al. (2016a) and Pitari et al. (2016b). CCSM-CAM4 is described in Tilmes et al. (2016).
A full section in the original manuscript is devoted to explaining the cirrus cloud formation in the ULAQ-CCM, via homogeneous freezing. An additional paragraph on the ice formation via heterogeneous freezing is now included in the revised manuscript.
Regarding the volcanic emissions, the simulations are in the future under a RCP4.5 scenario, so volcanic emissions are not considered.

The inconsistency here I think is problematic for the study. I'm not convinced you should look at this perturbation turning on and off surface temperature perturbations, and expect that the resulting impact on the model has any reference to reality since the system breaks any feedbacks that might modify the surface temperature.

Most of the available works on sulfate geoengineering have been performed using models with prescribed SSTs (as an example, Kuebbeler et al., 2012; Niemeier and Timmreck, 2015; Niemeier and Schmidt, 2017). We believe that showing what happens when turning on and off the surface temperature perturbation might be a valuable way to understand some of the feedbacks.
In addition, we would like to remind that the primary perturbation driving dynamical changes in the atmosphere is the lower stratospheric heating due to SG aerosols (see Kuebbeler et al., 2012). We show that SST changes end up increasing the atmospheric stabilization, which is primarily produced by the lower stratospheric aerosol warming.

Why should the surface temperature pattern be believed? CCSM-CAM4 does not have interactive chemistry or a stratosphere. How are the emissions put in? Wouldn't this be different than ULAQ? Especially at high latitudes, impacts are dependent on a stratospheric circulation that I don't think CCSM-CAM4 does correctly at all.

We believe that the surface temperature predicted by CCSM-CAM4 in case of a sulfate geoengineering injection can be used as long as it is clear that it is a first order approximation, because it responds to the direct SG effects (i.e. aerosol increased planetary albedo), allowing the ULAQ-CCM a more realistic study of the atmospheric response to the indirect effects (chemistry, ice) with respect to a case in which SSTs were kept fixed at the RCP4.5 reference values (G4K). This is clarified in the revised manuscript. In addition, in order to be more specific regarding CCSM-CAM4, we have asked the scientist responsible for those SG G4 simulations (Simone Tilmes) to give her contribution to the manuscript by further explaining some of the aspects of the model (as was done for Visioni et al., 2017b). Regarding the modeling of the stratosphere in CCSM-CAM4, we will also reference Lamarque et al. (2012), Neale et al. (2013) and Tilmes et al. (2016) in the revised manuscript.

Why not use WACCM4 Geoengineering experiments, which are at least based on a stratospheric model with interactive sulfur emissions.

The available WACCM4 Geoengineering simulations have not been performed using a fixed injection from 2020 and 2070 as prescribed by the GeoMIP protocol.

So how is what you are doing different than Kuebbler et al. (2012)? Why is this novel or unique?

As we explained before, we believe that including the two direct effects of SG aerosols in the CCM, as primary drivers for dynamical changes, it allows a more complete assessment of the SG impact on upper tropospheric ice formation, with respect to previous study by Kuebbeler et al. (2012) where SSTs were kept fixed at the reference RCP values.

Updrafts responsible for....

Corrected.

So most of the vertical velocity is heavily and crudely parameterized by gravity waves and TKE. The TKE is probably linked strongly to the temp gradients. Does the model actually use this vertical velocity in advection? Or ice nucleation? Please explain what is going on. It is not possible for the reader to understand whether the model formulation is realistic, though I am pretty convinced the perturbation (applying SSTs from another model) is NOT realistic for reasons described above.

Vertical advection of trace species in the model is treated using the large scale vertical velocity calculated in the dynamical core of the CCM. Ice formation via homogeneous freezing in the upper troposphere is produced by updraft on sub-grid scales (see Kärcher and Lohmann, 2002; Lohmann and Kärcher, 2002). The latter is parameterized using the TKE formulation, as explained in the same referenced studies. For what concerns the SST specification see above in response to the overall comment and in other specific comments.

Is a 3% change in a parameterized vertical velocity significant? Is 10% significantly different from 3%? From Figure 6, I don't think any of this is significant.

Figure 6 showed the variability of the calculated vertical velocity (large scale + f(TKE) mesoscale contribution from synoptic scale and gravity wave motions) and the time-averaged mean values. Changes in temperature and wind profiles produced by the SG aerosol forcing are related to a TOARF of the order of -1 W/m^2 and produce a change in TKE of the order of -120 cm^2/s^2 in the tropical upper troposphere in G4 relative to the Base case, i.e. close to -20%. Following the parameterization developed in Lohmann and Kärcher (2002), w is taken as the sum of the large-scale term (of the order of 0.2 cm/s in the tropical UT) and $0.7 \times TKE^{0.5}$ (of the order of 17 cm/s in the tropical UT) (see Eq. 1 in the revised manuscript). A change in TKE of approximately -120 cm^2/s^2 translates in a change of -1.8 cm/s of w, i.e. close to -10%. The G4K vertical profile of w is intermediate between G4 and Base, because TKE changes result only from the lower stratospheric aerosol heating, with surface temperature kept fixed at the reference RCP scenario. This ends up in a w change of approximately -3% in the tropical UT. The SG perturbation of the temperature profile is obviously small relative to baseline atmospheric conditions, both in G4 and G4K, but these small changes are exactly those impacting the atmospheric static stability and vertical motions. And differences in G4K and G4 are proved to be significant from this point of view.
To better clarify, we note that the variability of w in Figure 6 is essentially due to seasonal changes and non-zonal asymmetries of the TKE. But if we isolate a given month in the time series, the vertical velocity change due to SG is more comparable to the w variability in the time series. We attach a figure below (Fig. R2_1) showing this quantity, to show the reviewer what we mean.

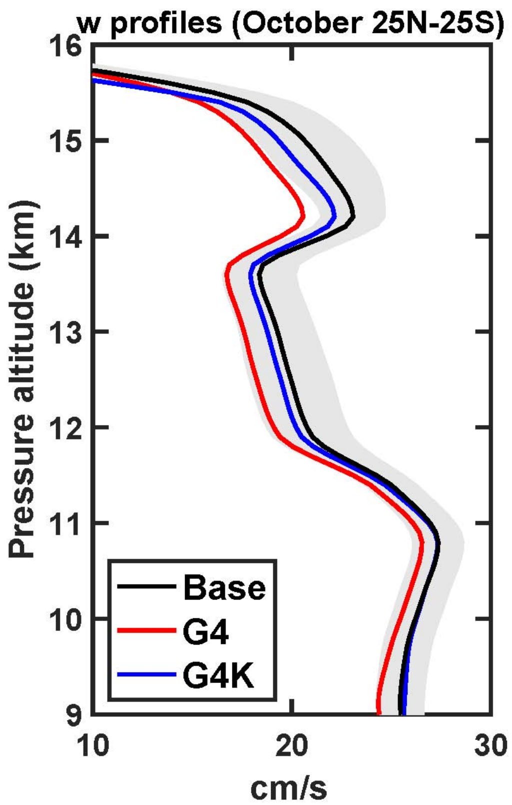

Fig. R2_1. October monthly mean of the upper tropospheric tropical profiles of vertical velocity (cm/s) in G4, G4K and Base experiments (years 2030-39). Shaded areas represent ±1σ for the ensemble over the October month in the 10 year period 2030-39.

MODIS ice effective radius is not a reasonable product, especially for thin tropical cirrus, unless you have a validation paper that says otherwise.

As per the reviewer request, we have tried to add some peer reviewed references to the MODIS ice effective radius, in particular Yang et al. (2007). We will also discuss some of the limitations regarding the retrieval of the ice effective radius (Delanoe and Hogan, 2008; Zhang et al.,2010).

The mention of what looks like a maximum updraft velocity here is an indication that the ULAQ ice nucleation needs to be better explained.

Ice nucleation is now presented in a more complete way in the revised manuscript.

This section needs to go before all the results presented earlier.

We have done what the reviewer suggested, also following the recommendation of reviewer 1.

It's not clear to me what fraction of ice formed in situ (T<238K) is from homogeneous and heterogeneous freezing. It would be useful to note the fraction homogenous (or heterogenous). This looks like it is in Figure 10c, but I don't think that is what I am interested in. What fraction of ice is heterogenously formed?

Cirrus ice formation in the ULAQ-CCM results from both homogeneous and heterogeneous freezing mechanisms and their competition. However, in our first draft of the manuscript we had decided to turn off the heterogeneous freezing mechanism, in order to focus on the SG aerosol induced perturbation to ice formation from homogeneous freezing only.

We acknowledge this specific point of the reviewer. The reduced updraft will affect ice formation from homogeneous freezing in a different way if part of the available water vapor goes to ice particles formed via heterogeneous freezing, which requires smaller supersaturation ratios, both on mineral dust and black carbon particles. Following the reviewer suggestion, we have decided to perform again our simulations with both mechanisms turned on, allowing their non-linear interaction. Results are substantially affected, with a resulting smaller indirect RF due to upper tropospheric ice changes induced by sulfate geoengineering.
Looking at the revised results of our numerical experiments, we are really indebted with the reviewer(s) for making this specific scientific point, helping us in a more correct assessment of the ice perturbation due to SG aerosol and its indirect radiative forcing.

This is a decent summary that the changes are due to changes in vertical velocity and tropospheric temperatures. How model dependent do you think these quantities are?

Results of our numerical experiments are obviously dependent on model features and design. However, one major point of our work was to systematically compare our results with observed ice-related quantities, on one hand, and to an independent modelling work (Kuebbeler et al., 2012) for the SG-related ice perturbation, on the other hand. It is shown that our results are consistent and that inclusion of SST changes may be significant, following a suggestion explicitly made in Kuebbeler et al. (2012).

Why the 5/8 scaling of the RF results?

We wanted to compare our results to their Clear Sky RF, and as a first approximation we scaled our results to their injection rate. However, we recognize that this might be confusing to the reader, and we now compare the direct results of our model with those from Kuebbeler et al. (2012).

How realistic is the decrease in updraft? Is it consistent with the overall circulation? I am concerned that fixing SSTs from another model will not yield a reasonable result, and it is likely to be a single model configuration, not even a general result. How can you convince me and other readers that the mechanism in ULAQ is reasonable, especially since it is imposed from another model and not-interactive, and from a model with no stratosphere.

We believe that we have widely responded above to these specific points. In particular, the use of SSTs as input parameter in CCMs is intrinsic in the CCM nature and formulation itself. A comparison of the SG aerosol optical depth and extinction from CCSM-CAM4 is presented in Fig. R2_2 and Fig. R2_3, respectively (attached below), with those predicted and fully interactive in the ULAQ-CCM (Visioni et al., 2017b). This proves that the two aerosol latitudinal and vertical distributions are consistent, so that the aerosol direct radiative forcing applied in CCSM-CAM4 and regulating SST changes due to SG is consistent with that in the ULAQ-CCM. Finally, it is not true that CCSM-CAM4 has no stratosphere.

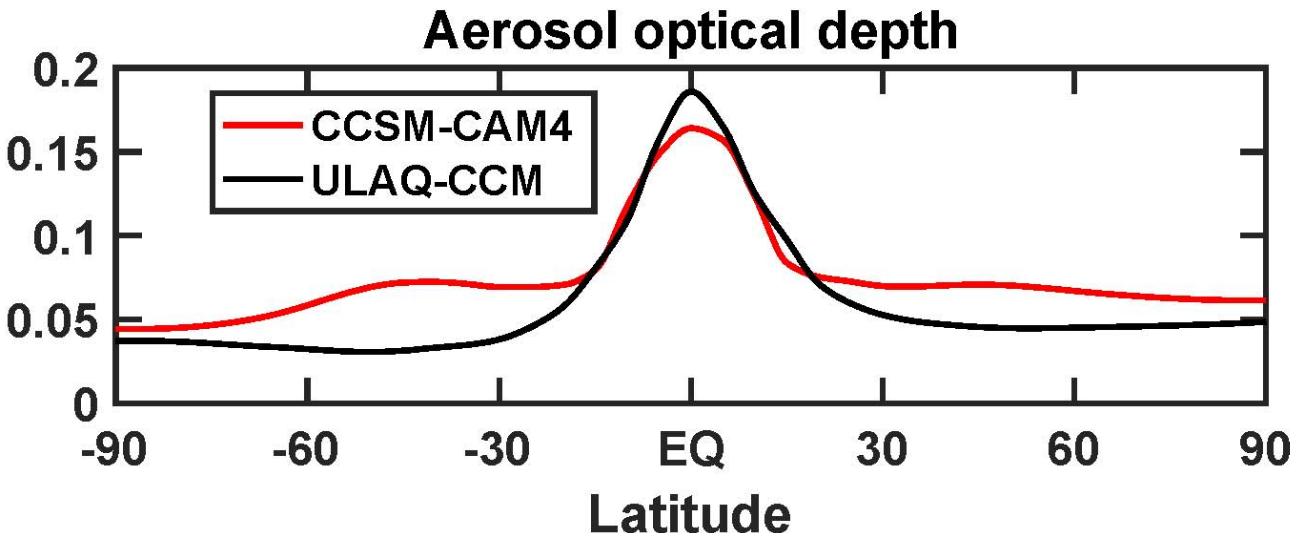

Fig. R2_2. Annually and zonally averaged SG aerosol optical depth at λ=0.55 μm used in CCSM-CAM4 and calculated in our study with the ULAQ-CCM.

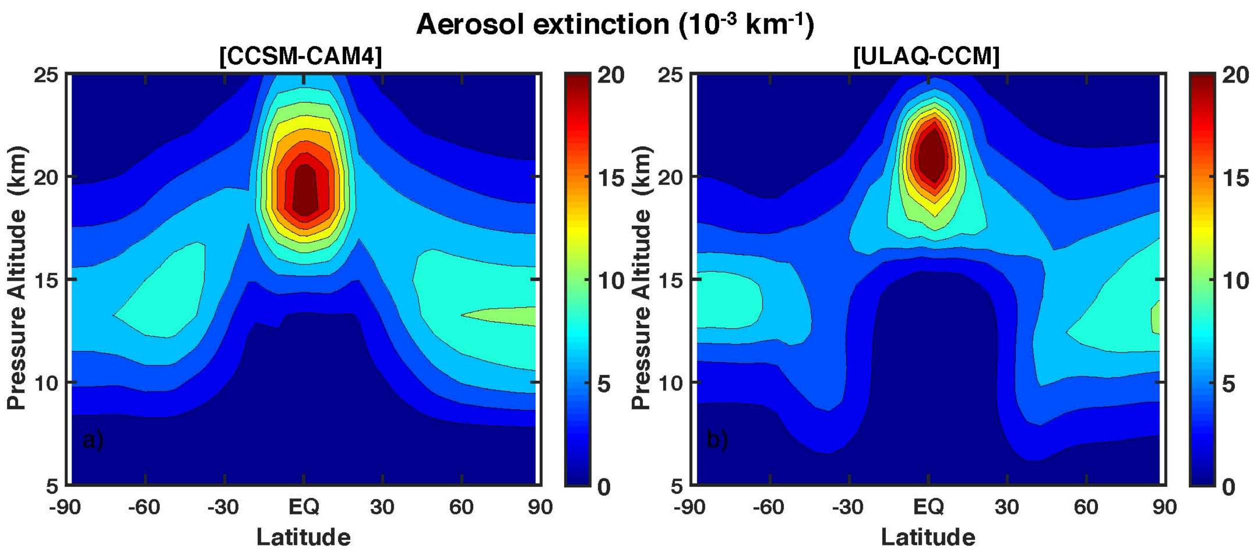

Fig. R2_3. Annually and zonally averaged SG aerosol extinction at λ=0.55 μm (10^{-3} km^{-1}) used in CCSM-CAM4 (left panel) and calculated in our study with the ULAQ-CCM (right panel).

References:

Bosilovich, M. G., Robertson, F. R., Takacs, L., Molod, A., and Mocko, D.: Atmospheric Water Balance and Variability in the MERRA-2 Reanalysis, Journal of Climate, 30, 1177–1196, doi:10.1175/JCLI-D-16-0338.1, https://doi.org/10.1175/JCLI-D-16-0338.1, 2017.

Chou, M. M. J. S. X. L.: A thermal infrared radiation parameterization for atmospheric studies, Tech. Rep. TM-2001-104606, NASA, NASA Goddard Space Flight Cent., Greenbelt, MD, 2001.

Delanoe, J., and R. J. Hogan (2008), A variational scheme for retrieving ice cloud properties from combined radar, lidar, and infrared radiometer, J. Geophys. Res., 113, D07204, doi:10.1029/2007JD00900

Duncan, D. I. and Eriksson, P.: An update on global atmospheric ice estimates from satellite observations and reanalyses, Atmos. Chem. Phys. Discuss., https://doi.org/10.5194/acp-2018-275, in review, 2018.

Gelaro, R., McCarty, W., Suárez, M. J., Todling, R., Molod, A., Takacs, L., Randles, C. A., Darmenov, A., Bosilovich, M. G., Reichle, R., Wargan, K., Coy, L., Cullather, R., Draper, C., Akella, S., Buchard, V., Conaty, A., da Silva, A. M., Gu, W., Kim, G. K., Koster, R., Lucchesi, R., Merkova, D., Nielsen, J. E., Partyka, G., Pawson, S., Putman, W., Rienecker, M., Schubert, S. D., Sienkiewicz, M., and Zhao, B.: The modern-era retrospective analysis for research and applications, version 2 (MERRA-2), J. Climate, 30, 5419–5454, https://doi.org/10.1175/JCLI-D-16-0758.1, 2017.

Kärcher, B. and Lohmann, U.: A parameterization of cirrus cloud formation: Homogeneous freezing of supercooled aerosols, Journal of Geophysical Research: Atmospheres, 107, doi:10.1029/2001JD000470, http://dx.doi.org/10.1029/2001JD000470, 2002.

Kuebbeler, M., Lohmann, U., and Feichter, J.: Effects of stratospheric sulfate aerosol geo-engineering on cirrus clouds, Geophysical Research Letters, 39, doi:10.1029/2012GL053797, http://dx.doi.org/10.1029/2012GL053797, l23803, 2012.

Lamarque, J.-F., Emmons, L. K., Hess, P. G., Kinnison, D. E., Tilmes, S., Vitt, F., Heald, C. L., Holland, E. A., Lauritzen, P. H., Neu, J., Orlando, J. J., Rasch, P. J., and Tyndall, G. K.: CAM-chem: description and evaluation of interactive atmospheric chemistry in the Community Earth System Model, Geosci. Model Dev., 5, 369-411, https://doi.org/10.5194/gmd-5-369-2012, 2012.

Lohmann, U. and Kärcher, B.: First interactive simulations of cirrus clouds formed by homogeneous freezing in the ECHAM general circulation model, Journal of Geophysical Research: Atmospheres, 107, AAC 8–1–AAC 8–13, doi:10.1029/2001JD000767, http: //dx.doi.org/10.1029/2001JD000767, 2002.

Morgenstern, O., Hegglin, M. I., Rozanov, E., O'Connor, F. M., Abraham, N. L., Akiyoshi, H., Archibald, A. T., Bekki, S., Butchart, N., Chipperfield, M. P., Deushi, M., Dhomse, S. S., Garcia, R. R., Hardiman, S. C., Horowitz, L. W., Jockel, P., Josse, B., Kinnison, D., Lin, M., Mancini, E., Manyin, M. E., Marchand, M., Marecal, V., Michou, M., Oman, L. D., Pitari, G., Plummer, D. A., Revell, L. E., Saint-Martin, D., Schofield, R., Stenke, A., Stone, K., Sudo, K., Tanaka, T. Y., Tilmes, S., Yamashita, Y., Yoshida, K., and Zeng, G.: Review of the global models used within phase 1 of the Chemistry–Climate Model Initiative (CCMI), Geoscientific Model Development, 10, 639–671, doi:10.5194/gmd-10-639-2017, https://www.geosci-model-dev.net/10/639/2017/, 2017.

Neale, R.B., J. Richter, S. Park, P.H. Lauritzen, S.J. Vavrus, P.J. Rasch, and M. Zhang: The Mean Climate of the Community Atmosphere Model (CAM4) in Forced SST and Fully Coupled Experiments. *J. Climate,* **26**, 5150–5168, https://doi.org/10.1175/JCLI-D-12-00236.1 , 2013.

Niemeier, U. and Schmidt, H.: Changing transport processes in the stratosphere by radiative heating of sulfate aerosols, Atmospheric Chemistry and Physics, 17, 14 871–14 886, doi:10.5194/acp-17-14871-2017, https://www.atmos-chem-phys.net/17/14871/2017/, 2017.

Pitari, G., Aquila, V., Kravitz, B., Robock, A., Watanabe, S., Cionni, I., De Luca, N., Di Genova, G., Mancini, E., and Tilmes, S.: Stratospheric ozone response to sulfate geoengineering: Results from the Geoengineering Model Intercomparison Project (GeoMIP), Journal of Geophysical Research: Atmospheres, 119, 2629–2653, 2014.

Pitari, G., Cionni, I., Di Genova, G., Visioni, D., Gandolfi, I., and Mancini, E.: Impact of Stratospheric Volcanic Aerosols on Age-of-Air and Transport of Long-Lived Species, Atmosphere, 7, http://www.mdpi.com/2073-4433/7/11/149, 2016a.

Pitari, G., Di Genova, G., Mancini, E., Visioni, D., Gandolfi, I., and Cionni, I.: Stratospheric Aerosols from Major Volcanic Eruptions: A Composition-Climate Model Study of the Aerosol Cloud Dispersal and e-folding Time, Atmosphere, 7, 75, doi:10.3390/atmos7060075, http://dx.doi.org/10.3390/atmos7060075, 2016b.

Randles, C. A., Kinne, S., Myhre, G., Schulz, M., Stier, P., Fischer, J., Doppler, L., Highwood, E., Ryder, C., Harris, B., Huttunen, J., Ma, Y., Pinker, R. T., Mayer, B., Neubauer, D., Hitzenberger, R., Oreopoulos, L., Lee, D., Pitari, G., Di Genova, G., Quaas, J., Rose, F. G., Kato, S., Rumbold, S. T., Vardavas, I., Hatzianastassiou, N., Matsoukas, C., Yu, H., Zhang, F., Zhang, H., and Lu, P.: Intercomparison of shortwave radiative transfer schemes in global aerosol modeling: results from the AeroCom Radiative Transfer Experiment, Atmospheric Chemistry and Physics, 13, 2347–2379, doi:10.5194/acp-13-2347-2013, http://www.atmos-chem-phys.net/13/2347/2013/, 2013.

Tilmes, S., Mills, M. J., Niemeier, U., Schmidt, H., Robock, A., Kravitz, B., Lamarque, J.-F., Pitari, G., and English, J. M.: A new Geoengineering Model Intercomparison Project (GeoMIP) experiment designed for climate and chemistry models, Geosci. Model Dev., 8, 43-49, https://doi.org/10.5194/gmd-8-43-2015, 2015.

Tilmes, S., Lamarque, J.-F., Emmons, L. K., Kinnison, D. E., Marsh, D., Garcia, R. R., Smith, A. K., Neely, R. R., Conley, A., Vitt, F., Val Martin, M., Tanimoto, H., Simpson, I., Blake, D. R., and Blake, N.: Representation of the Community Earth System Model (CESM1) CAM4-chem within the Chemistry-Climate Model Initiative (CCMI), Geosci. Model Dev., 9, 1853-1890, https://doi.org/10.5194/gmd-9-1853-2016, 2016.

Timmreck, C., Mann, G. W., Aquila, V., Hommel, R., Lee, L. A., Schmidt, A., Brühl, C., Carn, S., Chin, M., Dhomse, S. S., Diehl, T., English, J. M., Mills, M. J., Neely, R., Sheng, J., Toohey, M., and Weisenstein, D.: The Interactive Stratospheric Aerosol Model Intercomparison Project (ISA-MIP): Motivation and experimental design, Geosci. Model Dev. Discuss., https://doi.org/10.5194/gmd-2017-308, in review, 2018.

Visioni, D., Pitari, G., and Aquila, V.: Sulfate geoengineering: a review of the factors controlling the needed injection of sulfur dioxide, Atmos. Chem. Phys., 17, 3879-3889, https://doi.org/10.5194/acp-17-3879-2017, 2017a.

Visioni, D., Pitari, G., Aquila, V., Tilmes, S., Cionni, I., Di Genova, G., and Mancini, E.: Sulfate geoengineering impact on methane transport and lifetime: results from the Geoengineering Model Intercomparison Project (GeoMIP), Atmospheric Chemistry and Physics, 17, 11 209– 11 226, doi:10.5194/acp-17-11209-2017, https://www.atmos-chem-phys.net/17/11209/2017/, 2017b.

Visioni, D., Pitari, G., Tuccella, P., and Curci, G.: Sulfur deposition changes under sulfate geoengineering conditions: quasi-biennial oscillation effects on the transport and lifetime of stratospheric aerosols, Atmos. Chem. Phys., 18, 2787-2808, https://doi.org/10.5194/acp-18-2787-2018, 2018.

Yang, P., Zhang, L., Hong, G., Nasiri, S. L., Baum, B. A., Huang, H. L., King, M. D., and Platnick, S.: Differences Between Collection 4 and 5 MODIS Ice Cloud Optical/Microphysical Products and Their Impact on Radiative Forcing Simulations, IEEE Transactions on Geoscience and Remote Sensing, 45, 2886–2899, doi:10.1109/TGRS.2007.898276, 2007.

Zhang, Z., Platnick, S., Yang, P., Heidinger, A. K., and Comstock, J. M.: Effects of ice particle size vertical inhomogeneity on the passive remote sensing of ice clouds, Journal of Geophysical Research: Atmospheres, 115, doi:10.1029/2010JD013835, https://agupubs.onlinelibrary.wiley.com/doi/abs/10.1029/2010JD013835, 2010.

Upper tropospheric ice sensitivity to sulfate geoengineering

Daniele Visioni[1,2], Giovanni Pitari[1], Glauco di Genova[2], and Simone Tilmes[3]

[1]Department of Physical and Chemical Sciences, Universitá dell'Aquila, 67100 L'Aquila, Italy
[2]CETEMPS, Universitá dell'Aquila, 67100 L'Aquila, Italy
[3]National Center for Atmospheric Research, Boulder, CO 80305, USA

Abstract. Aside from the direct surface cooling that sulfate geoengineering (SG) would produce, the investigation ~~on possible side-effects~~ of the possible side effects of this method is still ongoing, ~~as for instance~~ such as, for instance, on upper tropospheric cirrus cloudiness. ~~Goal~~ The goal of the present study is to better understand the SG thermo-dynamical effects on the homogeneous freezing ice formation process. This is done by comparing the SG model simulations against a Representative Concentration Pathway 4.5 (RCP4.5~~reference case: in one case~~) reference case. In one case, the aerosol-driven surface cooling is included and coupled to the stratospheric warming resulting from the aerosol absorption of longwave radiation. In a second SG perturbed case, the surface temperatures are kept unchanged with respect to the reference RCP4.5 case. Surface cooling and lower stratospheric warming, together, tend to stabilize the atmosphere, thus decreasing ~~turbulence and water vapor~~ the turbulence and updraft velocities (-10% in our ~~modeling~~ modelling study). The net effect is an induced cirrus thinning, which may then produce a significant indirect negative radiative forcing (RF). This would go in the same direction as the direct effect of solar radiation scattering by the aerosols, thus influencing the amount of sulfur needed to counteract the positive RF due to the greenhouse gases. In our study, given ~~a~~ an 8 Tg-SO_2~~equatorial injection in~~/yr equatorial injection into the lower stratosphere, an all-sky net tropopause RF of ~~-2.13~~ -1.54 W/m^2 is calculated, of which ~~-0.96~~ -0.37 W/m^2 (~~45%)~~ 24%) is from the indirect effect on cirrus thinning (~~7.5~~5.2% reduction in ice optical depth). When the surface cooling is ignored, the ice optical depth reduction is lowered to ~~5~~3.1%, with an all-sky net tropopause RF of ~~-1.45~~ -1.42 W/m^2, of which ~~-0.21~~ -0.18 W/m^2 (~~14%)~~ 12%) is from cirrus thinning. ~~Relatively~~ Relative to the clear-sky net tropopause RF due to the SG aerosols (-2.06 W/m^2), the cumulative effect of the background clouds and cirrus thinning accounts for ~~-0.07~~ +0.52 W/m^2, due to the close compensation of large positive shortwave (+~~1.85~~ 1.56 W/m^2) and negative longwave adjustments (~~-1.92~~ -1.04 W/m^2). When the surface cooling is ignored, the net cloud adjustment becomes +~~0.71~~ 0.74 W/m^2, with the shortwave contribution (+~~1.97~~ 1.51 W/m^2) ~~significantly larger in magnitude than the longwave one (-1.26~~ almost twice as much as that of the longwave (-0.77 W/m^2). This highlights the importance of including all of the dynamical feedbacks of the SG aerosols.

1 Introduction

Sulfate geoengineering (SG) is one of the methods that have been proposed in the scientific community (Budyko (1974); Crutzen (2006); Niemeier and Tilmes (2017)) ~~in order~~ to cool our planet for a limited amount of time, in response to the warming caused by the increasing greenhouse gases of anthropogenic origin. SG proposes the injection of SO_2 ~~in~~ into the tropical lower stratosphere in order to produce an optically active cloud of H_2SO_4-H_2O supercooled liquid aerosols that would reflect part of the incoming solar radiation back to space. These aerosols, however, would at the same time warm the lower stratosphere by a few degrees. The idea stems from the cooling effect of past explosive volcanic ~~eruption~~ eruptions in the tropical region (the last being Pinatubo in 1991). These major eruptions injected large amounts of SO_2 ~~in~~ into the lower stratosphere and increased the planetary albedo. The resulting cooling effect has been clearly observed (Robock (2000)), although ~~the magnitude of this cooling~~ its magnitude is still being discussed (Canty et al. (2013)).

In the case of past volcanic eruptions, both the direct and indirect effects of episodic large ~~injection of sulfur in~~ injections of sulfur into the stratosphere have been observed and documented, this is obviously not possible for planned sustained sulfur ~~injection in~~ injections in the SG experiments. Because of this, the scientific community mainly relies on simulations using climate models and ~~comparison of~~ comparisons of the results among them, ~~as for instance~~ such as, for instance, under the GeoMIP project (Kravitz et al. (2011); Kravitz et al. (2013)). Different injection scenarios have been proposed and adopted in modelling experiments, the most used being the one with a constant sulfur injection rate at the ~~equator~~ Equator for a certain number of years ~~, in order~~ to understand the climate response to such an atmospheric perturbation. Simulations have also been performed to identify the optimal magnitude and location of the ~~sulfur injection, in order~~ stratospheric sulfur injection and to obtain the highest ratio between the radiative forcing (RF) and the injection magnitude (Niemeier and Schmidt (2017); Tilmes et al. (2017); Kleinschmitt et al. (2017)).

Amongst various side effects of SG, those with non-negligible ~~impact on~~ impacts on the RF were analysed and summarized in Visioni et al. (2017a). These are related to an enhancement of stratospheric ozone destruction (Tilmes et al. (2008); Pitari et al. (2014); Xia et al. (2017)), an increase in the concentration and lifetime of methane (Visioni et al. (2017b)), an increase of stratospheric water ~~vapor~~ vapour due to a ~~TTL~~ tropical tropopause layer warming (Pitari et al. (2014)) and~~most importantly~~ , most importantly, to a change in the probability of the formation of cirrus ice particles in the upper troposphere (UT) (Kuebbeler et al. (2012)). Regarding this latter effect, some studies have appeared in the recent literature that propose ways in which SG could affect the UT cirrus ice number density and optical depth. We will discuss them below and try to expand some aspects further in the present work.

~~Fig. 1 summarizes in a schematic way those dynamical and radiative processes related to UT ice formation that we analyze in detail ahead in this paper.~~ In an unperturbed atmosphere, the formation of UT ice particles may take place either by homogeneous or heterogeneous freezing (Karcher and Lohmann (2002); Hendricks et al. (2011)), with the former process normally dominating over the latter~~.~~ , at least in model simulations (Storelvmo and Herger (2014); Gasparini and Lohmann (2016); Gasparini et al. (2017)). Cziczo et al. (2013), however, reported that, in some areas, in-situ measurements show that heterogeneous freezing dominates over homogeneous freezing. Homogeneous freezing takes place when the ice ~~supersaturation~~ saturation ratio is relatively high (typically above ∼1.5), local temperatures are below the threshold for atmospheric ice particle formation (∼238 K) and supercooled solution droplets are present, namely, sulfate aerosols or ~~sulfate coated~~ sulfate-coated aerosols. Supersaturation conditions ~~is~~ are maintained by intense vertical motions ~~bringing water vapor~~ controlling the adiabatic cooling rate and bringing water vapour from the lower to the upper troposphere.

~~Cartoon of the sulfate geoengineering impact on cirrus ice particles, formed through homogeneous freezing, and schematic representation of ice induced changes in radiative fluxes.~~

Ice crystals formed in this way both reflect part of the incoming solar radiation (negative RF) and trap part of the outgoing planetary radiation, contributing to the greenhouse effect (positive RF). The sign of the combined effects could not easily be determined in a variety of atmospheric conditions. Normally, ~~however,~~ it has been shown that the net UT ice contribution to the RF is positive (Chen et al. (2000); Fusina et al. (2007); Gasparini et al. (2017)). This is, ~~anyway~~however, a rather delicate balance and strongly ~~depending on humidity and cloud cover~~ depends on the humidity, cloud cover and optical properties (Sanderson et al. (2008); Mitchell et al. (2008)), so that a robust atmospheric perturbation, such as the one that the SG could produce, may significantly affect it.

The perturbation to the UT ice could be twofold. On one hand, Cirisan et al. (2013) studied how the H_2SO_4-H_2O droplets resulting from the sulfur injection would interact with cirrus clouds, both microphysically and radiatively. ~~Even if an increase in~~ An upper tropospheric increase of the sulfate aerosol number concentration is expected under the SG conditions due to gravitational sedimentation and the large-scale transport of the particles below the tropopause from the lower stratosphere (LS). However, sulfuric acid liquid supercooled droplets are very inefficient ice nuclei (IN) ~~in the upper troposphere were found , the~~ for heterogeneous freezing. At the same time, the background number concentration of the UT aerosols acting as nuclei for homogeneous freezing is already much higher with respect to the ice particle number density. For this reason, a negligible increase of the active IN population would be found in the UT, and the same would hold true for the positive RF associated ~~to this effectwould be negligible, as the authors themselves state~~ with a possible increase of ice particles from this effect, as Cirisan et al. (2013) concluded in their study.

Kuebbeler et al. (2012), on the other hand, ~~analyzed~~ analysed the effects produced by dynamical changes due to the modification of the tropospheric thermal gradient produced by stratospheric geoengineering aerosols. In particular, the ~~lower stratosphere (LS)~~ LS warming, caused by increasing heating rates in the optically thick sulfate cloud, tends to decrease the tropospheric lapse rate. A subsequent decrease in the available turbulent kinetic energy (TKE) would follow and translate in ~~slowing down updraft of water vapor to the UT~~a slowing down of the updraft and of the adiabatic cooling rate, thus reducing the probability for sufficiently high supersaturation values capable ~~to produce~~ of producing ice crystals formation via homogeneous freezing. Their study found a resulting large net RF reduction in magnitude with respect to ~~clear sky~~ clear-sky conditions, where only the direct aerosol forcing is considered (-0.93 W/m^2 against -1.53 W/m^2). They ~~conclude~~ concluded that this forcing reduction results not only from the mere (passive) presence of background clouds ~~which~~ that affect the atmospheric radiative transfer ~~,~~ but also from the cirrus cloud thinning produced by the SG aerosols. This may obviously have clear ~~implication~~ implications regarding the potential of the SG to counterbalance global warming.

The aforementioned study, however, lacked an important part of the possible dynamical feedback of the SG, that is, the changes in sea surface temperatures (SSTs) that would result from the decreased incoming solar radiation. ~~Goal~~ The goal of the present study is to study the ~~SG~~ impact on cirrus ice particles formed via homogeneous freezing ~~, by include the two main radiative effects of stratospheric sulfate, i.e., local warming and surface cooling: this is made using~~ of a stratospheric sulfate injection and to understand how both the local stratospheric warming and the surface and tropospheric cooling can affect this process; to do this, we will use the composition-climate coupled model developed at the University of L'Aquila (ULAQ-CCM). We performed ~~a~~ an SG simulation with ~~a~~ an 8 Tg-SO_2/yr injection, using surface temperatures calculated in the atmosphere-ocean coupled model CCSM-CAM4, operated with the same sulfur injection (thus resulting in a general surface cooling, with respect to atmospheric unperturbed conditions). This perturbed experiment (named G4, according to the convention of Kravitz et al. (2011), regardless ~~from~~ of the time constant magnitude of the injection) ~~,~~ is compared against a baseline simulation without SG and using a background anthropogenic emission scenario corresponding to the Representative Concentration Pathway 4.5 (RCP4.5) (Taylor et al. (2012)) (named Base case in our study). ~~In order to~~ To properly compare our results with ~~the ones~~ those of Kuebbeler et al. (2012), a third simulation was performed with the same geoengineering sulfur injection of G4 ~~, but with~~ but with the surface temperatures fixed at the Base case values (named G4K).

The effects of the SG surface temperature changes on the lower stratospheric dynamics were already discussed in Visioni et al. (2017b); this time, we focus on their impact in the upper troposphere. ~~A flow-chart summary of the dynamical-radiative effects of SG on the UT is presented in Fig. 2, in a way that the SG-driven surface cooling effects are clearly highlighted. In particular, while both SG simulations (G4 and G4K) have the lower stratospheric warming in common, the surface (and consequently tropospheric) cooling is present only when surface temperatures are allowed to respond to the decreased incoming solar radiation (i.e., only in G4). This produces partially compensating effects on cirrus ice formation: a decrease in probability due to less water vapor updraft and an increase in probability due to colder temperatures in the UT. Colder temperatures, in fact, allow for a number density increase of ice particles (and their reduction in size), due to slower depositional growth and higher nucleation rate (Visioni et al. (2017a)). The predominant effect, as discussed ahead in Section 3, is the one related to changes in vertical motion, which produce an overall decrease in ice optical depth so that, in turn, more planetary radiation is allowed to escape to space with an indirect negative RF (i.e., reduced greenhouse effect).~~

~~Schematic summary of the sulfate geoengineering impact on dynamical processes driving changes of upper tropospheric ice particle formation through homogeneous freezing.~~

Unlike other side effects of sulfur injection ~~in~~ into the stratosphere, a comparison between the effects of a volcanic eruption and the SG on cirrus ice is ~~hard~~ difficult to draw. This is mainly ~~due to the fact that~~ because in a volcanic eruption episode (contrary to SG), a large amount of solid ash particles is injected ~~in~~ into the lower stratosphere together with SO_2. Part of these ~~dust~~ particles, after settling down below the tropopause, may contribute to ~~increase~~ increasing the number density of IN available for heterogeneous freezing in the UT. This could help explain some observed ~~increase~~ increases in UT ice particles after the Pinatubo eruption (~~Sassen et al. (2008)).~~ Sassen et al. (1995)). More recently, Friberg et al. (2005) showed that cirrus cloud reflectance and optical depth are reduced in the Northern Hemisphere in periods with more pronounced volcanic activity.

Understanding the RF contribution of the UT ice perturbation in a SG scenario is particularly crucial if the scientific community wants to design experiments whose goal is to meet a given climate target, as proposed in Kravitz et al. (2017) and MacMartin et al. (2017).

This paper is structured in ~~3~~ three subsequent sections plus the conclusions: in Section 2, we describe the CCSM-CAM4 and ULAQ-CCM ~~model and the set-up~~ models and the setup of the numerical experiments~~, discussing the dynamical drivers that may explain the ice perturbations described later on~~. Furthermore, in Section 2 we try to evaluate the ~~model~~ ULAQ-CCM skill in simulating the formation of the cirrus ice clouds, using re-analysis and satellite data. In Section 3, we discuss the ~~model calculated changes in~~ model-calculated changes in the thermo-dynamical properties of the atmosphere and in cirrus cloudiness (~~mass fraction,~~ size distribution, extinction, optical depth, number concentration~~, particle size~~) produced by ~~SG and finally~~ the SG, and finally, we show how these perturbations translate into tropopause radiative forcing terms.

2 ~~ULAQ-CCM~~ Model descriptions and setup of numerical experiments

~~The use of a composition-climate coupled model, as the ULAQ-CCM model, offers multiple advantages in this type of study: (a) on-line inclusion of interaction between aerosol and ice particles microphysics with chemistry, radiation, climate, dynamics and transport; (b) stratosphere-troposphere explicit interactions for the large-scale transport of gas and aerosol species (the model adopted high vertical resolution is important across the tropopause region); (c) sufficiently detailed chemistry both in the stratosphere and troposphere, with a robust design for heterogeneous chemical reactions on sulfuric acid aerosols, polar stratospheric cloud particles, upper tropospheric ice and liquid water cloud particles. This allows to account for atmospheric circulation changes produced by sulfate geoengineering. The ULAQ-CCM has many times proven to be capable of producing sound physical and chemical responses to both sulfate geoengineering (Pitari et al. (2014); Visioni et al. (2017b)) and for large explosive volcanic eruptions (Pitari (1993); Pitari et al. (2016b); Pitari et al. (2016a)).~~

~~In addition to a reference historical model experiment (1960-2015), we performed three sets of SG simulations: a baseline (Base) unperturbed case and two geoengineering experiments (G4 and G4K), both run with an injection of 8 Tg-SO_2/yr in the equatorial stratosphere between 18 and 25 km of altitude, as described in Kravitz et al. (2011) for the GeoMIP G4 experiment with sustained fixed injection of sulfur dioxide (5 Tg-SO_2/yr in that case). These numerical experiments were all run between years 2020-2069, with analyses focusing on the 2030-2039 decade; all take place under the same RCP4.5 reference scenario for well mixed greenhouse gases. The ULAQ-CCM is not an~~

2.1 CCSM-CAM4

The Community Climate System Model - Community Atmospheric Model version 4 (CCSM-CAM4) is an atmosphere-ocean coupled model ~~and uses a nudging technique for surface temperatures, taking them from the CCSM-CAM4 model, which was run under the same~~ that was used in this experiment to calculate the evolution of surface temperature for both the Base case

(RCP4.5 ~~and G4 conditions (8 Tg-SO_2/yr fixed injection in the equatorial lower stratosphere). In this way our main experiment G4 may account for the oceanic surface temperature response to SG (Fig. 4-5), even if only at a first order approximation since, as we will show, the cooling produced when also considering ice clouds modifications might be different.~~

~~A strong inter-hemispheric asymmetry in surface temperature changes produced by SG with 8 Tg-SO_2/yr injection is evident in both Fig. 4-5, with a negative anomaly in the Arctic region larger than 1 K with respect to south polar latitudes. The SG cooling impact on Arctic sea ice is such that larger negative surface temperature anomalies are favored in the Northern Hemisphere high latitudes for several months during the year, from fall to spring months (see Fig. 4a, Fig. 4b, Fig. 4d), thus increasing atmospheric stabilization with respect to the Southern Hemisphere. It should be noted, however, that the dynamical effects of this enhanced atmospheric stability in SG conditions (decreasing wave activity and turbulence) may be partially counterbalanced by the increased longitudinal variability of the induced cooling, mostly connected with positive surface temperature anomalies in the subpolar North Atlantic. These positive temperature anomalies in the North Atlantic sub-Arctic are a direct consequence of the increasing amount of polar sea ice in SG conditions, with southward transport of colder and saltier ocean waters in the sub-Arctic, with respect to RCP4.5 Base conditions (Tilmes et al. (2009)) . In this way, the North Atlantic subpolar downwelling of these cold surface waters to the deep ocean is favored with respect to Base conditions, thus producing positive anomalies in sea surface temperatures.~~

~~Seasonally averaged surface temperature anomalies G4-RCP4.5 (K), from the atmosphere-ocean coupled model CCSM-CAM4 (time average 2030-2069). Shaded areas are not statistically significant within $\pm 1\sigma$. Panels (a-d) refer to: December-January-February (a); March-April-May (b); June-July-August (c); September-October-November (d).~~

~~The SG induced warming on the Antarctic continent during wintertime (Fig. 4c), on the other hand, is a direct consequence of the geoengineering aerosol positive radiative forcing in the planetary longwave, which represent the net forcing at these high latitudes in the absence of sunlight. This radiative feature will be further discussed in Section 3. All these high-latitude positive temperature anomalies directly reflect in a large variability of the zonally averaged surface temperature changes presented in Fig. 5.~~

~~Annually and zonally averaged surface temperature anomalies G4-RCP4.5 (K), from the atmosphere-ocean coupled model CCSM-CAM4 (time average 2030-39). The shaded area represents $\pm 1\sigma$ of the zonally averaged temperature anomalies over the 10 year period.~~

~~Together with the G4 simulation, a sensitivity case (G4K) was run, with surface temperatures fixed at the RCP4.5 Base values. Here the experimental approach is similar to that of Kuebbeler et al. (2012) who ran a G4 simulation with 5 Tg-SO_2/yr injection and prescribed sea surface temperatures and sea ice from the RCP4.5 Base case. This is done in order to highlight not only the role of tropospheric temperature perturbations in cirrus ice formation (given a certain vertical velocity change), but mostly to calculate the updraft sensitivity to different conditions of tropospheric stabilization introduced by the stratospheric sulfate aerosol injection. Fig. 6 shows the differences in temperature and updraft in G4 and G4K with respect to the Base case. In G4 we observe a tropospheric cooling of $\simeq$1-2 K in the ice formation region throughout all latitudes, while the warming due to sulfate aerosol absorption of shortwave and longwave radiation is confined above the tropopause (Fig. 6a). When surface temperatures are kept fixed at the RCP4.5 baseline values with the SG perturbation (G4K case), the upper troposphere and~~

~~lower stratosphere temperature anomalies look very different (Fig. 6b). The tropospheric cooling is absent and the stratospheric warming produced by longwave and near-infrared solar radiation absorption is more uniformly spread across the lower stratosphere, with some penetration also in the UT (≃0-1 K). The latter is due to sulfate aerosol cross-tropopause large-scale transport (at mid-latitudes) and gravitational sedimentation (mostly relevant in the tropical region).Updraft responsible for upper tropospheric ice particle formation results from the sum of a rather small large-scale vertical velocity contribution (on the order of 1-2 cm/s) and a dominant part due to motions associated to synoptic scale disturbances and gravity waves (on the order of 10-20 cm/s); the latter is calculated as a function of the TKE (Lohmann and Karcher (2002)). The vertical velocity is reduced in G4 with respect to the Base case by ≃1-2 cm/s in the whole UT (Fig. 6c) (on the order of -10%, as visible in Fig. 7), due to the atmospheric stabilization caused by the reduction in the temperature gradient.~~

~~Zonally and time averaged changes of temperature (panels a,b) and vertical velocity (panels c,d) in experiments G4 (panels a,c) and G4K (panels b,d) with respect to the Base case (years 2030-39). The dashed lines show the mean tropopause height (with seasonal variability). The dash-dotted lines show the mean height (with seasonal variability) at which the temperature reaches 238 K, thus enabling homogeneous freezing.~~

~~The SG induced reduction of updraft velocities is significantly smaller in the G4K case (≃0.5 cm/s, on the order of -3% the baseline values), as clearly visible in Fig. 6d. This will represent the major change in our approach for studying the UT ice sensitivity to SG, with respect to the one adopted in Kuebbeler et al. (2012). According to our calculations, when taking into account both the main radiative effects of geoengineering stratospheric aerosols (i.e., lower stratospheric heating on one hand, surface and tropospheric cooling on the other hand) the resulting impact on tropospheric turbulence and updraft is significantly enhanced with respect to the case in which only the stratospheric warming is considered. A noticeable difference in~~ scenario) and a geoengineering case with the ~~G4K w-anomalies with respect to the G4 ones is at low altitudes over the polar regions, where the G4K negative values are larger than in G4. This may be largely explained by the increasing longitudinal variability of surface temperatures in the G4 case, mainly in the sub-Arctic region (see previous discussion relative to Fig. 4).~~

~~Tropical and extratropical average profiles of the updraft velocity are shown in Fig. 7, for both Base and G4 conditions. The G4K curve (not shown) is intermediate between the previous two. The pronounced variability of the vertical velocity is expected as a consequence of time, latitude and longitude fluctuations of TKE. This will produce a significant dispersion of the ice particle size distribution (see ahead in Section 3).~~

~~Average upper tropospheric profiles of the vertical velocity (cm/s) in G4 and Base experiments (years 2030-39). Panels (a) and (b) are for the tropics and extratropics, respectively (see legends). The vertical velocity w is obtained as the sum of the large scale value and the one calculated as a function of turbulent kinetic energy (see Lohmann and Karcher (2002)), which essentially accounts for synoptic scale and gravity wave motions. Shaded areas of the same color represent~~ ~~$\pm 1\sigma$~~ ~~for the ensemble over the 10 year period 2030-39.~~

~~A compact summary of model features in these numerical experiments is presented in Table 1; relevant aerosol and ice quantities calculated in the~~ same sulfur injection as the ULAQ-CCM ~~are summarized in Table 2 in comparison with available satellite observations. The first two rows in Table 2 compare the ULAQ-CCM results for stratospheric sulfate optical depth (OD) and tropical effective radius~~ ~~(r_{eff})~~ ~~against SAGE-II and AVHRR satellite observations (Thomason et al. (1997); Long and Stowe (1994)),~~

~~under post-Pinatubo conditions (Pitari et al. (2016a)). This is done to highlight the realistic representation of gas-particle conversion and aerosol microphysics processes in the model, along with aerosol large scale transport in the lower stratosphere in case of a major tropical volcanic eruption, which may be used as a proxy for SG with an equatorial SO_2 injection. A comparison of aerosol effective radii under volcanic and background conditions (see rows 2 and~~ model, described in Tilmes et al. (2015). For these simulations, the model was run without interactive chemistry. The resolution of the model is 1.9° × 2.5° with 26 vertical levels and the top of the model is at 3 ~~in Table 2), clearly shows the effects of sulfuric acid condensation on the size extension of the aerosol accumulation mode and how this is represented in the model. The bottom 5 rows in Table 2 compare global budget calculations for upper tropospheric ice particles with values obtained from MERRA reanalyses (ice mass fraction) and MODIS retrieval (ice effective radius). Simultaneous use of these two products allows an indirect calculation of the ice optical depth (row 7 of Table 2), as discussed ahead in Section 2.2. The ULAQ-CCM OD underestimation is mostly related to the ice mass fraction lower values in the largest portion of the upper troposphere (see row 5 of Table 2) and may be in part explained with the inclusion of a relatively narrow interval for updraft velocities (w<30 cm/s), as well as with the inclusion of a single pathway for ice particle formation in the model (i.e., via homogeneous freezing).~~ hPa. The model has been fully described in Neale et al. (2013) and Tilmes et al. (2016) and has been shown to compare well against observations in the stratosphere in Lamarque et al. (2012). Ice clouds are diagnosed from a purely relative humidity-based formulation (Neale et al. (2013)). The ~~ULAQ-CCM has been widely described in recent literature, along with in-depth process-evaluation.For the sake of completeness, however, we discuss in the following two sub-headings some of the model features, in particular those relevant for stratospheric sulfate aerosols and upper tropospheric cirrus ice particle formation.~~

~~Summary of ULAQ-CCM features and numerical experiments for the present study. Years of simulation 1960-2015 2020-2069 Type of simulation Reference Base (RCP4.5) + G4 + G4K Ensemble size 2 1 +2 + 2 Horizontal and vertical resolution Chemistry Dynamics Calculated[1] Calculated[2] QBO Nudged (from equatorial wind obs.) Nudged (iteration of observed cycles of eqt. winds) Altitude of equatorual injection 18 -25 km of SO_2 in G4 (~~results of an 8 Tg-SO_2/~~yr) - (Gaussian Distribution)~~

~~Summary of time-averaged sulfate aerosol and cirrus ice particle related quantities, as calculated in the ULAQ-CCM and compared with available satellite observations. Sulfate aerosols: sectional approach (Pitari et al. (2002); Pitari et al. (2014)). Cirrus ice particles: parameterization for homogenous freezing based on Karcher and Lohmann (2002), but including effects of the aerosol size distribution; a probabilistic approach is adopted for the ice supersaturation ratio. Standard deviations are calculated over the time series of globally averaged monthly mean values. Stratospheric sulfate optical depth 0.11 ± 0.02 (~~yr injection on the surface temperatures and the effects of the inclusion of the perturbed SSTs in the ULAQ-CCM ~~)~~ model have been already discussed in Visioni et al. (2017b).

~~[post-Pinatubo conditions] 0.13 ± 0.02 (SAGE II) [reference (September 1991 - August 1992)] 0.13 ± 0.02 (AVHRR) Sulfate r_{eff} (μm) (30-100 hPa, 25S-25N) [post-Pinatubo conditions] 0.54 ± 0.06 (ULAQ-CCM [reference (September 1991 - August 1992)] 0.58 ± 0.06 (SAGE II) Sulfate r_{eff} (μm) (30-100 hPa, 25S-25N) [volcanic unperturbed conditions] 0.19± 0.02 (ULAQ-CCM [reference (1999 - 2000)] 0.22 ± 0.02 (SAGE II) Ice mass fraction (mg/kg) (150-200 hPa) 3.3 ± 0.3 (ULAQ-CCM) [reference (2003 - 2012)] 3.5 ± 0.4 (MERRA) Ice mass fraction (mg/kg) (200-300 hPa) 4.3 ± 0.6 (ULAQ-CCM) [reference~~

~~(2003 - 2012)] 5.5 ± 0.8 (MERRA) Ice mass fraction (mg/kg) (350-400 hPa) 2.5 ± 0.4 (ULAQ-CCM) [reference (2003 - 2012)] 2.6 ± 0.5 (MERRA) Upper tropospheric ice r_{eff} (μm) 32.0 ± 3.6 (ULAQ-CCM) [reference (2003 - 2012)] 33.4 ± 2.1 (MODIS) Upper tropospheric ice optical depth 0.40 ± 0.03 (ULAQ-CCM) [reference (2003 - 2012)] 0.62 ± 0.04 (MERRA+MODIS)~~

2.2 ULAQ-CCM

2.3 ~~Stratospheric sulfate aerosols~~

The University of L'Aquila composition-climate coupled model was described in its first version in Pitari et al. (2002); subsequent model versions were documented in ~~modeling~~ modelling intercomparison campaigns (Eyring et al. (2006); Morgenstern et al. (2010); Morgenstern et al. (2017)). Model updates in the horizontal and vertical resolution, photolysis cross sections, the treatment of Schumann-Runge bands and radiative transfer code were described and tested in Pitari et al. (2014) and Chipperfield et al. (2014). The shortwave radiative module has been documented and tested for tropospheric aerosols in Randles et al. (2013) and ~~also~~ for volcanic stratospheric aerosols in Pitari et al. (2016a). It makes use of a two-stream delta-Eddington approximation and is on-line in the model for both photolysis and solar heating rate calculations. A companion broadband, k-distribution longwave radiative module is used for the heating rate and the top-of-atmosphere radiative forcing calculations in the planetary infrared spectrum (Chou (2001)).

A critical atmospheric region in the SG studies is the upper troposphere and lower stratosphere (UTLS). An extensive model evaluation based on specific physical and chemical aspects was made in Gettelman et al. (2010) and Hegglin et al. (2010)). Subsequent model improvements in this region were discussed in Pitari et al. (2016b). The treatment of surface temperatures, and their importance for the lower stratospheric dynamics and species transport under a geoengineering scenario, has been discussed in Visioni et al. (2017b). Another very important aspect to be taken into account for large-scale species transport in the lower stratosphere is the role of the quasi-biennial oscillation (QBO) in SG studies. It has been discussed ~~under~~ from different points of view in some recent studies (Aquila et al. (2014); Niemeier and Schmidt (2017); ~~Visioni et al., 2017c~~Visioni et al. (2018)). A nudging procedure for the QBO is ~~used~~ adopted in the ULAQ-CCM, based on an observed historical data series of equatorial mean zonal winds (Morgenstern et al. (2017)).

For the sake of completeness, we discuss in the following two sub-headings some of the model features, in particular those relevant for stratospheric sulfate aerosols and upper tropospheric cirrus ice particle formation.

Table 1. Summary of ULAQ-CCM features and numerical experiments for the present study.

Years of simulation	1960-2015	2020-2069
Type of simulation	Reference	Base (RCP4.5) + G4 + G4K
Ensemble size	2	1 +2 + 2
Horizontal and vertical resolution	5° × 6°, L126 log-pressure top: 0.04 hPa	
Chemistry	On-line (strat & trop)	
Dynamics	Calculated[1]	Calculated[2]
QBO	Nudged (from eqt. wind obs.)	Nudged (iteration of observed cycles of eqt. winds)
Altitude of equatorual injection of SO_2 in G4 (8 Tg-SO_2/yr)	-	18-25 km (Gaussian Distribution)

[1] Sea surface temperatures from observations; calculated land temperatures

[2] Surface temperatures from CCSM-CAM4, separately for Base and G4 (Visioni et al. (2017b))

[3] Surface temperatures from CCSM-CAM4, Base values also used for G4K

2.2.1 Stratospheric sulfate aerosols

In SG experiments G4 and G4K, SO_2 is injected at the ~~equator~~ Equator (0° longitude) ~~,~~ throughout the altitude range 18-25 km with a Gaussian distribution ~~centered~~ centred at 21.5 km. The OH oxidation of SO_2 starts the production of supercooled H_2O-H_2SO_4 particles, whose size distribution is calculated in an aerosol microphysics module with a sectional approach, starting from gas-particle interaction processes (nucleation, H_2SO_4 condensation and H_2O growth) and then including aerosol particle coagulation. Removal processes ~~from~~ are included via gravitational settling across the tropopause and evaporation in the upper stratosphere (Visioni et al. (2018)).

In the troposphere, the ULAQ-CCM includes sulfate production from ~~DMS~~ the dimethyl sulfide (DMS) and SO_2 emissions, with gas phase and aqueous/ice SO_2 oxidation (by OH and H_2O_2, O_3, respectively) to produce SO_4 (Feichter et al. (1996); Clegg and Abbatt (2001)). The tropospheric and stratospheric SOx budget in the ULAQ-CCM (for unperturbed background conditions) was recently discussed in Pitari et al. (2016c), with a focus on the role of non-explosive volcanic sulfur emissions, and in Visioni et al. (2018), in connection with the SG.

Aerosol extinction, optical thickness, single scattering albedo and surface area density are calculated on-line at all model grid-points every hour. This allows the interactive calculation of up/down diffuse radiation and absorption of solar near-infrared and planetary radiation by SG aerosols, with explicit full coupling of the aerosol, chemistry and radiation modules in the ULAQ-CCM. This justifies the 'composition-climate' name for this coupled model, which is more general than the usual 'chemistry-climate' model name.

The ULAQ-CCM ability ~~in producing~~ to produce the correct confinement of sulfate aerosols in the tropical stratosphere has already been documented in the literature, with a comparison against SAGE II data following the Pinatubo eruption or looking at the SG conditions (see Pitari et al. (2014); Pitari et al. (2016a); Visioni et al. (2017b)). ~~Figure 8a shows the average tropical~~

~~vertical profiles of SO_4 mixing ratio, for both Base and SG experiments (with 8 Tg-SO_2 injection). Changes in zonally averaged net heating rates, temperatures and zonal winds are also shown in Fig. 8, panels (b), (c) and (d), respectively. They help to understand how SG sulfate changes act as drivers for dynamical changes in the UT , with significant effects on ice particle formation. In Fig. 8a it is interesting to note a somewhat smaller tropical aerosol confinement in the G4K case. This is consistent with the findings of Visioni et al. (2017b): the aerosol-driven surface cooling in G4 (contrary to G4K) favors a decreased wave activity and a consequent decrease in poleward mass fluxes from the tropical reservoir, for both gas and aerosol species. On the other hand, the increased H_2SO_4 tropical amount available for aerosol formation tends to produce larger particles with smaller equivalent optical thickness (see Niemeier and Schmidt (2017); Visioni et al. (2018)). On light of this, smaller stratospheric heating rate anomalies are calculated in G4 with respect to G4K (Fig. 8b): in the latter casewe then expect an enhanced temperature increase in the tropical lower stratosphere (Fig. 8c), coupled to a slight tropospheric warming due to SG aerosol sedimentation below the tropopause. The latter, in addition, results to be greatly overbalanced by tropospheric convective cooling produced by the aerosol-driven surface cooling in G4 (contrary to G4K). As a result, the G4 atmosphere is more efficiently stabilized with respect to G4K and the positive/negative anomalies of T/u shears in the UT (Fig. 8cd) favor a decrease of TKE (and updraft velocities) in G4 with respect to G4K (Fig. 6).~~

~~All features of SW and LW heating rate anomalies in Fig. 8b can be fully explained taking into account the aerosol-O_3 coupled effects (Pitari et al. (2014)). The sign of tropical ozone changes under SG conditions depends on altitude: O_3 decreases below $\sim$25 km and increases above this height: this helps explain the positive/negative heating anomalies in SW and LW components above 25 km altitude.~~

~~Average tropical vertical profiles (25S-25N, years 2030-39) of: SO_4 volume mixing ratio for G4, G4K and Base experiments (ppbv, panel a); G4-Base changes of net, shortwave and longwave heating rates (K/day, panel b) (LW is calculated with temperature fixed at Base values) (net heating rate changes are also shown for G4K-Base, with blue line); G4-Base and G4K-Base temperature changes (K, panel c); G4-Base and G4K-Base changes of mean zonal winds (m/s, panel d). Shaded areas of the same color represent $\pm$ 1 σ for the ensemble over the 10 year period 2030-39.~~

2.2.2 Upper tropospheric ice

2.3 ~~Upper tropospheric ice particles~~

~~Formation of UT ice particles is parameterized in the~~ The formation of UT ice particles may take place via heterogeneous and homogeneous freezing mechanisms. In the latter case, the ULAQ-CCM ~~by adopting~~ adopts the approach initially described in Karcher and Lohmann (2002), which assumes ice crystals formed only via homogeneous freezing of solution droplets as a function of local UT temperatures and updraft velocities, ~~but including also~~ also including the effects of a variable aerosol size distribution. ~~As discussed above in Section 2, these~~ These updraft velocities are obtained as the sum of a dominant term related to the TKE and a much smaller contribution from the large-scale tropospheric circulation (Lohmann and Karcher (2002)). Typical vertical velocity net values are on the order of ~~15-25~~ 10-20 cm/s (~~Fig. 7~~see Section 3.1) and allow the formation of thin cirrus.

For the ice supersaturation ratio, we adopt a simplified probabilistic approach, starting from the knowledge of climatological frequencies of the UT relative humidity (RH$_{ICE}$), from which a mean value and a standard deviation can be calculated, assuming a normal distribution. Local ice super-saturation conditions (RH$_{ICE}$>100%) are a result of turbulent ascent and can be found in the UT~~. More precisely, when air is located~~ , in the vertical layer below the tropopause (where turbulent updraft conditions may be found) and above an altitude ~~with~~ where T < 238 K (i.e., the assumed threshold for ~~ice particle formation from water vapor freezing)~~ the spontaneous freezing of solution droplets). Here, the conditions for ice formation are met and we may calculate the probability that RH$_{ICE}$>1.5 (P$_{HOM}$). This represent the assumed threshold for homogeneous freezing to be activated, which is considerably higher with respect to the threshold for heterogeneous freezing to take place (RH$_{ICE}$>$\sim$~~1.2) (Hendricks et al. , 2011).The~~ 1.3) (Hendricks et al. (2011)). This represents the probability that an ice particle could be formed via heterogeneous freezing on a pre-existing population of ice condensation nuclei (P$_{HET}$), typically mineral dust or BC particles transported from the surface (N$_{IN}$).

The size distribution and number density n$_{HET}$ of ice particles formed via heterogeneous freezing is calculated starting from the formulation of Hendricks et al. (2011) using the ULAQ microphysical scheme adopted for polar stratospheric ice particle formation (Pitari et al. (2002)). N$_{IN}$ is the sum of grid-point model-predicted concentrations of mineral dust and black carbon aerosols (N$_{DU}$ and N$_{BC}$, respectively) and is used as the population of available condensation nuclei, with PHET being the probability that RH$_{ICE}$ > 1.3 at any model grid point. The problem in this case is on the actual availability of solid ice nuclei~~, typically mineral dust transported from the surface or freshly emitted non-hydrophobic aviation BC particles from aviation~~. A low fraction of activated IN is suggested in the literature (~~0.1%),~~ f$_{DU}$=1% for mineral dust and f$_{BC}$=0.25% for BC) because the large majority of IN will rapidly be coated by sulfate (Hendricks et al. (2011)). ~~Under~~ The number density n$_{HET}$ is then obtained as:

$$n_{HET} = (f_{BC}N_{BC} + f_{DU}N_{DU})P_{HET} \tag{1}$$

The specification of the active ice fraction for both mineral dust and BC represents the major source of uncertainty for UT ice particle formation via heterogeneous freezing. With the above assumptions and under typical UT conditions, homogeneous freezing normally dominates ice particle formation, with respect to the heterogeneous freezing mechanism (Cziczo et al. (2009); Hendricks et al. (2011)). However, this may not be considered a general conclusion~~and~~ , assumed to be valid in all thermodynamics conditions and any local atmospheric composition, as it has been shown for instance in Cziczo et al. (2013), where a predominance of heterogeneous freezing over homogeneous may be found.

The calculated mass fraction of ice formed ~~this way~~ in the ULAQ-CCM through both freeing mechanisms is shown in Fig. ~~9~~1ac for two pressure layers, 150-200 hPa and 350-400 hPa, where the ice formation is greater in the tropics and mid-high latitudes, respectively. These calculations are compared against the MERRA data (Bosilovich et al. (2017), Gelaro et al. (2017)), averaged over the same decade (Fig. ~~9~~1bd). Tropical ice formation shows a strong land-ocean asymmetry ~~,~~ due to significantly higher P_{HOM} and P_{HET} values over land. For both pressure layers, the magnitude and spatial distribution of the ice mass ~~fraction is comparable between~~ mixing ratio are comparable between the ULAQ-CCM and MERRA. Regarding the datasets used in this work to compare against our model results, note that there is a large spread amongst retrievals (such as MODIS or CALIPSO) and amongst reanalyses (Zhang et al. (2010); Duncan and Eriksson (2018)). In particular, MERRA-2 appears to be in the lower end of the spectrum in regards to some quantities, such as ice water path. Considering that the dataset only considers non precipitating ice (Duncan and Eriksson (2018)), this quantity might be however closer to the one simulated in our model, and thus allow for a more correct comparison.

While the probability of homogeneous ice formation is defined ~~this way~~as above, the number density and size of the ice particles formed this way is determined by the local ~~temperature and vertical velocity~~temperatures and vertical velocities, in addition to the competing ice formation mechanism via heterogeneous freezing. The lower the temperature, the faster the nucleation rate~~, thus~~; thus, more ice crystals can be formed. On the other hand, higher vertical velocities ~~produce higher RH conditions~~ increase the saturation ratio, leading to more ice crystals formed before ~~the deposition of the water in the~~ water deposition on ice crystals reduces ~~the RH conditions~~ supersaturation below the threshold. The spatial distribution of the cirrus ice optical depth (OD) in the model is calculated as:

$$\tau_{ice} = \Delta z \sum_i \sum_j Q_{ext} \pi r_{ij}^2 n_{ij}(r) \tag{2}$$

where $Q_{ext} \sim 2$ at all visible wavelengths for ice particle sizes on the order of 5-50 μm~~,~~; i is an index for the vertical layers, and the sum is over all the vertical layers in the UT~~with PHOM>0,~~; j is an index for the particle size bins, and the sum is over the whole size distribution; r_{ij}ij is the ~~particles~~ particle radius at the i-th layer and j-th bin; and n_{ij} is the corresponding ice number density.

~~Eq.~~ Equation 2 can easily be applied ~~in the modeland the result is~~ to the model, and the results are shown in Fig. ~~10~~2a. An evaluation can be made ~~using again the ice water mass fraction~~ again using the ice mixing ratio from MERRA (shown in Fig. ~~9~~1bc for two specific pressure layers), together with ~~MODIS derived~~ the MODIS-derived values of the ice particle effective radius (https://giovanni.gsfc.nasa.gov) ~~.~~ (Yang et al. (2007)). Intrinsic limitations regarding the retrieval of this quantity are discussed in **?** and Zhang et al. (2010). With these two products we have indirectly derived τ_{ice} at every horizontal grid point in Eq. (2), using the hydrostatic equation:

$$\tau_{ice} = Q_{ext} \frac{3}{2} \frac{\Delta p}{g} \frac{1}{\rho_{ice}} \sum_i \frac{\chi_i}{r} \tag{3}$$

where the sum is~~again over all~~, again, over all the vertical layers (~~each thick~~ constant Δp=50 hPa), g is the acceleration of gravity, ρ_{ice} is the ice bulk density, r is the MODIS effective radius; and χ_i is the MERRA ice mass fraction at the ith layer.

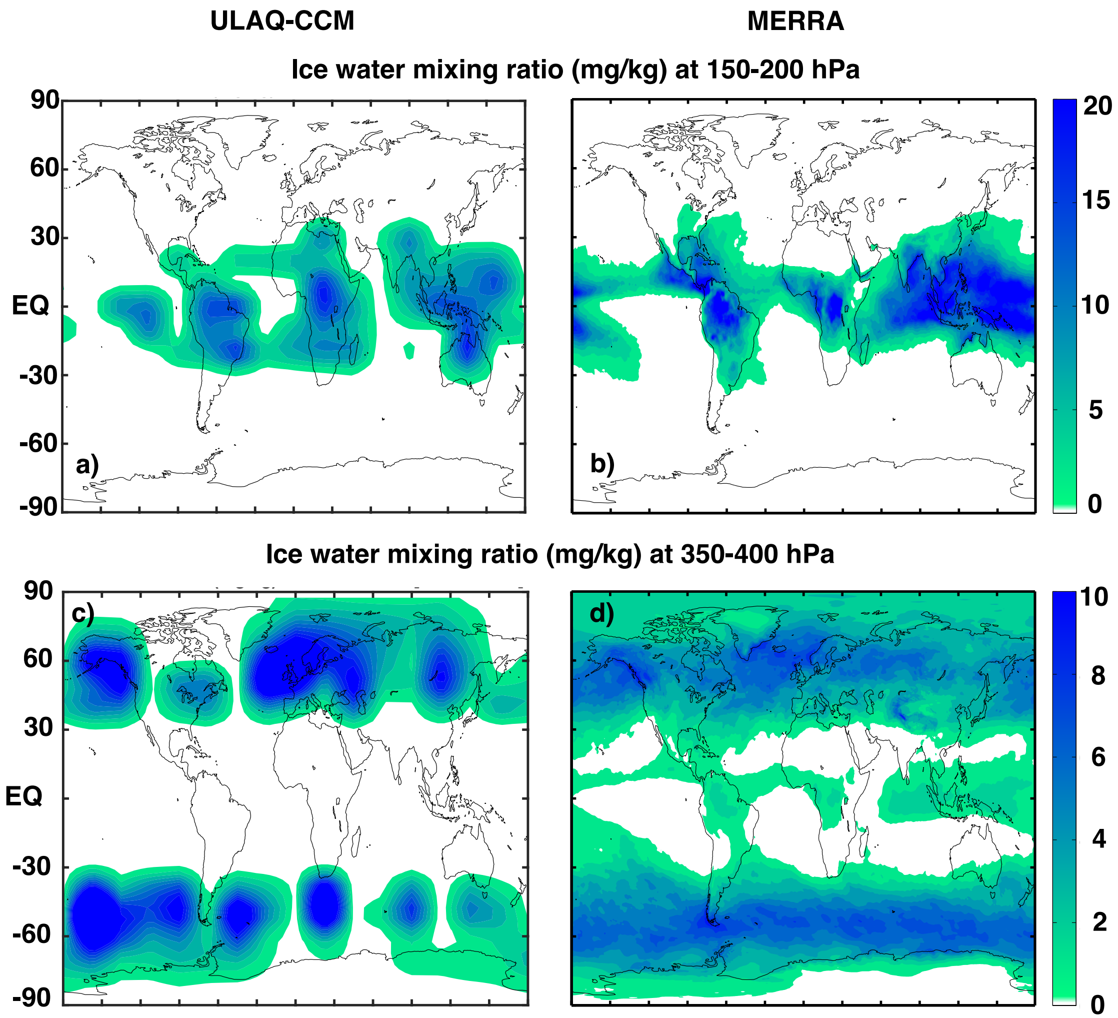

Figure 1. Lat/lon maps of the ice mass ~~fraction~~ mixing ratio (mg/kg-air) for pressure layers representative of tropical (panels a,b) and extratropical (panels c,d) upper troposphere. Panels (a,c) are for the ULAQ-CCM; panels (b,d) are for MERRA data (Bosilovich et al. (2017)). Time average is on years 2003-2012.

Doing so, we obtain an optical depth shown in Fig. ~~10~~2b. The two ODs are comparable in terms of spatial distribution, with the highest values in the tropics over land. ~~Absolute~~ The absolute values in the ULAQ-CCM, however, ~~result to be~~ are significantly smaller over the tropics. This should not surprise, in principle, ~~due to the fact that~~ because we are considering ~~only sub-visible ice cloudsformed through homogeneous freezing~~thin ice clouds, with a relatively narrow interval for updraft velocities (w<30 cm/s) so that events leading to thick cirrus formation are not considered. ~~In addition, ice formation from heterogeneous freezing~~

~~Ice optical depth at λ=0.55 μm, from ULAQ-CCM calculations (a) and from MERRA ice mass fractions (100 <p< 450 hPa) (Bosilovich et al. (2017)) with MODIS particle effective radius (b). Time average is on years 2003-2012 (MODIS data downloaded from https://giovanni.gsfc.nasa.gov, version MOD08M3v6).~~

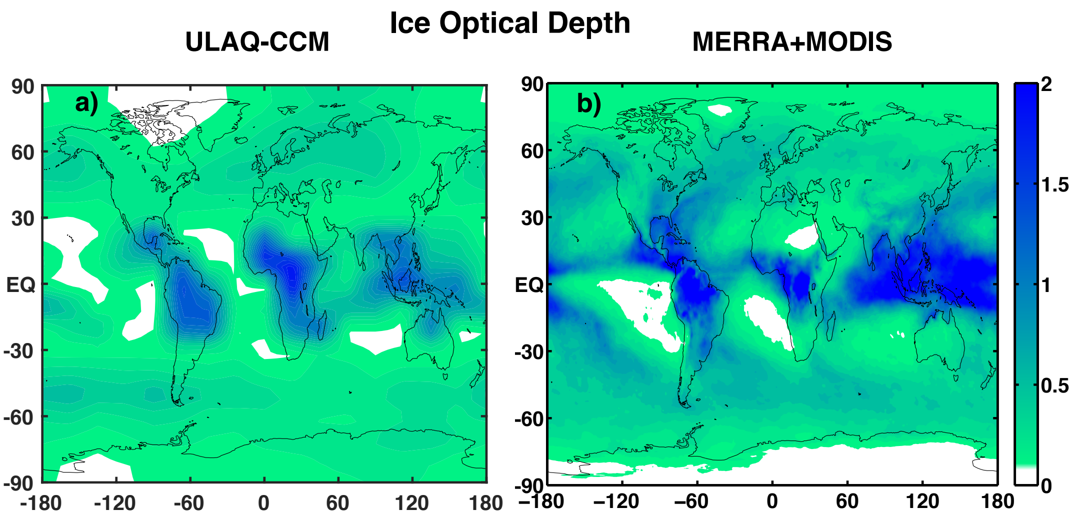

Figure 2. Ice optical depth at λ=0.55 μm, from ULAQ-CCM calculations (a) and from the MERRA ice mass fractions (100 <p< 450 hPa) (Bosilovich et al. (2017)) with MODIS particle effective radius (b). Time is averaged over the years 2003-2012 (MODIS data downloaded from https://giovanni.gsfc.nasa.gov, version MOD08M3v6).

~~on large IN, as mineral dust particles for example, is not taken into account in our modelling approach.~~

In Fig. 3, we show the model-predicted fraction of ice formed through heterogeneous freezing in terms of optical depth (Fig.3a) and zonally averaged extinction (Fig.3b). In both panels, we see that a large part of the ice particles formed through heterogeneous freezing is located in the tropical band at lower altitudes, where a higher concentration of mineral dust and BC ice nuclei can be transported from the surface. In those regions, the fraction of ice formed this way can be as much as 80% of the total.

In Fig. ~~11~~4ab we show the model calculated vertical profiles of ice particle number density averaged over the tropics (Fig. ~~11~~4a) and the ~~extra-tropics~~ extratropics (Fig. ~~11~~4b), with superimposed the time variability produced by changing conditions of vertical velocity, temperature and P$_{HOM}$, P$_{HET}$. The ice number density maxima are located at rather different altitudes in the two latitude bands, close to 13 km in the tropics and ~~to~~ 8 km elsewhere. This is clearly expected from the latitudinal variability of the tropopause height.

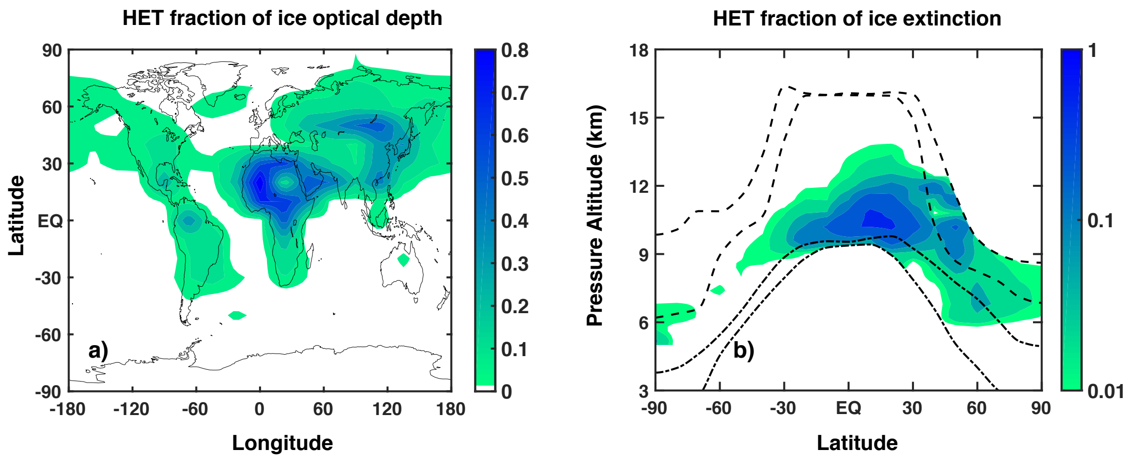

Figure 3. Fraction of total ice formed through heterogeneous freezing in ULAQ-CCM averaged over the years 2003-2012, as a function of latitude and longitude for the total optical depth (a) and as a function of altitude and latitude for the zonally averaged extinction (b). In panel (b), the colour scale is logarithmic, starting at 0.01 (i.e., 1% of total ice extinction) up to 1 (100%).

With a procedure similar to the one described above for the ice OD, we may derive a first order approximation of the ice number density from the MERRA ice mass ~~fractions~~ mixing ratio and MODIS radii. ~~Similarly~~ Similar to Eq. 3, for the ice number density n_i at each vertical layer we obtain the following expression:

$$n_i = \frac{3}{4\pi}\frac{1}{\rho_{ice}}\frac{1}{r^3}\chi_i \tag{4}$$

~~Results~~ The results from Eq. 4 (red circles in Fig. ~~11~~4ab) show that while the model and the indirectly derived points agree in terms of the general vertical distribution and localization of the vertical maxima in the extratropics, the ULAQ-CCM tends, however, to have smaller number densities in the tropics in the 10-13 km layer. Again, this should not surprise in light of the fact that we are focusing on a specific type of cirrus cloud particles.

Figure ~~11~~4c shows the ~~model calculated values of PHOM~~model-calculated values of P_{HOM}, as a 2D zonally averaged distribution. Using these PHOM values, it is possible to scale a n_i value measured in the mid-latitude airborne campaign of Strom et al. (1997) during a young cirrus formation, ~~in order~~ to derive an average climatological value to be considered consistent with our ~~modeling~~ modelling approach. They measured a mid-latitude ice concentration value n=0.3 cm^{-3} in a young cirrus cloud at T=220 K and p=320 hPa. If we scale this result with our corresponding P_{HOM}=12±3%, a 'climatological-mean' value n=0.025±0.005 cm^{-3} is obtained, close to our model prediction value of 0.031± 0.008 cm^{-3} (Fig. ~~11~~4b).

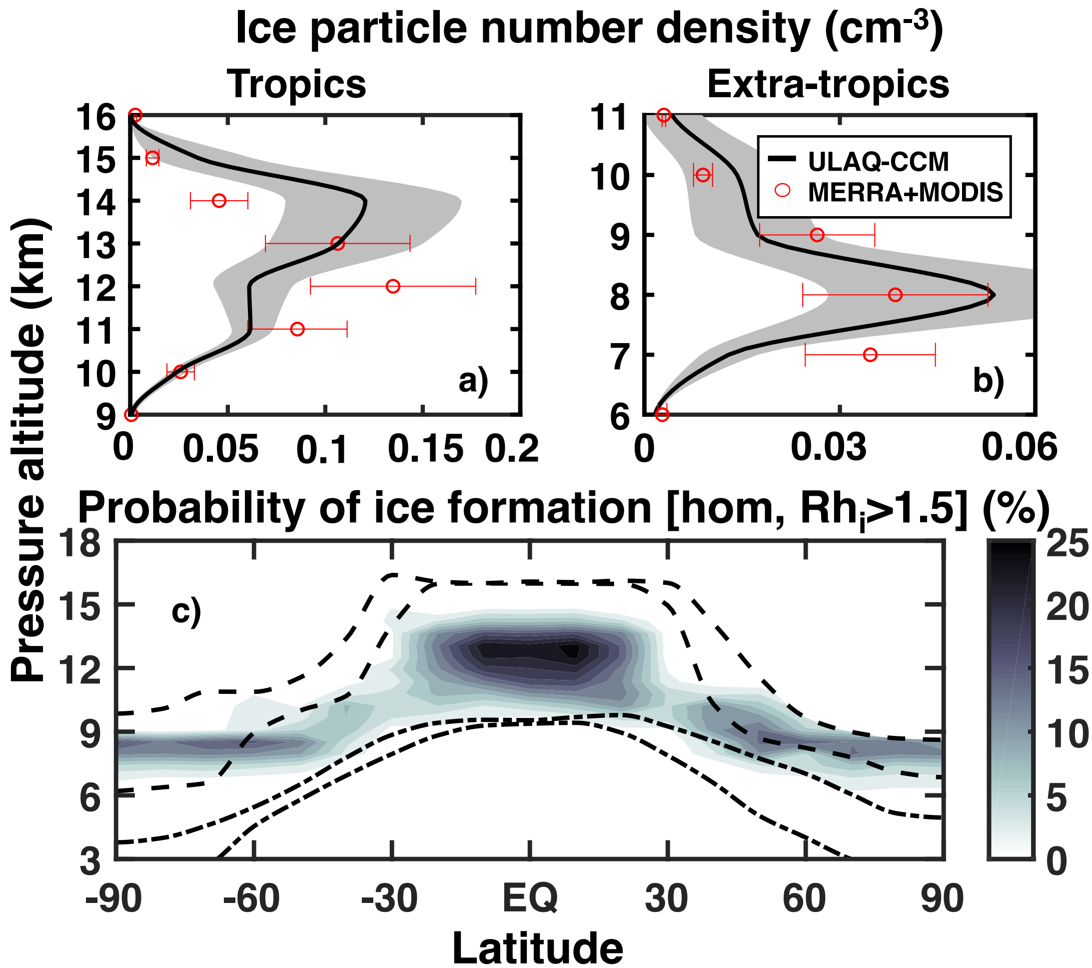

Figure 4. Average upper tropospheric profiles of ice particle number density (cm^{-3}), for the tropics (25S-25N) and extratropics (35S-90S, 35N-90N), in panels (a) and (b), respectively. ~~The time average~~ Time is ~~on~~ averaged over the years 2003-2012. Shaded areas represent $\pm 1\sigma$ for the ensemble over the ~~10 year~~ 10-year period. ~~Red~~ The red circles show indirectly derived values from the MERRA ice mass ~~fraction~~ mixing ratio and MODIS effective radius (see text). Panel (c) shows the zonally averaged probability of ice formation via homogeneous freezing (percent), as a function of altitude and latitude. ~~Dashed~~ The dashed lines show the mean tropopause height (with seasonal variability). ~~Dash-dotted~~ The dash-dotted lines show the mean height (with seasonal variability) at which ~~the~~ T=238 K (homogeneous freezing allowed for colder temperatures).

Table 2. Summary of globally time-averaged sulfate aerosol and cirrus ice particle related quantities, as calculated in the ULAQ-CCM and compared with available satellite observations. Sulfate aerosols: sectional approach (Pitari et al. (2002); Pitari et al. (2014)). Cirrus ice particles: parameterization for homogenous (HOM) and heterogeneous (HET) freezing are summarized in the text and based on the formulation of Karcher and Lohmann (2002) (HOM), but including the effects of the aerosol size distribution, and Hendricks et al. (2011) (HET); a probabilistic approach is adopted for the ice supersaturation ratio. Standard deviations are calculated over the time series of globally averaged monthly mean values. On the global average, our model predicts a 90% fraction of the ice optical depth formed via homogeneous freezing.

Stratospheric sulfate optical depth [post-Pinatubo conditions] [reference (September 1991 - August 1992)]	0.11 ± 0.02 (ULAQ-CCM) 0.13 ± 0.02 (SAGE II) 0.13 ± 0.02 (AVHRR)
Sulfate r_{eff} (μm) (30-100 hPa, 25S-25N) [post-Pinatubo conditions] [reference (September 1991 - August 1992)]	0.54 ± 0.06 (ULAQ-CCM 0.58 ± 0.06 (SAGE II)
Sulfate r_{eff} (μm) (30-100 hPa, 25S-25N) [volcanic unperturbed conditions] [reference (1999 - 2000)]	0.19 ± 0.02 (ULAQ-CCM) 0.22 ± 0.02 (SAGE II)
Ice mass mixing ratio (mg/kg) (150-200 hPa) [reference (2003 - 2012)]	3.3 ± 0.2 (ULAQ-CCM) (HOM) 0.1 ± 0.1 (ULAQ-CCM) (HET) 3.5 ± 0.4 (MERRA)
Ice mass mixing ratio (mg/kg) (200-300 hPa) [reference (2003 - 2012)]	3.8 ± 0.5 (ULAQ-CCM) (HOM) 0.6 ± 0.2 (ULAQ-CCM) 5.5 ± 0.8 (MERRA)
Ice mass mixing ratio (mg/kg) (350-400 hPa) [reference (2003 - 2012)]	2.4 ± 0.4 (ULAQ-CCM) (HOM) 0.1 ± 0.1 (ULAQ-CCM) (HET) 2.6 ± 0.5 (MERRA)
Upper tropospheric ice r_{eff} (μm) [reference (2003 - 2012)]	31.3 ± 3.1 (ULAQ-CCM) (HOM) 34.6 ± 3.8 (ULAQ-CCM) (HET) 33.4 ± 2.1 (MODIS)
Upper tropospheric ice optical depth [reference (2003 - 2012)]	0.37 ± 0.03 (ULAQ-CCM) (HOM) 0.04 ± 0.01 (ULAQ-CCM) (HET) 0.62 ± 0.04 (MERRA+MODIS)

3 ~~Ice perturbation due to sulfate geoengineering~~

Relevant aerosol and ice quantities calculated in the ULAQ-CCM are summarized in Table 2 in comparison with available satellite observations. The first two rows in Table 2 compare the ULAQ-CCM results for stratospheric sulfate optical depth (OD) and the tropical effective radius (r_{eff}) against SAGE-II and AVHRR satellite observations (Thomason et al. (1997); Long and Stowe (1994)), under post-Pinatubo conditions (Pitari et al. (2016a)). This is done to highlight the realistic representation of the gas-particle conversion and aerosol microphysics processes in the model, along with the aerosol large-scale transport in the lower stratosphere in case of a major tropical volcanic eruption, which may be used as a proxy for SG with an equatorial SO_2 injection. A comparison of the aerosol effective radii under volcanic and background conditions (see rows 2 and 3 in Table 2) clearly shows the effects of the sulfuric acid condensation on the size extension of the aerosol accumulation mode and how this is represented in the model.

The bottom 5 rows in Table 2 compare the global budget calculations for upper tropospheric ice particles with values obtained from the MERRA reanalyses (ice mass mixing ratio) and MODIS retrieval (ice effective radius). The simultaneous use of these two products allows an indirect calculation of the ice optical depth (row 7 of Table 2), as previously discussed. The ULAQ-CCM OD underestimation is mostly related to the ice mass mixing ratio lower values in the largest portion of the upper troposphere (see row 5 of Table 2) and may be, in part, explained with the inclusion of a relatively narrow interval for updraft velocities ($w<30$ cm/s).

The values are given separately for the ice formed through homogeneous and heterogeneous freezing.

~~In the previous sectionwe~~

2.1 Setup of the numerical experiments and role of perturbed SSTs

The use of a composition-climate coupled model, such as the ULAQ-CCM model, offers multiple advantages in this type of study: (a) the on-line inclusion of interaction between aerosol and ice particles microphysics with chemistry, radiation, climate, dynamics and transport; (b) the stratosphere-troposphere explicit interactions for the large-scale transport of gas and aerosol species (the model adopted high vertical resolution is important across the tropopause region); (c) the sufficiently detailed chemistry both in the stratosphere and troposphere, with a robust design for heterogeneous chemical reactions on sulfuric acid aerosols, polar stratospheric cloud particles, and upper tropospheric ice and liquid water cloud particles. This allows us to account for the atmospheric circulation changes produced by sulfate geoengineering. The ULAQ-CCM model has many times proven to be capable of producing sound physical and chemical responses to both sulfate geoengineering (Pitari et al. (2014); Visioni et al. (2017b)) and for large explosive volcanic eruptions (Pitari (1993); Pitari et al. (2016b); Pitari et al. (2016a)).

In addition to a reference historical model experiment (1960-2015), we performed three sets of SG simulations: a baseline (Base) unperturbed case and two geoengineering experiments (G4 and G4K), both run with an injection of 8 Tg-SO_2/yr into the equatorial stratosphere between 18 and 25 km of altitude, as described in Kravitz et al. (2011) for the GeoMIP G4 experiment with a sustained fixed injection of sulfur dioxide (5 Tg-SO_2/yr in that case). These numerical experiments were all run between years 2020 and 2069, with analyses focusing on the 2030 to 2039 decade; all take place under the same RCP4.5 reference scenario for well-mixed greenhouse gases. The ULAQ-CCM is not an atmosphere-ocean coupled model and uses a nudging technique for surface temperatures, taking them from the CCSM-CAM4 model, which was run under the same RCP4.5 and G4 conditions (8 Tg-SO_2/yr fixed injection into the equatorial lower stratosphere). In this way our main experiment G4 may account for the oceanic surface temperature response to SG (Fig. 4-5). We acknowledge that the perturbation introduced in the dynamics of ULAQ-CCM by the external SSTs changes is a first-order approximation, considering that CCSM-CAM4 has not been run with a coupled chemistry and a much simpler cirrus parametrization that produces negligible changes in the geoengineering experiment (Neale et al. (2013)). However, we believe it to be still a consistent one, considering that the main effect produced by the sulfate injection is the direct aerosol effect (Visioni et al. (2017a)) and that the prescribed stratospheric aerosol field in the SG simulation in CCSM-CAM4 (Tilmes et al. (2015)) is comparable to the one produced by the sulfate injection in ULAQ-CCM. With this in mind, in the next paragraph we discuss the SSTs perturbation and their significance for this study.

A strong inter-hemispheric asymmetry in the surface temperature changes produced by the SG with an 8 Tg-SO_2/yr injection is evident in both Figs. 5-6, with a negative anomaly in the Arctic region that is approximately 1 K larger than that of the high southern latitudes. The SG cooling impact on the Arctic sea ice is such that larger negative surface temperature anomalies are favoured in the Northern Hemisphere high latitudes for several months during the year, from the fall to spring months (see Fig. 5a, Fig. 5b, Fig. 5d), thus increasing atmospheric stabilization with respect to the Southern Hemisphere. Note, however, that the dynamical effects of this enhanced atmospheric stability in the SG conditions (decreasing wave activity and turbulence) may be partially counterbalanced by the increased longitudinal variability of the induced cooling, mostly connected with positive surface temperature anomalies in the subpolar North Atlantic. These positive temperature anomalies in the North Atlantic sub-Arctic are a direct consequence of the increasing amount of polar sea ice in the SG conditions, with the southward transport of colder and saltier ocean waters in the sub-Arctic, with respect to the RCP4.5 Base conditions (Tilmes et al. (2009)). In this way, the North Atlantic subpolar downwelling of these cold surface waters to the deep ocean is favoured with respect to the Base conditions, thus producing positive anomalies in sea surface temperatures.

Although not statistically significant, the SG-induced warming on the Antarctic continent during wintertime (Fig. 5c) is a direct consequence of the geoengineering aerosol positive radiative forcing in the planetary longwave, which represents the net forcing at these high latitudes in the absence of sunlight. This radiative feature will be further discussed in Section 3. All these high-latitude positive temperature anomalies directly reflect in the large variability of the zonally averaged surface temperature changes presented in Fig. 6.

Together with the G4 simulation, a sensitivity case (G4K) was run, with surface temperatures fixed at the RCP4.5 Base values. Here, the experimental approach is similar to that of Kuebbeler et al. (2012) who ran a G4 simulation with a 5 Tg-SO_2/yr injection and prescribed sea surface temperatures and sea ice from the RCP4.5 Base case. This is done not only to highlight the

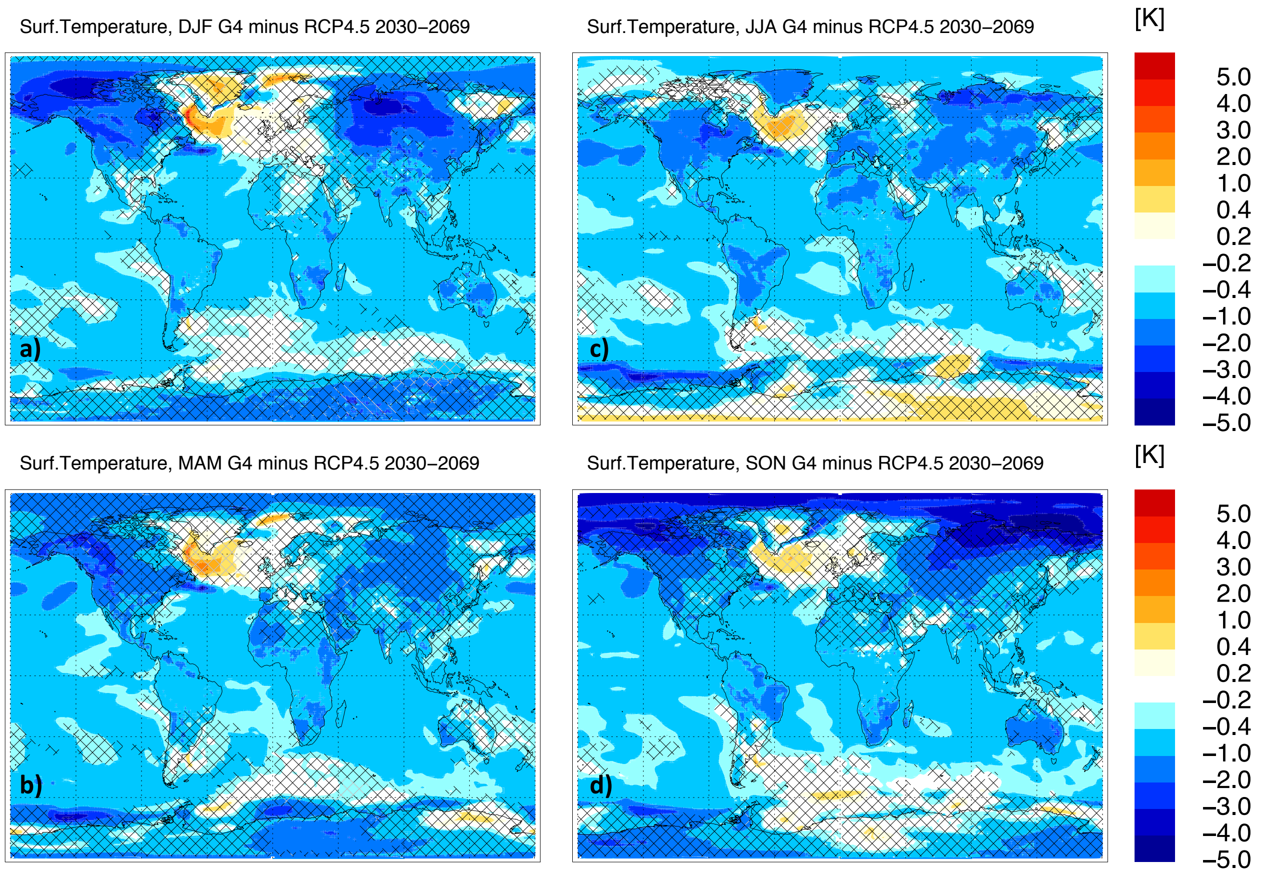

Figure 5. Seasonally averaged surface temperature anomalies G4-RCP4.5 (K) from the atmosphere-ocean coupled model CCSM-CAM4 (time average 2030-2069). The shaded areas are not statistically significant within $\pm 1\sigma$. Panels (a-d) refer to: December-January-February (a); March-April-May (b); June-July-August (c); September-October-November (d).

role of the tropospheric temperature perturbations in cirrus ice formation (given a certain vertical velocity change) but mostly to calculate the updraft sensitivity to different conditions of tropospheric stabilization introduced by the stratospheric sulfate aerosol injection.

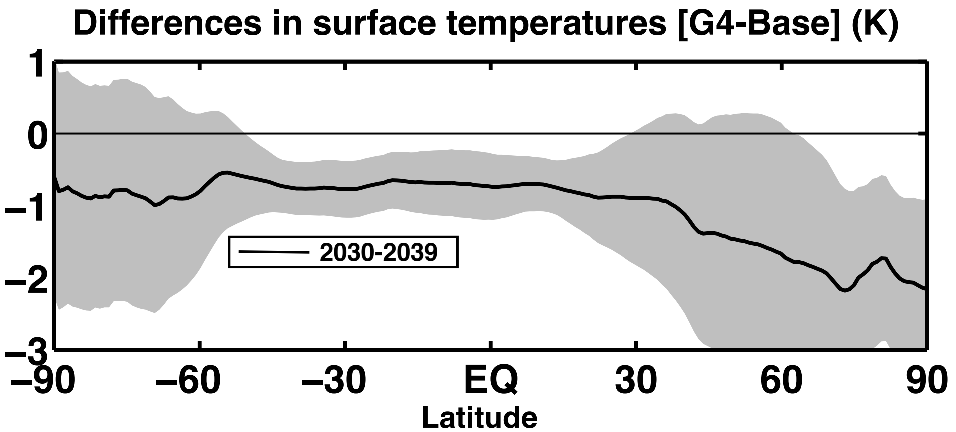

Figure 6. Annually and zonally averaged surface temperature anomalies G4-RCP4.5 (K), from the atmosphere-ocean coupled model CCSM-CAM4 (time average 2030-39). The shaded area represents $\pm 1\sigma$ of the zonally averaged temperature anomalies over the 10-year period.

3 Model response to sulfate geoengineering

In this section, we will show the ULAQ-CCM response to the stratospheric sulfate injection. Some of the perturbations have already been discussed in previous works, in particular regarding stratospheric dynamics changes (Pitari et al. (2014); Visioni et al. (2017b)). Here, we will focus on the thermo-dynamical changes in the upper troposphere and, consequently, on changes in the formation of cirrus ice clouds.

3.1 Thermo-dynamical changes in the troposphere

Figure 7 shows the differences in temperature and updraft in G4 and G4K with respect to the Base case. In G4, we observe a tropospheric cooling of $\simeq$1-2 K in the ice formation region throughout all latitudes, while the warming due to the sulfate aerosol absorption of shortwave and longwave radiation is confined above the tropopause (Fig. 7a). When surface temperatures are kept fixed at the RCP4.5 baseline values with the SG perturbation (G4K case), the upper troposphere and lower stratosphere temperature anomalies look very different (Fig. 7b). The tropospheric cooling is absent and the stratospheric warming produced by longwave and near-infrared solar radiation absorption is more uniformly spread across the lower stratosphere, with some penetration also in the UT ($\simeq$0-1 K). The latter is due to the sulfate aerosol cross-tropopause fluxes that are due to the large-scale transport (at mid-latitudes) and gravitational sedimentation (mostly relevant in the tropical region).
The updrafts responsible for the upper tropospheric ice particle formation result from the sum of a rather small large-scale vertical velocity contribution (on the order of 1-2 cm/s) and a dominant part due to motions associated with synoptic scale disturbances and gravity waves (on the order of 10-20 cm/s); the latter is calculated as a function of the TKE (Lohmann and Karcher (2002)) with the exact formulation reported in Eq. 5:

$$w_{TOT} = w_{LS} + 0.7\sqrt{TKE} \quad (5)$$

The vertical velocity is reduced in G4 with respect to the Base case by $\simeq$1-2 cm/s in the whole UT (Fig. 7c) (on the order of -10%, as visible in Fig. 8), due to the atmospheric stabilization caused by a reduction in the temperature vertical gradient.

Fig. 9a shows the average tropical vertical profiles of the SO_4 mixing ratio, for both the Base and SG experiments (with an 8 Tg-SO_2 injection). The changes in zonally averaged net heating rates, temperatures and zonal winds are also shown in Fig. 8, panels (b), (c) and (d), respectively. They help explain how the SG sulfate changes act as drivers for dynamical changes in the UT, with significant effects on ice particle formation.
In Fig. 9a, it is interesting to note a somewhat smaller tropical aerosol confinement in the G4K case. This is consistent with the findings of Visioni et al. (2017b): the aerosol-driven surface cooling in G4 (contrary to G4K) favours a decreased wave activity and a consequent decrease in poleward mass fluxes from the tropical reservoir, for both gas and aerosol species. On the other hand, the increased H_2SO_4 tropical amount available for aerosol formation tends to produce larger particles with smaller equivalent optical thickness (see Niemeier and Schmidt (2017); Visioni et al. (2018)). In light of this, smaller stratospheric heating rate anomalies are calculated in G4 with respect to G4K (Fig. 9b): in the latter case, we then expect an

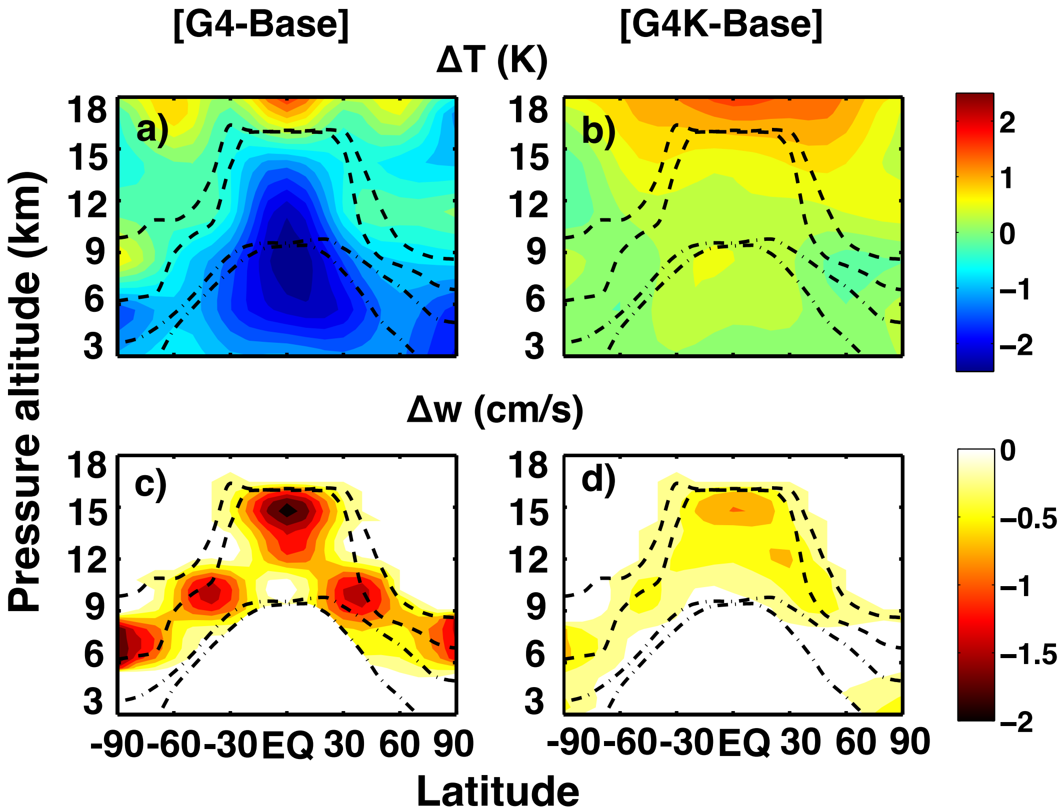

Figure 7. Zonally and time-averaged changes of temperature (panels a,b) and vertical velocity (panels c,d) in experiments G4 (panels a,c) and G4K (panels b,d) with respect to the Base case (years 2030-39). The dashed lines show the mean tropopause height (with seasonal variability). The dash-dotted lines show the mean height (with seasonal variability) at which the temperature reaches 238 K, thus enabling homogeneous freezing.

enhanced temperature increase in the tropical lower stratosphere (Fig. 9c), coupled to a slight tropospheric warming due to the SG aerosol sedimentation below the tropopause. The latter, in addition, causes the results to be greatly overbalanced by tropospheric convective cooling produced by the aerosol-driven surface cooling in G4 (contrary to G4K). As a result, the G4 atmosphere is more efficiently stabilized with respect to G4K, and the positive/negative anomalies of T/u shears in the UT (Fig. 9cd) favour a decrease of the TKE (and updraft velocities) in G4 with respect to G4K (Fig. 7).

All features of the SW and LW heating rate anomalies in Fig. 9b can be fully explained taking into account the aerosol-O_3 coupled effects (Pitari et al. (2014)). The sign of tropical ozone changes under the SG conditions depends on altitude. The O_3 decreases below ∼25 km and increases above this height; this helps explain the positive/negative heating anomalies in SW and LW components above 25-km altitude.

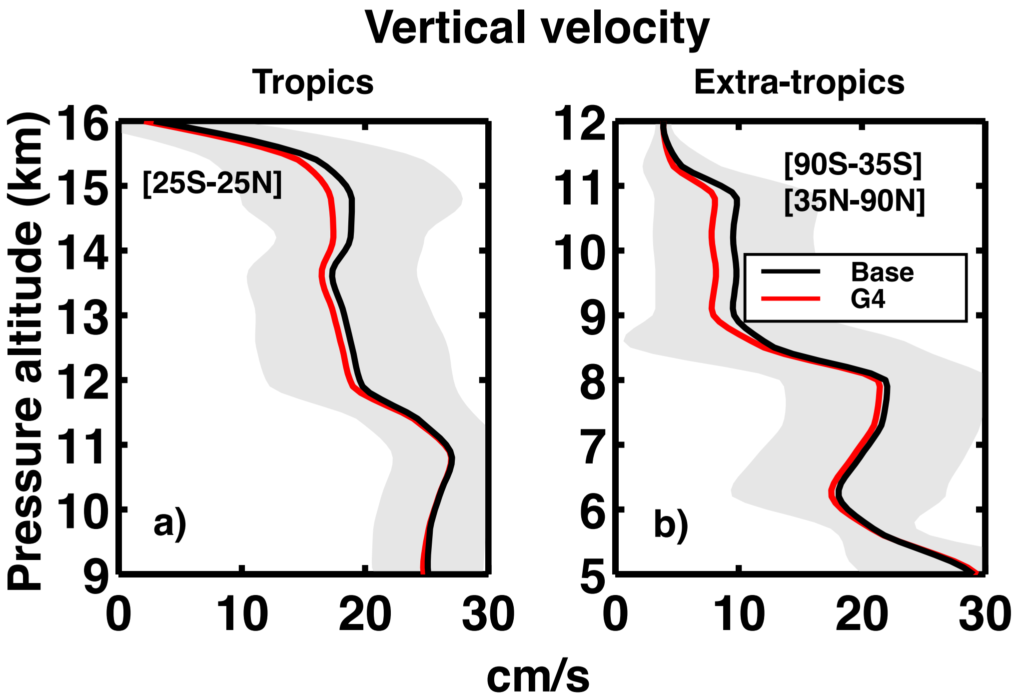

Figure 8. Average upper tropospheric profiles of the vertical velocity (cm/s) in G4 and Base experiments (years 2030-39). Panels (a) and (b) are for the tropics and extratropics, respectively (see legends). The vertical velocity w is obtained as the sum of the large-scale value and that calculated as a function of the TKE (see Lohmann and Karcher (2002) and Eq. 5), which essentially accounts for the synoptic scale and gravity wave motions. The shaded areas of the same color represent $\pm 1\sigma$ for the ensemble over the 10-year period 2030 to 39.

The SG induced reduction of updraft velocities is significantly smaller in the G4K case ($\simeq$0.5 cm/s, on the order of -3% the baseline values), as clearly visible in Fig. 7d. This will represent the major change in our approach to studying the UT ice sensitivity to SG with respect to the one adopted in Kuebbeler et al. (2012). According to our calculations, when taking into account both the main radiative effects of geoengineering stratospheric aerosols (i.e., lower stratospheric heating on one hand, surface and tropospheric cooling on the other hand), the resulting impact on tropospheric turbulence and updraft is significantly enhanced with respect to the case in which only the stratospheric warming is considered. A noticeable difference in the G4K w-anomalies with respect to those of G4 is at low altitudes over the polar regions, where the G4K negative values are larger than in G4. This may be largely explained by the increasing longitudinal variability of surface temperatures in the G4 case, mainly in the sub-Arctic region (see previous discussion relative to Fig. 5).

The tropical and extratropical average profiles of the updraft velocity are shown in Fig. 8 for both the Base and G4 conditions. The G4K curve (not shown) is intermediate between the previous two. The pronounced variability of the vertical velocity is expected as a consequence of time, latitude and longitude fluctuations of the TKE. This will produce a significant dispersion of the ice particle size distribution (see ahead in Section 3.2).

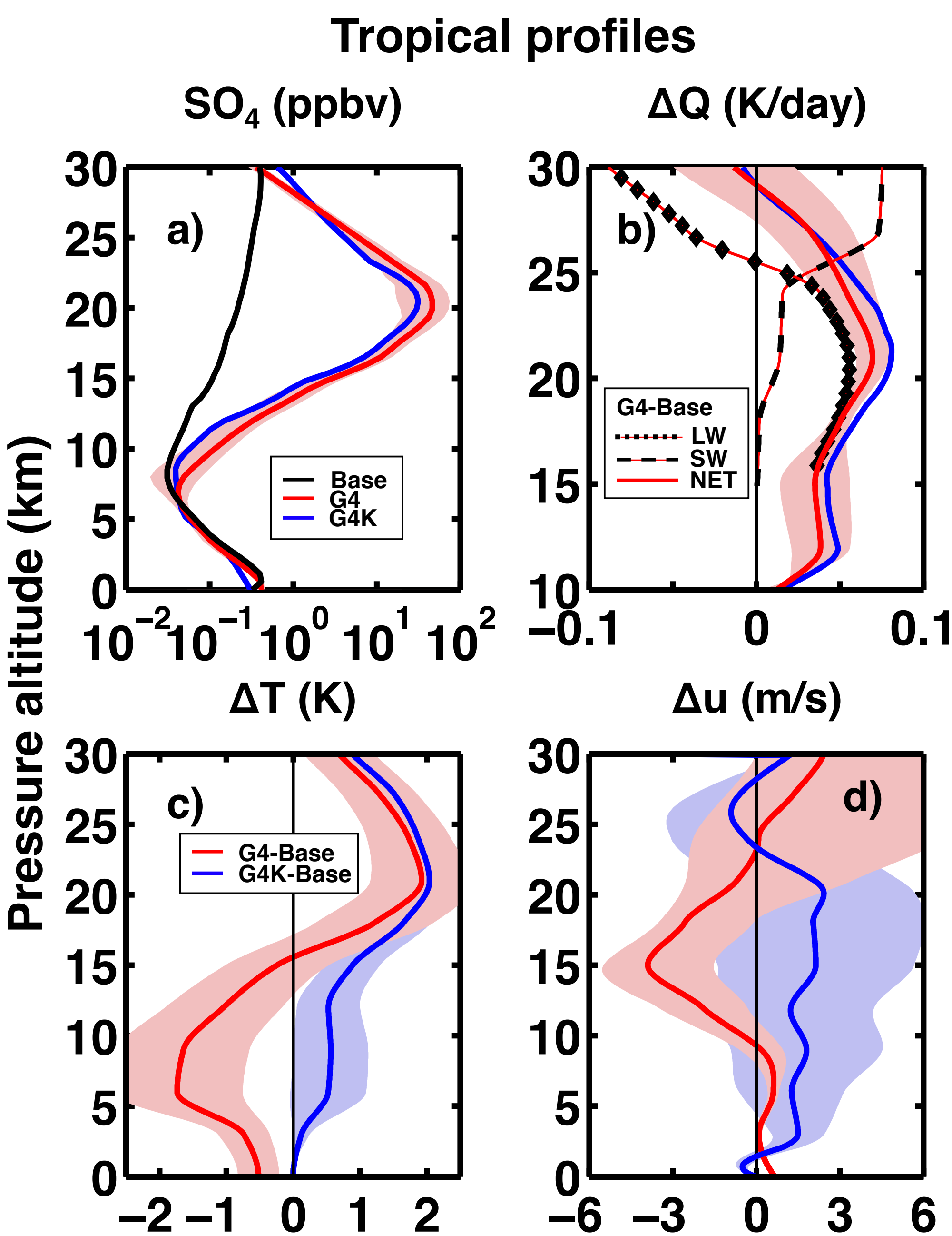

Figure 9. Average tropical vertical profiles (25S-25N, years 2030-39) of the SO_4 volume mixing ratio for G4, G4K and Base experiments (ppbv, panel a); G4-Base changes of net, shortwave and longwave heating rates (K/day, panel b) (LW is calculated with temperature fixed at Base values) (net heating rate changes are also shown for G4K-Base, with the blue line); G4-Base and G4K-Base temperature changes (K, panel c); G4-Base and G4K-Base changes of mean zonal winds (m/s, panel d). The shaded areas of the same colour represent $\pm 1\ \sigma$ for the ensemble over the 10-year period 2030 to 39.

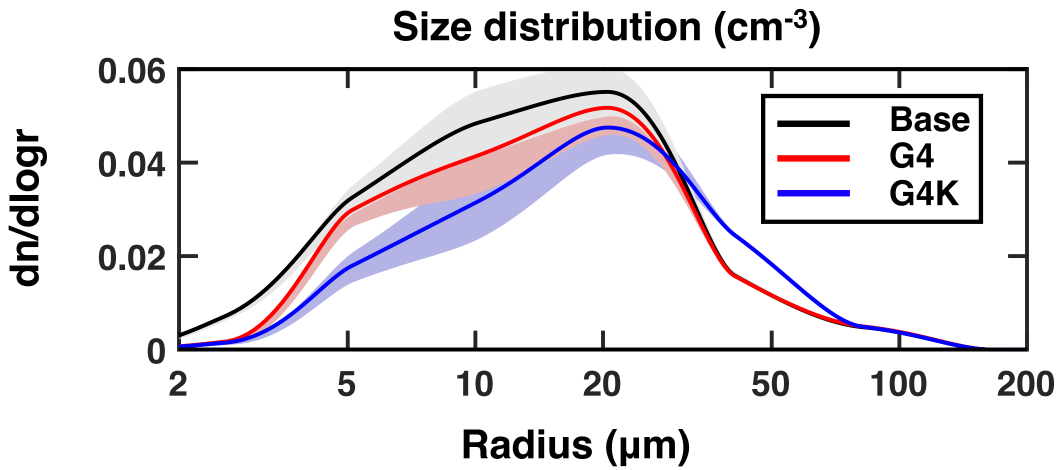

Figure 10. Globally and time-averaged number density values of ice crystals as a function of particle radius (dn/dlogr, cm^{-3}) (years 2030-39). Shaded areas of the same colour represent $\pm 1\ \sigma$ for the ensemble over the 10-year period 2030-39. The calculated global mean values of the ice particle effective radius are as follows: Base $\rightarrow$ 31.3$\pm$3.1 μm; G4 $\rightarrow$ 33.1$\pm$3.4 μm; G4K $\rightarrow$ 36.9$\pm$4.0 μm. The reference MODIS value in Table 2 is 33.4$\pm$2.1 μm.

3.2 Tropospheric ice perturbations due to sulfate geoengineering

In Section 2.2.2, we showed that the ULAQ-CCM parametrization for ice particle formation through ~~homogeneous~~ both homogeneous and heterogeneous freezing produces a spatial distribution of the UT ice particles reasonably comparable to available data ~~,~~ in terms of ice number concentration, OD, mass ~~fraction~~ mixing ratio and effective radius. We now move to analyse the ~~model calculated~~ model-calculated SG perturbation of some of these quantities ~~, by comparing~~ by comparing the G4 and G4K simulations against the Base case. As we have previously discussed and shown in Fig. ~~6~~7-~~8~~9, these perturbations are essentially produced and regulated by decreasing vertical velocities ~~,~~ (-1.7 cm/s and -0.8 cm/s, in the tropical region below the tropopause, for G4 and G4K, respectively) and by changing the tropospheric temperatures (-1.2 K and +0.5 K, in the tropical UT region, for G4 and G4K, respectively).

~~The model calculated globally and time averaged~~

The model-calculated globally and time-averaged size distribution of the ice particles is presented in Fig. ~~12~~ 10 for the three experiments, along with their globally averaged effective radius. A significant change in size distribution is highlighted in Fig. ~~12,~~ 10 in both SG experiments with respect to not only the Base case, but also ~~between~~ G4 and G4K. The common feature in both SG cases is the expected decreased particle population over the whole radial spectrum with respect to the Base experiment. This is due to the increased atmospheric stabilization forced by the SG aerosols ~~,~~ with reduced updraft velocities

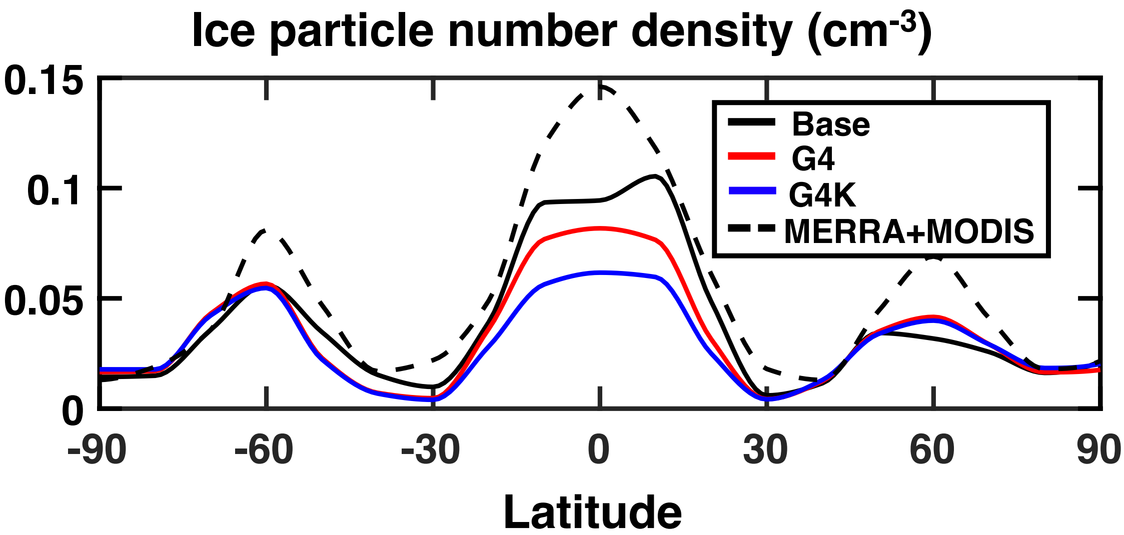

Figure 11. Zonally and time-averaged total number density values of ice crystals as a function of latitude (n, cm^{-3}) (years 2030-39), as calculated in the ULAQ-CCM (for Base, G4, G4K experiments) and compared with indirectly derived values from the MERRA ice mass fraction and MODIS effective radius (Eq. 4). Number densities are calculated at pressure layers 150-200 hPa for 25S-25N, 200-250 hPa for 25-35 (N/S), 250-300 hPa for 35-45 (N/S), 300-350 for 45-55 (N/S) and 350-400 for 55-90 (N/S).

and consequent decrease of the UT ice supersaturation probability.

The UT temperature anomalies, however, are very different in the two SG experiments with respect to the Base case (see Fig. 6). As a consequence of this, the tropospheric cooling produced in G4 by the surface temperature adjustment to the stratospheric aerosol negative RF ~~favors~~ favours a number density increase of ice particles with respect to the G4K experiment ~~, but~~ but is still less than in the Base case (see also Fig. ~~13~~11), due to the dominant impact of the reduced updraft. Cooler temperatures, in fact, cause a faster nucleation of the ice particles, quickly removing water ~~vapor~~ vapour available for the freezing itself ~~, thus~~ and limiting the condensational growth of ice particles (Kuebbeler et al. (2012); Visioni et al. (2017a)). At the same time, the velocity and temperature negative anomalies partially compensate each other also in the particle size spectrum, with a resulting effective radius in G4 larger with respect to the one in the unperturbed atmosphere (~~37.2~~33.1±~~4.0~~ 3.4 μm and ~~32.0~~31.3±~~3.6~~ 3.1 μm, respectively) ~~,~~ but smaller than that in G4K. In this latter case, the UT is slightly warmed up with respect to the Base case (see Fig. ~~6),~~ 7) so that both the velocity and temperature anomalies tend to increase the particle size (~~39.0~~36.9±~~4.2~~ 4.0 μm). Globally, the ULAQ-CCM baseline values of the effective radius fall well inside the MODIS range of variability (33.4±2.1 μm).

~~Globally and time averaged number density values of ice crystals as a function of particle radius (dn/dlogr, cm^{-3}) (years 2030-39). Shaded areas of the same color represent $\pm 1\ \sigma$ for the ensemble over the 10 year period 2030-39. Calculated global mean values of the ice particle effective radius are as follows: Base $\rightarrow$ 32.0$\pm$3.6 μm; G4 $\rightarrow$ 37.2$\pm$4.0 μm; G4K $\rightarrow$ 39.0$\pm$4.2 μm. The reference MODIS value in Table 2 is 33.4$\pm$2.1 μm.~~

~~Zonally and time averaged total number density values of ice crystals as a function of latitude (n, cm^{-3}) (years 2030-39), as calculated in the ULAQ-CCM (for Base, G4, G4K experiments) and compared with indirectly derived values from MERRA ice mass fraction and MODIS effective radius (Eq. 4). Number densities are calculated at pressure layers 150-200 hPa for 25S-25N, 200-250 hPa for 25-35 (N/S), 250-300 hPa for 35-45 (N/S), 300-350 for 45-55 (N/S) and 350-400 for 55-90 (N/S).~~

As visible in Fig. ~~13~~ 11 the calculated ice number densities follow the zonal mean ~~behavior~~ behaviour of the MERRA+MODIS indirectly derived values, with the ~~already~~ previously discussed underestimation tendency, mainly in the tropical region (see Fig. ~~11~~4).

3.2.1 Optical depth

3.3 ~~Optical depth~~

~~Ice extinction anomalies~~ The ice extinction anomalies of G4-Base that are calculated in the ULAQ-CCM are negative in the whole UT (Fig. ~~14ab) ,~~ 12ab) due to the decreasing number density of the particles ~~,~~ caused by the reduced vertical velocities in the SG dynamical conditions (see Fig. ~~6-7~~7-8). Although the UT cooling in G4 tends to partially offset the effects of the updraft decrease on the ice particle number density, the overall impact is of a general decrease of the UT ice extinction ~~,~~ and is even more pronounced than in G4K where the tropospheric cooling is not taken into account. In the latter case, however, the particle effective radius is larger than in G4, as discussed above for Fig. ~~12~~10. These size distribution changes ~~not only affect~~ affect not only ice extinction, but also the shortwave and longwave radiative responses per unit optical depth (see ahead Section 3.2.2).

Following the procedure described in Section 2.2 (see Eq. 3), an evaluation of the model calculated ice extinction profiles is attempted (Fig. ~~14~~12cd). This is made using indirectly derived values from the MERRA ice mass ~~fraction and~~ mixing ratio and the MODIS effective radii, as in Eq. 6 below. Here, $\chi_{ext,i}$ is the ice extinction at the i-th vertical layer and $\rho_{atm,i}$ is the atmospheric mass density at the same vertical layer:

$$\chi_{ext,i} = Q_{ext} \frac{3}{2} \frac{\rho_{atm,i}}{\rho_{ice}} \frac{\chi_i}{r} \qquad (6)$$

The ULAQ-CCM tropical underestimation of the ice extinction below 13 km is consistent with that of the ice number density and is partly justified by the specific assumptions made on cirrus cloud formation in the model, as pointed out in the discussion of Fig. ~~11~~4.

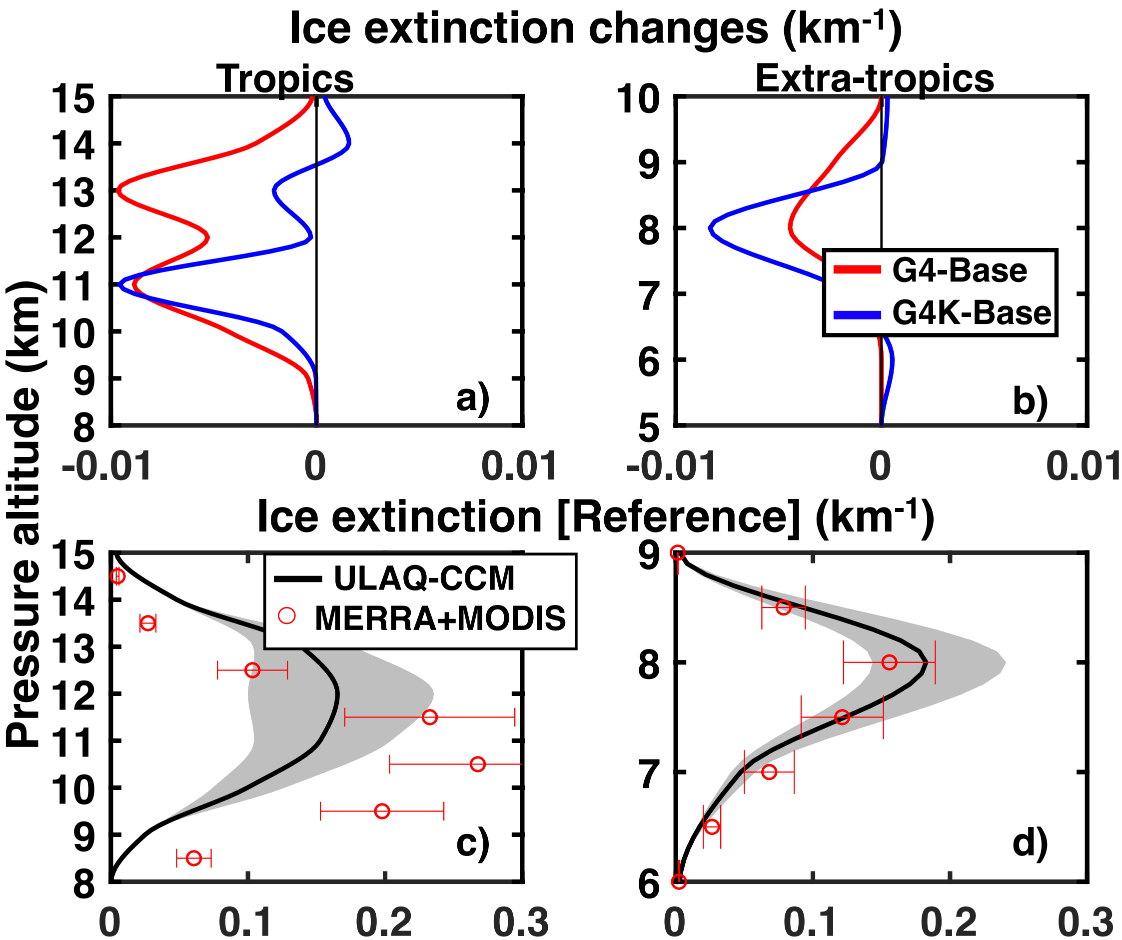

Figure 12. Average upper tropospheric profiles of ice particle extinction (λ=0.55 μm) (km-1) ~~,~~ for the tropics (25S-25N) and extratropics (35S-90S, 35N-90N) ~~,~~ in panels (a,c) and (b,d), respectively. Panels (a,b): ice extinction changes for G4-Base (red curves) and G4K-Base (blue curves) (years 2030-39). Panels (c,d): comparison of ULAQ-CCM calculated values of ice extinction with indirectly derived values from the MERRA ice mass ~~fraction~~ mixing ratio and MODIS effective radius (red circles) (see text). ~~Time~~ The time average is ~~on~~ over the years 2003-2012. ~~Shaded~~ The shaded areas represent ±1 σ for the ensemble over the ~~10 year~~ 10-year period.

The net result on the ice optical depth (i.e., the vertical integral of ice extinction) is shown in Fig. ~~15~~13. In general, a latitude-dependent OD reduction comparable to that found in Kuebbeler et al. (2012) is present in G4K, while in the G4 case (as expected from the extinction anomalies) a further decrease is calculated mainly in the tropics, even though ~~tropospheric~~ the UT temperatures are cooler. The effects regarding the temperature and updraft cannot be easily separated, but the colder tropospheric temperatures in G4 with respect to G4K reduce the particle size increase respect to the Base case, producing an additional decrease in the optical depth. The coupled effects of the velocity and temperature anomalies on the ice particle

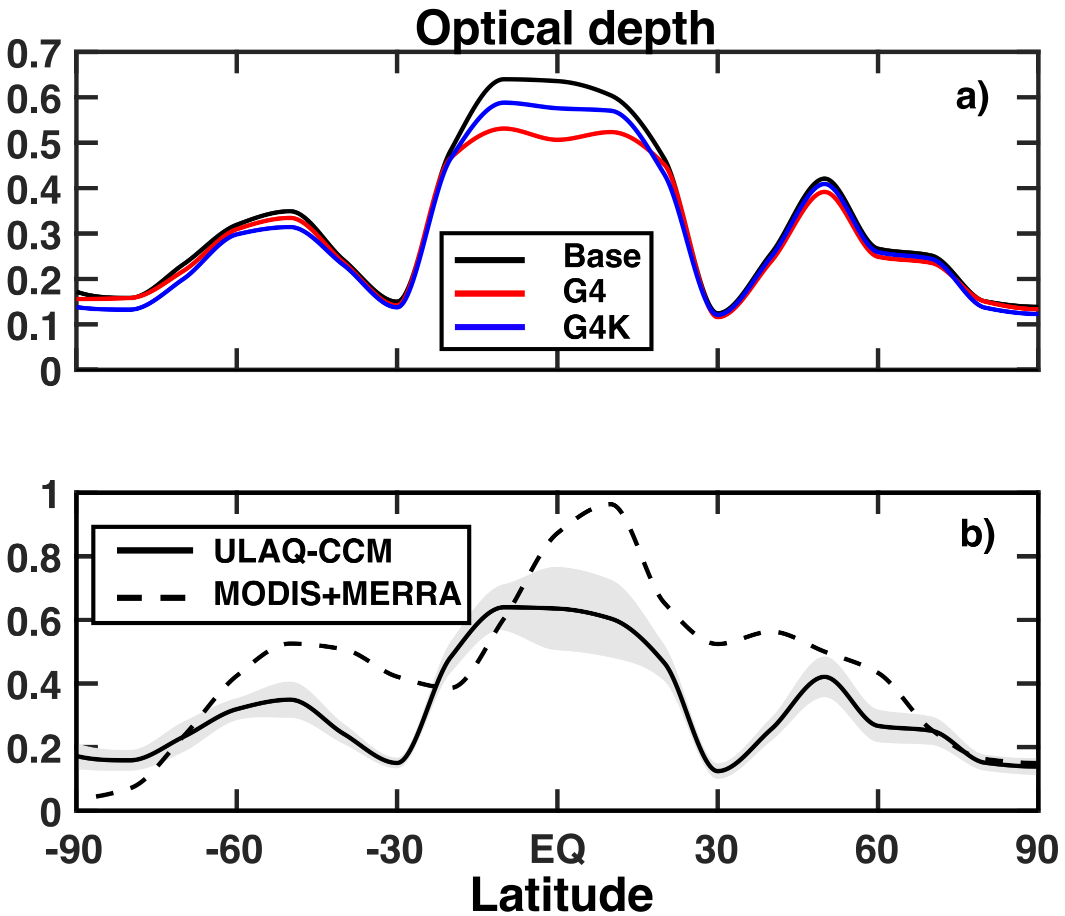

Figure 13. Zonally and ~~time averaged~~ time-averaged values of the ice optical depth (λ=0.55 μm) for the ULAQ-CCM Base, G4 and G4K experiments (solid black, red and blue lines, respectively) (panel a) and Base case comparison with the MERRA+MODIS indirectly derived values (dashed black line) (panel b). ~~Model~~ The model results are for years 2030-39; the MERRA+MODIS data are for years 2003-12. The shaded area represents $\pm 1\ \sigma$ for the ensemble over the ~~10 year~~ 10-year period 2030-39.

number density and size produce the most relevant impact in our study, pointing out ~~to~~ the importance of allowing surface temperatures to respond to the stratospheric aerosol radiative forcing.

3.3 ~~Radiative forcing~~

3.2.1 Consequences on radiative forcing

The ~~well tested~~ well-tested radiative transfer code on-line in the ULAQ-CCM (Chou (2001); Randles et al. (2013); SPARC (2013)) ~~,~~ has been used to calculate the shortwave and longwave components of the tropopause radiative forcing due to SG aerosols (direct forcing) and to UT ice changes (indirect forcing). As discussed so far, the latter are largely produced by the SG-driven dynamical perturbations on the homogeneous freezing process for ice formation~~(indirect forcing) in Table 3. Results~~. The ice radiative effects have been calculated using up-to-date wavelength-dependent refractive index available in the literature (Warren (1984); Warren and Brandt (2008); Curtis et al. (2005)) and compared against previous results under similar conditions, such as those by Schumann et al. (2012).

The results are shown separately for the G4 and G4K experiments, both with respect to the RCP4.5 Base case. Following the ~~above~~ previously discussed thinning of the UT ice clouds, a positive SW RF is calculated ~~,~~ because of the decreased scattering of the incoming solar radiation by the ice particles. However, such an effect is largely covered by the negative LW RF due to a lessened capacity of the ice particles to trap outgoing planetary radiation~~, therefore~~; therefore, the obtained net effect on RF is negative, as shown in Table 3. This indirect negative RF is smaller but ~~of the same order of magnitude of the negative direct~~ still significant when compared to the negative direct net RF due to the ~~increased solar radiation scattering by SG aerosols~~ SG aerosols (∼30% of it).

It is interesting to note that the shortwave component of the ice RF is indeed smaller than the longwave component, ~~but~~ however, not as much as one could expect from the very different normalized RFs (i.e., forcing per unit OD) at a given particle radius. The reason is that both the SW and LW normalized RFs are decreasing with the increasing particle radius, but the relative changes of these normalized RF components are significantly different between the SW and LW. According to our radiative calculations, the SW normalized values decrease (in magnitude) from -12.1 W/m^2 to -5.7 W/m^2 (-53%) with the ice effective radius increasing from 15 μm to 40 μm, whereas the LW normalized RF values remain quasi-constant on average value +53 W/m^2, with a smooth 3% decrease over the same radius interval. The resulting SW RF is then controlled not only by the negative OD changes (~~-0.030~~ -0.020 in G4 and ~~-0.020~~ -0.012 G4K) ~~,~~ but also by the magnitude of the particle radius increase, which is larger in G4K than in G4, both with respect to the Base case (see ~~above~~ discussion of Fig. ~~12~~10).

Table 3. Top three rows: globally and ~~time averaged~~ time-averaged values of the upper tropospheric ice optical depth changes and RF differences (W/m^2) between the SG perturbed experiments and the RCP4.5 Base case ~~,~~ due to changes in ice crystal concentration and size. Middle three rows: globally averaged values of stratospheric sulfate aerosol optical depth changes and RF differences (W/m^2) defined as above ~~,~~ due to changes in aerosol concentration and size. Bottom three rows: total OD and RF changes (i.e., ice + sulfate). All results are for all-sky conditions (i.e., including the presence of background cloudiness) and with an 8 Tg-SO_2/yr injection. The RFs are calculated at the tropopause with adjustment of stratospheric temperatures. ~~Time~~ The time average is ~~on~~ over the years 2030-39.

Exp [all sky]	**Ice OD change**	**RF SW**	**RF LW**	**RF Net**
G4-Base	~~-0.030~~ -0.020	+~~0.75~~ 0.46	~~-1.71~~ -0.83	~~-0.96~~ -0.37
G4K-Base	~~-0.020~~ -0.012	+~~0.81~~ 0.35	~~-1.02~~ -0.53	~~-0.21~~ -0.18
Exp [all sky]	**SO_4 OD change**	**RF SW**	**RF LW**	**RF Net**
G4-Base	+0.079	-2.03	+0.86	-1.17
G4K-Base	+0.083	-2.14	+0.90	-1.24
Exp [all sky]	**Total OD change**	**RF SW**	**RF LW**	**RF Net**
G4-Base	~~-0.030~~ -0.020+0.079	~~-1.28~~ -1.57	~~-0.85~~ +0.03	~~-2.13~~ -1.54
G4K-Base	~~-0.020~~ -0.012+0.083	~~-1.33~~ -1.79	~~-0.12~~ +0.37	~~-1.45~~ -1.42

Table 4. Rearrangement of the results presented in Table 3, with the calculated cloud adjustments (bottom three rows) in clear-sky RF components (top three rows). ~~Cloud~~ The cloud adjustments for the SW and LW RF contributions are shown separately for the mere presence of background atmospheric clouds (left) and for the cirrus thinning (right): the former is calculated as the difference between the all-sky and clear-sky aerosol RFs, with the all-sky including the background warm clouds and fixed UT ice clouds.

Exp [clear sky]	**RF SW**		**RF LW**		**RF Net**
G4-Base	-3.13		+1.07		-2.06
G4K-Base	-3.30		+1.14		-2.16
Cloud adjustment	**RF SW**		**RF LW**		**RF Net**
G4-Base	+1.10	+~~0.75~~ 0.46	-0.21	~~-1.71~~ -0.83	+0.52
G4K-Base	+1.16	+~~0.81~~ 0.35	-0.24	~~-1.02~~ -0.53	+0.74

Table 4 presents, in a compact form, the globally and time averaged ULAQ-CCM results for the cloud adjustments of clear-sky RF components due to the SG stratospheric aerosols. The SW and LW cloud adjustments are roughly comparable to the ones calculated in Kuebbeler et al. (2012) (+1.11 W/m^2 and -0.51 W/m^2, respectively, calculated at the top of atmosphere for ~~a~~ an SG experiment with a 5 Tg-SO_2/yr injection). These numbers could be ~~directly~~ compared with those obtained in the ULAQ-CCM G4K case ~~, if a 5/~~(although for an 8 ~~sealing of the total RF results is made (as a rough first approximation). Following this procedure, we obtain SW and LW cloud adjustments of~~ Tg-SO2/yr injection), i.e., +~~1.23~~ 1.51 W/m^2 and ~~-0.79~~ -0.77 W/m^2 for SW and LW, respectively, ~~for the 'sealed G4K experiment',~~ with a net value of +~~0.44~~ 0.52 W/m^2 ~~,~~ against

+0.60 W/m^2 in Kuebbeler et al. (2012).

In the (more realistic) G4 simulation performed by the ULAQ-CCM model, the SW cloud adjustment is only ~~a bit~~ slightly smaller than in the G4K, while a ~~much~~ significantly larger negative LW component is calculated. This ends up in a net adjustment of ~~-0.07~~ +0.52 W/m^2 in the G4 against +~~0.71~~ 0.72 W/m^2 in the G4K experiment. A latitude-dependent view of these results is presented in Fig. 16. The black solid line shows the net positive adjustment (SW+LW) due to the mere presence of background clouds, whose increased reflectivity enhances the downward scattered solar radiation by the stratospheric aerosol layer. According to our model calculations, the negative LW is the dominant component of the cloud adjustment due to cirrus ice thinning, and this is particularly true for the more realistic G4 simulation. In this latter case, significantly larger values of the LW adjustment are found over the tropics with respect to G4K, ~~consistently~~ consistent with the ice extinction profile changes in Fig. ~~14~~12a.

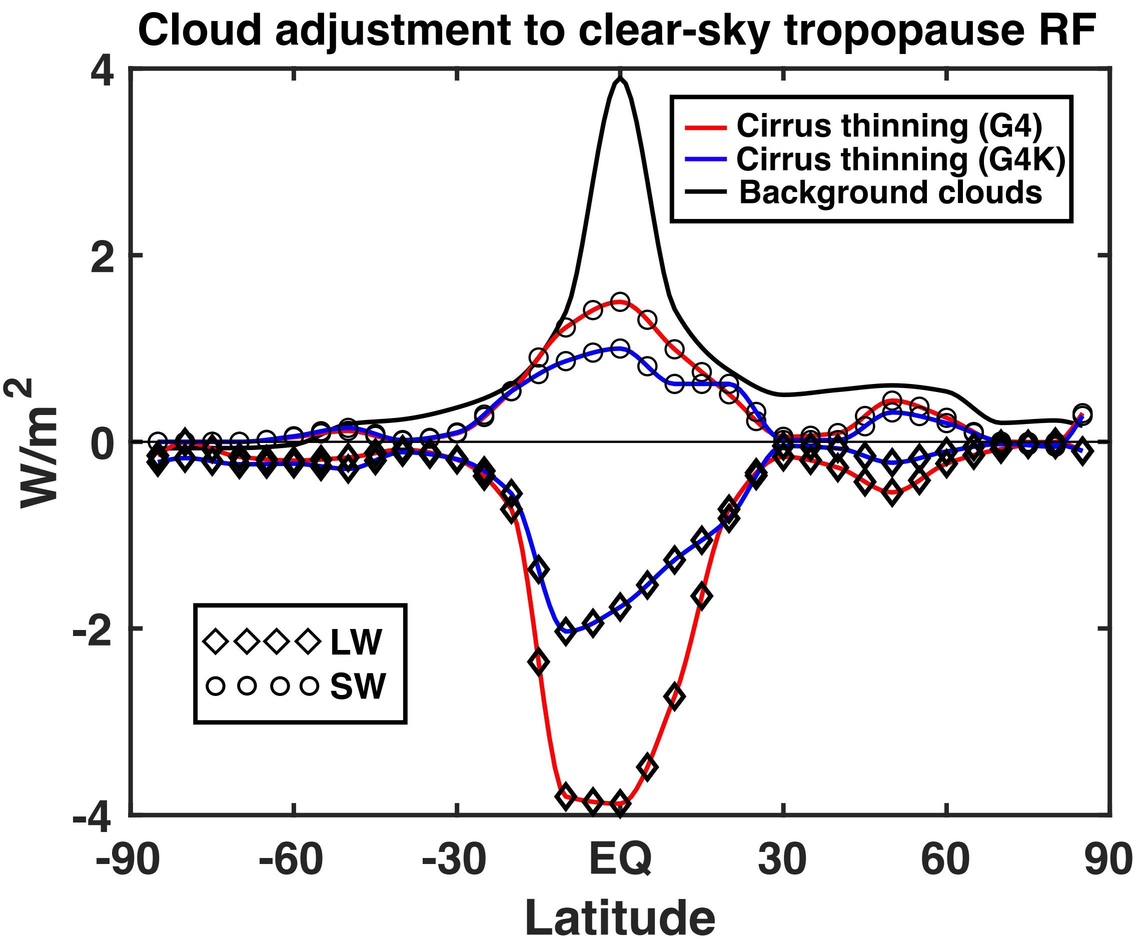

Figure 14. Cloud adjustments in the clear-sky SG aerosol RF (W/m^2). See legends for line meaning. The positive adjustment due to (passive) background clouds (black solid line) shows the net value (SW+LW), which is, however, largely controlled by the SW contribution (see Table 4).

4 Conclusions

Sulfate geoengineering is considered, amongst other solar radiation management (SRM) techniques, one of the most promising. One reason for this (and unlike other methods) is that we have a natural proxy for the stratospheric sulfate injection, i.e., past explosive volcanic eruptions in the tropical belt. This does not mean that SG does not still pose some scientific questions that need to be answered thoroughly, as pointed out by MacMartin et al. (2016). For instance, models still show many significant differences regarding the confinement of stratospheric sulfate aerosols in the tropical pipe Pitari et al. (2014).

In recent years, some experiments have been proposed where SG is used to meet different climate targets (MacMartin et al. (2017); Kravitz et al. (2017)). However, to properly do so, a clear understanding is needed of how multiple side effects of this technique can modify the net RF (Visioni et al., 2017a). While some of these effects produce a negligible difference in forcing, such as those from gas species perturbations (CH_4, O_3, stratospheric H_2O) (Visioni et al. (2017b)), this might not be the case for changes produced in the formation of thin cirrus ice clouds.

This latter indirect effect was already ~~analyzed~~ analysed in two previous works~~:~~. Cirisan et al. (2013) looked at the potential impact of IN changes in the UT, finding a negligible positive TOA forcing (+0.02 W/m^2, up to 0.04 W/m^2) due to the number density increase of H_2SO_4-H_2O aerosols transported down in the UT from the lower stratosphere. Kuebbeler et al. (2012), on the other hand, have studied the effects of dynamical changes caused by the ~~aerosol induced~~ aerosol-induced stratospheric warming and their consequences on UT ice formation via homogeneous freezing.They found a considerable negative TOA forcing in the longwave spectrum (-0.51 W/m^2), greatly attributable to the SG-induced ice optical depth reduction. In the present study, we focused on these same indirect dynamical effects, adding the potential impact of the SG ~~aerosol induced~~ aerosol-induced surface cooling (G4 experiment), which was not explicitly considered in the study of Kuebbeler et al. (2012). Their approach was also included for comparison in our study, by means of a sensitivity study (G4K) conducted with the ULAQ-CCM, where we keep the surface temperature fixed at the RCP4.5 baseline values ~~,~~ so that we ~~could~~ can quantify more precisely the surface cooling impact on the UT thin cirrus clouds.

A compact view of the ~~surface cooling~~ SG effects on UT ice formation ~~was~~ is presented in Fig. ~~2~~15. On one hand, the ~~aerosol induced~~ aerosol-induced stratospheric warming and surface cooling combined together ~~,~~ produce a further atmospheric stabilization with an even larger reduction in tropospheric updraft with respect to the G4K case. This lowers the UT probability for ice supersaturation and thus less ~~favorable~~ favourable conditions for homogeneous freezing. On the other hand, this ice formation limiting effect is partially counterbalanced by the ~~convectively-driven~~ convectively driven tropospheric cooling, which is not observed in the G4K case.

The resulting changes in ice particle number density and size distribution, when combined, translate into a globally averaged decrease of the ice optical depth ($\Delta\tau$=~~-0.030~~-0.020, at λ=0.55 μm), i.e., ~~-7.5~~-5.2% of the baseline OD. This reduction is larger than the one in G4K relative to the Base case ($\Delta\tau$=~~-0.020, -5~~-0.012, -3.1%), pointing ~~out~~ to the dominant and controlling role of the reduced updraft velocities. According to our model results, these OD changes (coupled to increases in ice particle

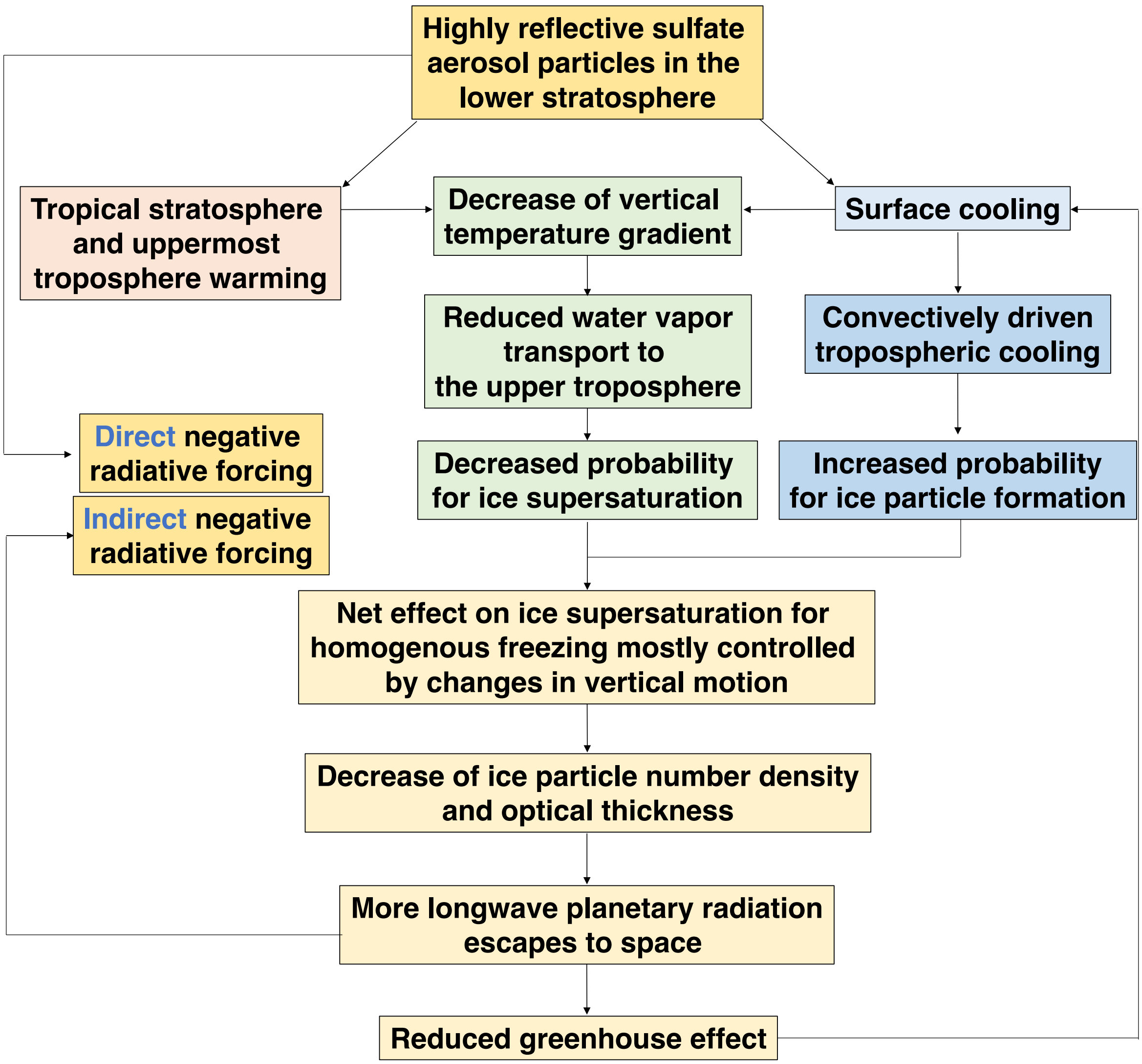

Figure 15. Schematic summary of the sulfate geoengineering impact on the dynamical processes driving changes of upper tropospheric ice particle formation through homogeneous freezing.

effective radii) translate in net tropopause RFs of ~~-0.96~~ -0.37 W/m^2 and ~~-0.21~~ -0.18 W/m^2, for G4 and G4K experiments, respectively, produced only by the cirrus ice thinning effect of SG. These two cloud adjustments result from a combination of the SW and LW RF contributions, ~~that~~ which account for +~~0.75~~ 0.46 W/m^2 and +~~0.81~~ 0.35 W/m^2 in the SW (for G4 and G4K, respectively) and ~~-1.71~~ -0.83 W/m^2 and ~~-1.02~~ -0.53 W/m^2 in the LW (again for G4 and G4K).

We can compare these ice thinning forcing contributions with the net tropopause all-sky RF produced by the stratospheric SG aerosols, i.e., of -1.17 W/m^2 and -1.24 W/m^2, for the G4 and G4K experiments, respectively~~: according~~. According to our model, the net negative RF due to the cirrus ice cloud thinning ~~,~~ is (in G4) ~~of the same order of magnitude of the~~ close to 30% of the direct effect of the sulfate particles themselves. This might have consequences in the definition of the sulfate injection efficiency in terms of RF per Tg-S/yr injected, especially if such efficiency is used to determine the amount of SO_2 that needs to be injected ~~in~~ into the stratosphere to achieve climate targets (MacMartin et al. (2017); Kravitz et al. (2017)).

Fig. 16 summarizes, in a schematic way, the thermo-dynamical processes leading to the changes in cirrus ice formation and the radiative response caused by these changes in the Earth?s radiative balance, as analysed in detail in this paper, together with the direct radiative effect of the sulfate particles.

Furthermore, one last consideration is necessary regarding ~~RFs in~~ the RFs in the SG scenarios and the unperturbed atmosphere~~;~~, more specifically, regarding the cloud adjustment to clear-sky RFs due to the stratospheric sulfate aerosols. In our fully interactive aerosol simulation (G4), we obtain a total cloud adjustment (from both cirrus ice thinning and passive background clouds) ~~close to zero (-0.07~~ of +0.52 W/m^2 ~~),~~ due to compensating large adjustments in the LW and SW. The SW adjustment results in part from the mere presence of (passive) background clouds and in part from the changing size distribution of UT ice particles. The increasing particle size is more pronounced in the partially interactive aerosol simulation (G4K), thus producing a larger positive SW contribution ~~, with a consequent net positive cloud adjustment~~ (+~~0.71~~ 0.74 W/m^2).
This latter value is ~~fully comparable to the one~~ comparable to that calculated in the similar experiment of Kuebbeler et al. (2012) (+0.60 W/m^2, with a 5 Tg-SO_2 injection). It means that the lower stratospheric warming produced by the SG aerosols acts indirectly on atmospheric dynamics with a strong feedback on the UT cirrus clouds ~~,~~ so that a simple reduction of the incoming solar radiation is not a good proxy for the eventual injection of sulfate particles ~~in~~ into the stratosphere. When the ~~aerosol induced~~ aerosol-induced surface cooling is coupled to the lower stratospheric warming, the net cloud adjustment is significantly reduced; however, the clear-sky balance of the SW and LW RF contributions is greatly altered by the presence of background clouds coupled to the UT ice thinning.

One important caveat to the conclusions of this study, is that the physical processes behind the UT ice particle formation are highly idealized in our parameterization. Nonetheless, the results it produces in the reference (historical) simulation are generally comparable with the MERRA reanalysis and some satellite data. In addition, the calculated SG dynamical anomalies in the stratosphere are consistent with those from other ~~modeling~~ modelling studies (Pitari et al. (2014); Niemeier and Schmidt (2017)). Finally, taking into account the consistency with the findings from the study of Kuebbeler et al. (2012), we may reasonably conclude that our results regarding the thinning of the UT ice clouds under SG conditions are sufficiently robust. However, considering how complex is the balance between the UT ice formation changes and their radiative forcing is (Sanderson et al. (2008); Mitchell et al. (2008)), the results in the present cannot be considered conclusive and exhaustive. Additional results using different and more complete physical parametrizations (both regarding the ice formation processes

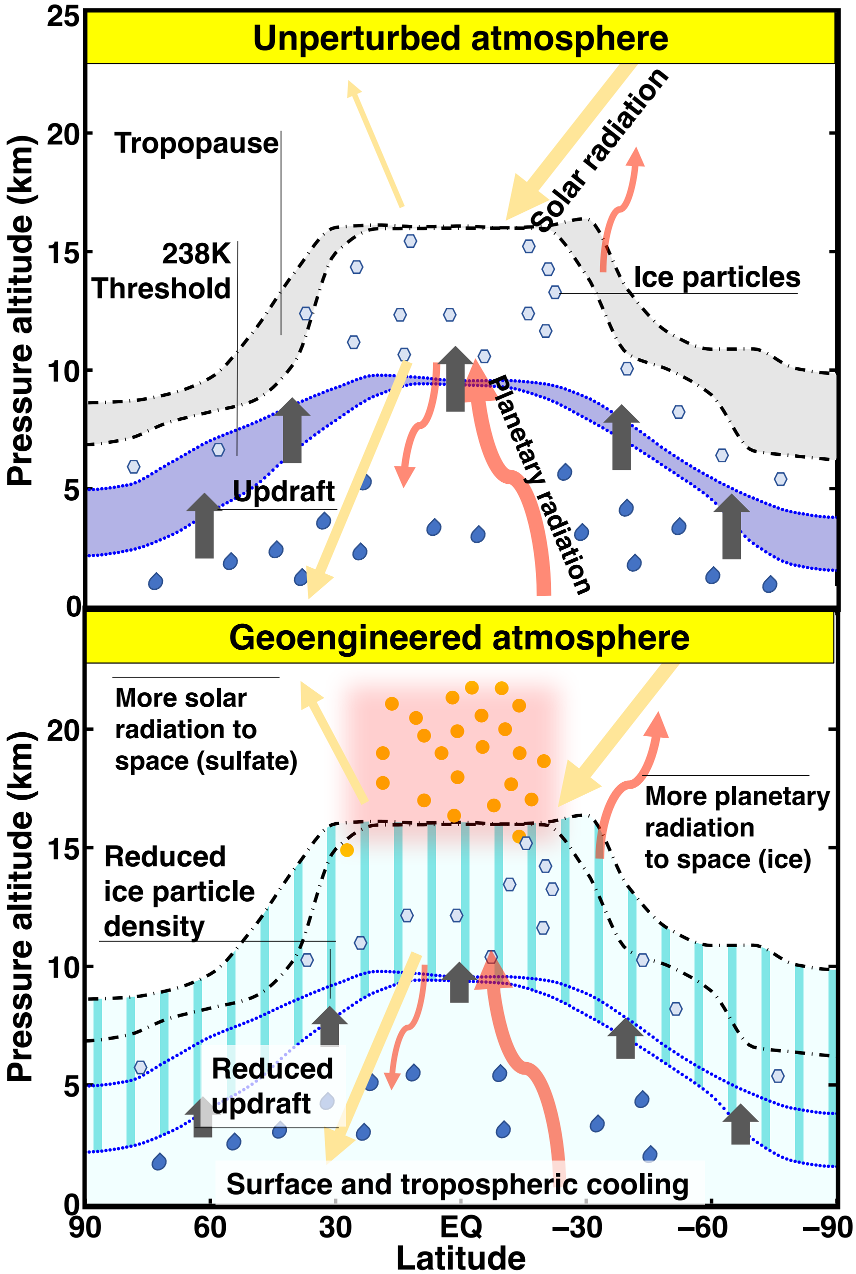

Figure 16. Cartoon of the sulfate geoengineering impact on cirrus ice particles formed through freezing and schematic representation of ice-induced changes in radiative fluxes.

and a wider range of updraft velocities), together with an on-line ocean coupling, may help clarify the net contribution of ice clouds in a sulfate geoengineering scenario.

Acknowledgements. Some of the analyses and visualizations used in this study were produced with the Giovanni online data system, developed and maintained by the NASA GES DISC. We also acknowledge the MODIS mission scientists and associated NASA personnel for the production of the data used in this research effort. ~~We thank Simone Tilmes (NCAR) for providing surface temperature data from the atmosphere-ocean coupled model CCSM-CAM4, to be used in the ULAQ-CCM numerical simulations.~~ One of the authors (GP) would like to thank Bernd Karcher for helpful discussions on the physical processes behind aerosol-ice interactions and for providing the heterogeneous freezing numerical code used in the ULAQ-CCM. Finally, the authors are indebted with two anonymous reviewers for their helpful suggestions that improved this study in a significant way.

References

Aquila, V., Garfinkel, C., Newman, P., Oman, L., and Waugh, D.: Modifications of the quasi-biennial oscillation by a geoengineering perturbation of the stratospheric aerosol layer, Geophysical Research Letters, 41, 1738–1744, 2014.

Bosilovich, M. G., Robertson, F. R., Takacs, L., Molod, A., and Mocko, D.: Atmospheric Water Balance and Variability in the MERRA-2 Reanalysis, Journal of Climate, 30, 1177–1196, doi:10.1175/JCLI-D-16-0338.1, https://doi.org/10.1175/JCLI-D-16-0338.1, 2017.

Budyko, M. I.: The Climate of the Future, American Geophysical Union, doi:10.1002/9781118665251.ch7, http://dx.doi.org/10.1002/9781118665251.ch7, 1974.

Canty, T., Mascioli, N. R., Smarte, M. D., and Salawitch, R. J.: An empirical model of global climate - Part 1: A critical evaluation of volcanic cooling, Atmospheric Chemistry and Physics, 13, 3997–4031, doi:10.5194/acp-13-3997-2013, http://www.atmos-chem-phys.net/13/3997/2013/, 2013.

Chen, T., Zhang, Y., and Rossow, W. B.: Sensitivity of Atmospheric Radiative Heating Rate Profiles to Variations of Cloud Layer Overlap, Journal of Climate, 13, 2941–2959, doi:10.1175/1520-0442(2000)013<2941:SOARHR>2.0.CO;2, https://doi.org/10.1175/1520-0442(2000)013<2941:SOARHR>2.0.CO;2, 2000.

Chipperfield, M. P., Liang, Q., Strahan, S. E., Morgenstern, O., Dhomse, S. S., Abraham, N. L., Archibald, A. T., Bekki, S., Braesicke, P., Di Genova, G., Fleming, E. L., Hardiman, S. C., Iachetti, D., Jackman, C. H., Kinnison, D. E., Marchand, M., Pitari, G., Pyle, J. A., Rozanov, E., Stenke, A., and Tummon, F.: Multimodel estimates of atmospheric lifetimes of long-lived ozone-depleting substances: Present and future, Journal of Geophysical Research: Atmospheres, 119, 2555–2573, doi:10.1002/2013JD021097, http://dx.doi.org/10.1002/2013JD021097, 2014.

Chou, M. M. J. S. X. L.: A thermal infrared radiation parameterization for atmospheric studies, Tech. Rep. TM-2001-104606, NASA, NASA Goddard Space Flight Cent., Greenbelt, MD, 2001.

Cirisan, A., Spichtinger, P., Luo, B. P., Weisenstein, D. K., Wernli, H., Lohmann, U., and Peter, T.: Microphysical and radiative changes in cirrus clouds by geoengineering the stratosphere, Journal of Geophysical Research: Atmospheres, 118, 4533–4548, doi:10.1002/jgrd.50388, http://dx.doi.org/10.1002/jgrd.50388, 2013.

Clegg, S. M. and Abbatt, J. P. D.: Oxidation of SO_2 by H_2O_2 on ice surfaces at 228 K: a sink for SO_2 in ice clouds, Atmospheric Chemistry and Physics, 1, 73–78, doi:10.5194/acp-1-73-2001, https://www.atmos-chem-phys.net/1/73/2001/, 2001.

Crutzen, P. J.: Albedo Enhancement by Stratospheric Sulfur Injections: A Contribution to Resolve a Policy Dilemma?, Climatic Change, 77, 211–220, doi:10.1007/s10584-006-9101-y, http://dx.doi.org/10.1007/s10584-006-9101-y, 2006.

Curtis, D. B., Rajaram, B., Toon, O. B., and Tolbert, M. A.: Measurement of the temperature-dependent optical constants of water ice in the 15–200 µm range, Appl. Opt., 44, 4102–4118, doi:10.1364/AO.44.004102, http://ao.osa.org/abstract.cfm?URI=ao-44-19-4102, 2005.

Cziczo, D. J., Froyd, K. D., Gallavardin, S. J., Moehler, O., Benz, S., Saathoff, H., and Murphy, D. M.: Deactivation of ice nuclei due to atmospherically relevant surface coatings, Environmental Research Letters, 4, 044 013, http://stacks.iop.org/1748-9326/4/i=4/a=044013, 2009.

Cziczo, D. J., Froyd, K. D., Hoose, C., Jensen, E. J., Diao, M., Zondlo, M. A., Smith, J. B., Twohy, C. H., and Murphy, D. M.: Clarifying the Dominant Sources and Mechanisms of Cirrus Cloud Formation, Science, 340, 1320–1324, doi:10.1126/science.1234145, http://science.sciencemag.org/content/340/6138/1320, 2013.

Duncan, D. I. and Eriksson, P.: An update on global atmospheric ice estimates from satellite observations and reanalyses, Atmospheric Chemistry and Physics Discussions, 2018, 1–20, doi:10.5194/acp-2018-275, https://www.atmos-chem-phys-discuss.net/acp-2018-275/, 2018.

Eyring, V., Butchart, N., Waugh, D. W., Akiyoshi, H., Austin, J., Bekki, S., Bodeker, G. E., Boville, B. A., Bruhl, C., Chipperfield, M. P., Cordero, E., Dameris, M., Deushi, M., Fioletov, V. E., Frith, S. M., Garcia, R. R., Gettelman, A., Giorgetta, M. A., Grewe, V., Jourdain, L., Kinnison, D. E., Mancini, E., Manzini, E., Marchand, M., Marsh, D. R., Nagashima, T., Newman, P. A., Nielsen, J. E., Pawson, S., Pitari, G., Plummer, D. A., Rozanov, E., Schraner, M., Shepherd, T. G., Shibata, K., Stolarski, R. S., Struthers, H., Tian, W., and Yoshiki, M.: Assessment of temperature, trace species, and ozone in chemistry-climate model simulations of the recent past, Journal of Geophysical Research: Atmospheres, 111, n/a–n/a, doi:10.1029/2006JD007327, d22308, 2006.

Feichter, J., Kjellstram, E., Rodhe, H., Dentener, F., Lelieveldi, J., and Roelofs, G.-J.: Simulation of the tropospheric sulfur cycle in a global climate model, Atmospheric Environment, 30, 1693 – 1707, doi:https://doi.org/10.1016/1352-2310(95)00394-0, http://www.sciencedirect.com/science/article/pii/1352231095003940, joint 8th CAGCP and 2nd IGAC Conference on Global Atmospheric Chemistry, 1996.

Friberg, J., Martinsson, B. G., Sporre, M. K., Andersson, S. M., Brenninkmeijer, C. A. M., Hermann, M., Velthoven, P. F. J., and Zahn, A.: Influence of volcanic eruptions on midlatitude upper tropospheric aerosol and consequences for cirrus clouds, Earth and Space Science, 2, 285–300, doi:10.1002/2015EA000110, https://agupubs.onlinelibrary.wiley.com/doi/abs/10.1002/2015EA000110, 2005.

Fusina, F., Spichtinger, P., and Lohmann, U.: Impact of ice supersaturated regions and thin cirrus on radiation in the midlatitudes, Journal of Geophysical Research: Atmospheres, 112, n/a–n/a, doi:10.1029/2007JD008449, http://dx.doi.org/10.1029/2007JD008449, d24S14, 2007.

Gasparini, B. and Lohmann, U.: Why cirrus cloud seeding cannot substantially cool the planet, Journal of Geophysical Research: Atmospheres, 121, 4877–4893, doi:10.1002/2015JD024666, https://agupubs.onlinelibrary.wiley.com/doi/abs/10.1002/2015JD024666, 2016.

Gasparini, B., Munch, S., Poncet, L., Feldmann, M., and Lohmann, U.: Is increasing ice crystal sedimentation velocity in geoengineering simulations a good proxy for cirrus cloud seeding?, Atmospheric Chemistry and Physics, 17, 4871–4885, doi:10.5194/acp-17-4871-2017, https://www.atmos-chem-phys.net/17/4871/2017/, 2017.

Gelaro, R., McCarty, W., Suárez, M. J., Todling, R., Molod, A., Takacs, L., Randles, C. A., Darmenov, A., Bosilovich, M. G., Reichle, R., Wargan, K., Coy, L., Cullather, R., Draper, C., Akella, S., Buchard, V., Conaty, A., da Silva, A. M., Gu, W., Kim, G.-K., Koster, R., Lucchesi, R., Merkova, D., Nielsen, J. E., Partyka, G., Pawson, S., Putman, W., Rienecker, M., Schubert, S. D., Sienkiewicz, M., and Zhao, B.: The Modern-Era Retrospective Analysis for Research and Applications, Version 2 (MERRA-2), Journal of Climate, 30, 5419–5454, doi:10.1175/JCLI-D-16-0758.1, https://doi.org/10.1175/JCLI-D-16-0758.1, 2017.

Gettelman, A., Liu, X., Ghan, S. J., Morrison, H., Park, S., Conley, A. J., Klein, S. A., Boyle, J., Mitchell, D. L., and Li, J.-L. F.: Global simulations of ice nucleation and ice supersaturation with an improved cloud scheme in the Community Atmosphere Model, Journal of Geophysical Research: Atmospheres, 115, n/a–n/a, doi:10.1029/2009JD013797, http://dx.doi.org/10.1029/2009JD013797, d18216, 2010.

Hegglin, M. I., Gettelman, A., Hoor, P., Krichevsky, R., Manney, G. L., Pan, L. L., Son, S.-W., Stiller, G., Tilmes, S., Walker, K. A., Eyring, V., Shepherd, T. G., Waugh, D., Akiyoshi, H., Anel, J. A., Austin, J., Baumgaertner, A., Bekki, S., Braesicke, P., Bruhl, C., Butchart, N., Chipperfield, M. P., Dameris, M., Dhomse, S., Frith, S., Garny, H., Hardiman, S. C., Jockel, P., Kinnison, D. E., Lamarque, J. F., Mancini, E., Michou, M., Morgenstern, O., Nakamura, T., Olivie, D., Pawson, S., Pitari, G., Plummer, D. A., Pyle, J. A., Rozanov, E., Scinocca, J. F., Shibata, K., Smale, D., Teyssedre, H., Tian, W., and Yamashita, Y.: Multimodel assessment of the upper troposphere and lower stratosphere: Extra-tropics, Journal of Geophysical Research: Atmospheres, 115, D00M09, doi:10.1029/2010JD013884, https://hal.archives-ouvertes.fr/hal-00510687, 2010.

Hendricks, J., Karcher, B., and Lohmann, U.: Effects of ice nuclei on cirrus clouds in a global climate model, Journal of Geophysical Research: Atmospheres, 116, doi:10.1029/2010JD015302, http://dx.doi.org/10.1029/2010JD015302, d18206, 2011.

Karcher, B. and Lohmann, U.: A parameterization of cirrus cloud formation: Homogeneous freezing of supercooled aerosols, Journal of Geophysical Research: Atmospheres, 107, doi:10.1029/2001JD000470, http://dx.doi.org/10.1029/2001JD000470, 2002.

Kleinschmitt, C., Boucher, O., and Platt, U.: Sensitivity of the radiative forcing by stratospheric sulfur geoengineering to the amount and strategy of the SO_2 injection studied with the LMDZ-S3A model, Atmospheric Chemistry and Physics Discussions, 2017, 1–34, doi:10.5194/acp-2017-722, https://www.atmos-chem-phys-discuss.net/acp-2017-722/, 2017.

Kravitz, B., Robock, A., Boucher, O., Schmidt, H., Taylor, K. E., Stenchikov, G., and Schulz, M.: The Geoengineering Model Intercomparison Project (GeoMIP), Atmospheric Science Letters, 12, 162–167, doi:10.1002/asl.316, http://dx.doi.org/10.1002/asl.316, 2011.

Kravitz, B., Robock, A., and Irvine, P.: Robust Results From Climate Model Simulations of Geoengineering, Eos, Transactions American Geophysical Union, 94, 292–292, doi:10.1002/2013EO330005, http://dx.doi.org/10.1002/2013EO330005, 2013.

Kravitz, B., MacMartin, D. G., Mills, M. J., Richter, J. H., Tilmes, S., Lamarque, J.-F., Tribbia, J. J., and Vitt, F.: First Simulations of Designing Stratospheric Sulfate Aerosol Geoengineering to Meet Multiple Simultaneous Climate Objectives, Journal of Geophysical Research: Atmospheres, 122, 12,616–12,634, doi:10.1002/2017JD026874, http://dx.doi.org/10.1002/2017JD026874, 2017JD026874, 2017.

Kuebbeler, M., Lohmann, U., and Feichter, J.: Effects of stratospheric sulfate aerosol geo-engineering on cirrus clouds, Geophysical Research Letters, 39, doi:10.1029/2012GL053797, http://dx.doi.org/10.1029/2012GL053797, l23803, 2012.

Lamarque, J.-F., Emmons, L. K., Hess, P. G., Kinnison, D. E., Tilmes, S., Vitt, F., Heald, C. L., Holland, E. A., Lauritzen, P. H., Neu, J., Orlando, J. J., Rasch, P. J., and Tyndall, G. K.: CAM-chem: description and evaluation of interactive atmospheric chemistry in the Community Earth System Model, Geoscientific Model Development, 5, 369–411, doi:10.5194/gmd-5-369-2012, https://www.geosci-model-dev.net/5/369/2012/, 2012.

Lohmann, U. and Karcher, B.: First interactive simulations of cirrus clouds formed by homogeneous freezing in the ECHAM general circulation model, Journal of Geophysical Research: Atmospheres, 107, AAC 8–1–AAC 8–13, doi:10.1029/2001JD000767, http://dx.doi.org/10.1029/2001JD000767, 2002.

Long, C. S. and Stowe, L. L.: using the NOAA/AVHRR to study stratospheric aerosol optical thicknesses following the Mt. Pinatubo Eruption, Geophysical Research Letters, 21, 2215–2218, doi:10.1029/94GL01322, http://dx.doi.org/10.1029/94GL01322, 1994.

MacMartin, D. G., Kravitz, B., Long, J. C. S., and Rasch, P. J.: Geoengineering with stratospheric aerosols: What do we not know after a decade of research?, Earth's Future, 4, 543–548, doi:10.1002/2016EF000418, http://dx.doi.org/10.1002/2016EF000418, 2016EF000418, 2016.

MacMartin, D. G., Kravitz, B., Tilmes, S., Richter, J. H., Mills, M. J., Lamarque, J.-F., Tribbia, J. J., and Vitt, F.: The Climate Response to Stratospheric Aerosol Geoengineering Can Be Tailored Using Multiple Injection Locations, Journal of Geophysical Research: Atmospheres, 122, 12,574–12,590, doi:10.1002/2017JD026868, http://dx.doi.org/10.1002/2017JD026868, 2017JD026868, 2017.

Mitchell, D. L., Rasch, P., Ivanova, D., McFarquhar, G., and Nousiainen, T.: Impact of small ice crystal assumptions on ice sedimentation rates in cirrus clouds and GCM simulations, Geophysical Research Letters, 35, n/a–n/a, doi:10.1029/2008GL033552, http://dx.doi.org/10.1029/2008GL033552, l09806, 2008.

Morgenstern, O., Giorgetta, M. A., Shibata, K., Eyring, V., Waugh, D. W., Shepherd, T. G., Akiyoshi, H., Austin, J., Baumgaertner, A. J. G., Bekki, S., Braesicke, P., Bruhl, C., Chipperfield, M. P., Cugnet, D., Dameris, M., Dhomse, S., Frith, S. M., Garny, H., Gettelman, A., Hardiman, S. C., Hegglin, M. I., Jockel, P., Kinnison, D. E., Lamarque, J.-F., Mancini, E., Manzini, E., Marchand, M., Michou, M., Nakamura, T., Nielsen, J. E., Olivie, D., Pitari, G., Plummer, D. A., Rozanov, E., Scinocca, J. F., Smale, D., Teyssedre, H., Toohey, M., Tian, W., and Yamashita, Y.: Review of the formulation of present-generation stratospheric chemistry-climate models and associated external forcings, Journal of Geophysical Research: Atmospheres, 115, n/a–n/a, doi:10.1029/2009JD013728, http://dx.doi.org/10.1029/2009JD013728, d00M02, 2010.

Morgenstern, O., Hegglin, M. I., Rozanov, E., O'Connor, F. M., Abraham, N. L., Akiyoshi, H., Archibald, A. T., Bekki, S., Butchart, N., Chipperfield, M. P., Deushi, M., Dhomse, S. S., Garcia, R. R., Hardiman, S. C., Horowitz, L. W., Jockel, P., Josse, B., Kinnison, D., Lin, M., Mancini, E., Manyin, M. E., Marchand, M., Marecal, V., Michou, M., Oman, L. D., Pitari, G., Plummer, D. A., Revell, L. E., Saint-Martin, D., Schofield, R., Stenke, A., Stone, K., Sudo, K., Tanaka, T. Y., Tilmes, S., Yamashita, Y., Yoshida, K., and Zeng, G.: Review of the global models used within phase 1 of the Chemistry–Climate Model Initiative (CCMI), Geoscientific Model Development, 10, 639–671, doi:10.5194/gmd-10-639-2017, https://www.geosci-model-dev.net/10/639/2017/, 2017.

Neale, R. B., Richter, J., Park, S., Lauritzen, P. H., Vavrus, S. J., Rasch, P. J., and Zhang, M.: The Mean Climate of the Community Atmosphere Model (CAM4) in Forced SST and Fully Coupled Experiments, Journal of Climate, 26, 5150–5168, doi:10.1175/JCLI-D-12-00236.1, https://doi.org/10.1175/JCLI-D-12-00236.1, 2013.

Niemeier, U. and Schmidt, H.: Changing transport processes in the stratosphere by radiative heating of sulfate aerosols, Atmospheric Chemistry and Physics, 17, 14 871–14 886, doi:10.5194/acp-17-14871-2017, https://www.atmos-chem-phys.net/17/14871/2017/, 2017.

Niemeier, U. and Tilmes, S.: Sulfur injections for a cooler planet, Science, 357, 246–248, doi:10.1126/science.aan3317, http://science.sciencemag.org/content/357/6348/246, 2017.

Pitari, G.: A Numerical Study of the Possible Perturbation of Stratospheric Dynamics Due to Pinatubo Aerosols: Implications for Tracer Transport, Journal of the Atmospheric Sciences, 50, 2443–2461, doi:10.1175/1520-0469(1993)050<2443:ANSOTP>2.0.CO;2, https://doi.org/10.1175/1520-0469(1993)050<2443:ANSOTP>2.0.CO;2, 1993.

Pitari, G., Mancini, E., Rizi, V., and Shindell, D. T.: Impact of Future Climate and Emission Changes on Stratospheric Aerosols and Ozone, Journal of the Atmospheric Sciences, 59, 414–440, doi:10.1175/1520-0469(2002)059<0414:IOFCAE>2.0.CO;2, https://doi.org/10.1175/1520-0469(2002)059<0414:IOFCAE>2.0.CO;2, 2002.

Pitari, G., Aquila, V., Kravitz, B., Robock, A., Watanabe, S., Cionni, I., De Luca, N., Di Genova, G., Mancini, E., and Tilmes, S.: Stratospheric ozone response to sulfate geoengineering: Results from the Geoengineering Model Intercomparison Project (GeoMIP), Journal of Geophysical Research: Atmospheres, 119, 2629–2653, 2014.

Pitari, G., Cionni, I., Di Genova, G., Visioni, D., Gandolfi, I., and Mancini, E.: Impact of Stratospheric Volcanic Aerosols on Age-of-Air and Transport of Long-Lived Species, Atmosphere, 7, http://www.mdpi.com/2073-4433/7/11/149, 2016a.

Pitari, G., Di Genova, G., Mancini, E., Visioni, D., Gandolfi, I., and Cionni, I.: Stratospheric Aerosols from Major Volcanic Eruptions: A Composition-Climate Model Study of the Aerosol Cloud Dispersal and e-folding Time, Atmosphere, 7, 75, doi:10.3390/atmos7060075, http://dx.doi.org/10.3390/atmos7060075, 2016b.

Pitari, G., Visioni, D., Mancini, E., Cionni, I., Di Genova, G., and Gandolfi, I.: Sulfate Aerosols from Non-Explosive Volcanoes: Chemical-Radiative Effects in the Troposphere and Lower Stratosphere, Atmosphere, 7, doi:10.3390/atmos7070085, http://www.mdpi.com/2073-4433/7/7/85, 2016c.

Randles, C. A., Kinne, S., Myhre, G., Schulz, M., Stier, P., Fischer, J., Doppler, L., Highwood, E., Ryder, C., Harris, B., Huttunen, J., Ma, Y., Pinker, R. T., Mayer, B., Neubauer, D., Hitzenberger, R., Oreopoulos, L., Lee, D., Pitari, G., Di Genova, G., Quaas, J., Rose, F. G., Kato, S., Rumbold, S. T., Vardavas, I., Hatzianastassiou, N., Matsoukas, C., Yu, H., Zhang, F., Zhang, H., and Lu, P.: Intercomparison of shortwave radiative transfer schemes in global aerosol modeling: results from the AeroCom Radiative Transfer Experiment, Atmospheric Chemistry and Physics, 13, 2347–2379, doi:10.5194/acp-13-2347-2013, http://www.atmos-chem-phys.net/13/2347/2013/, 2013.

Robock, A.: Volcanic eruptions and climate, Reviews of Geophysics, 38, 191–219, doi:10.1029/1998RG000054, http://dx.doi.org/10.1029/1998RG000054, 2000.

Sanderson, B. M., Piani, C., Ingram, W. J., Stone, D. A., and Allen, M. R.: Towards constraining climate sensitivity by linear analysis of feedback patterns in thousands of perturbed-physics GCM simulations, Climate Dynamics, 30, 175–190, doi:10.1007/s00382-007-0280-7, https://doi.org/10.1007/s00382-007-0280-7, 2008.

Sassen, K., Starr, D. O., Mace, G. G., Poellot, M. R., Melfi, S., Eberhard, W. L., Spinhirne, J. D., Eloranta, E., Hagen, D. E., and Hallett, J.: The 5–6 December 1991 FIRE IFO II Jet Stream Cirrus Case Study: Possible Influences of Volcanic Aerosols, Journal of the Atmospheric Sciences, 52, 97–123, doi:10.1175/1520-0469(1995)052<0097:TDFIIJ>2.0.CO;2, 1995.

Sassen, K., Wang, Z., and Liu, D.: Global distribution of cirrus clouds from CloudSat/Cloud-Aerosol lidar and infrared pathfinder satellite observations (CALIPSO) measurements, Journal of Geophysical Research: Atmospheres, 113, 2008.

Schumann, U., Mayer, B., Graf, K., and Mannstein, H.: A Parametric Radiative Forcing Model for Contrail Cirrus, Journal of Applied Meteorology and Climatology, 51, 1391–1406, doi:10.1175/JAMC-D-11-0242.1, https://doi.org/10.1175/JAMC-D-11-0242.1, 2012.

SPARC: Chapter 5: Model Estimates of Lifetimes in SPARC Report on Lifetimes of Stratospheric Ozone-Depleting Substances, Their Replacements, and Related Species. Chipperfield, M. and Q. Liang, et al. , Tech. rep., SPARC, http://www.sparc-climate.org/publications/sparc-reports/, 2013.

Storelvmo, T. and Herger, N.: Cirrus cloud susceptibility to the injection of ice nuclei in the upper troposphere, Journal of Geophysical Research: Atmospheres, 119, 2375–2389, doi:10.1002/2013JD020816, https://agupubs.onlinelibrary.wiley.com/doi/abs/10.1002/2013JD020816, 2014.

Strom, J., Strauss, B., Anderson, T., Schrader, F., Heintzenberg, J., and Wendling, P.: In Situ Observations of the Microphysical Properties of Young Cirrus Clouds, Journal of the Atmospheric Sciences, 54, 2542–2553, doi:10.1175/1520-0469(1997)054<2542:ISOOTM>2.0.CO;2, http://dx.doi.org/10.1175/1520-0469(1997)054<2542:ISOOTM>2.0.CO;2, 1997.

Taylor, K. E., Stouffer, R. J., and Meehl, G. A.: An overview of CMIP5 and the experiment design, Bulletin of the American Meteorological Society, 93, 485, 2012.

Thomason, L. W., Poole, L. R., and Deshler, T.: A global climatology of stratospheric aerosol surface area density deduced from Stratospheric Aerosol and Gas Experiment II measurements: 1984?1994, Journal of Geophysical Research: Atmospheres, 102, 8967–8976, doi:10.1029/96JD02962, http://dx.doi.org/10.1029/96JD02962, 1997.

Tilmes, S., Muller, R., and Salawitch, R.: The Sensitivity of Polar Ozone Depletion to Proposed Geoengineering Schemes, Science, 320, 1201–1204, doi:10.1126/science.1153966, http://science.sciencemag.org/content/320/5880/1201, 2008.

Tilmes, S., Garcia, R. R., Kinnison, D. E., Gettelman, A., and Rasch, P. J.: Impact of geoengineered aerosols on the troposphere and stratosphere, Journal of Geophysical Research: Atmospheres, 114, doi:10.1029/2008JD011420, http://dx.doi.org/10.1029/2008JD011420, d12305, 2009.

Tilmes, S., Mills, M. J., Niemeier, U., Schmidt, H., Robock, A., Kravitz, B., Lamarque, J.-F., Pitari, G., and English, J. M.: A new Geoengineering Model Intercomparison Project (GeoMIP) experiment designed for climate and chemistry models, Geoscientific Model Development, 8, 43–49, doi:10.5194/gmd-8-43-2015, https://www.geosci-model-dev.net/8/43/2015/, 2015.

Tilmes, S., Lamarque, J.-F., Emmons, L. K., Kinnison, D. E., Marsh, D., Garcia, R. R., Smith, A. K., Neely, R. R., Conley, A., Vitt, F., Val Martin, M., Tanimoto, H., Simpson, I., Blake, D. R., and Blake, N.: Representation of the Community Earth System Model (CESM1) CAM4-chem within the Chemistry-Climate Model Initiative (CCMI), Geoscientific Model Development, 9, 1853–1890, doi:10.5194/gmd-9-1853-2016, https://www.geosci-model-dev.net/9/1853/2016/, 2016.

Tilmes, S., Richter, J. H., Mills, M. J., Kravitz, B., MacMartin, D. G., Vitt, F., Tribbia, J. J., and Lamarque, J.-F.: Sensitivity of Aerosol Distribution and Climate Response to Stratospheric SO2 Injection Locations, Journal of Geophysical Research: Atmospheres, pp. n/a–n/a, doi:10.1002/2017JD026888, http://dx.doi.org/10.1002/2017JD026888, 2017JD026888, 2017.

Visioni, D., Pitari, G., and Aquila, V.: Sulfate geoengineering: a review of the factors controlling the needed injection of sulfur dioxide, Atmos. Chem. Phys., 17, 3879–3889, doi:10.5194/acp-17-3879-2017, http://www.atmos-chem-phys.net/17/3879/2017/, 2017a.

Visioni, D., Pitari, G., Aquila, V., Tilmes, S., Cionni, I., Di Genova, G., and Mancini, E.: Sulfate geoengineering impact on methane transport and lifetime: results from the Geoengineering Model Intercomparison Project (GeoMIP), Atmospheric Chemistry and Physics, 17, 11 209–11 226, doi:10.5194/acp-17-11209-2017, https://www.atmos-chem-phys.net/17/11209/2017/, 2017b.

Visioni, D., Pitari, G., Tuccella, P., and Curci, G.: Sulfur deposition changes under sulfate geoengineering conditions: quasi-biennial oscillation effects on the transport and lifetime of stratospheric aerosols, Atmospheric Chemistry and Physics, 18, 2787–2808, doi:10.5194/acp-18-2787-2018, https://www.atmos-chem-phys.net/18/2787/2018/, 2018.

Warren, S. G.: Optical constants of ice from the ultraviolet to the microwave, Appl. Opt., 23, 1206–1225, doi:10.1364/AO.23.001206, http://ao.osa.org/abstract.cfm?URI=ao-23-8-1206, 1984.

Warren, S. G. and Brandt, R. E.: Optical constants of ice from the ultraviolet to the microwave: A revised compilation, Journal of Geophysical Research: Atmospheres, 113, doi:10.1029/2007JD009744, https://agupubs.onlinelibrary.wiley.com/doi/abs/10.1029/2007JD009744, 2008.

Xia, L., Nowack, P. J., Tilmes, S., and Robock, A.: Impacts of Stratospheric Sulfate Geoengineering on Tropospheric Ozone, Atmospheric Chemistry and Physics Discussions, 2017, 1–38, doi:10.5194/acp-2017-434, http://www.atmos-chem-phys-discuss.net/acp-2017-434/, 2017.

Yang, P., Zhang, L., Hong, G., Nasiri, S. L., Baum, B. A., Huang, H. L., King, M. D., and Platnick, S.: Differences Between Collection 4 and 5 MODIS Ice Cloud Optical/Microphysical Products and Their Impact on Radiative Forcing Simulations, IEEE Transactions on Geoscience and Remote Sensing, 45, 2886–2899, doi:10.1109/TGRS.2007.898276, 2007.

Zhang, Z., Platnick, S., Yang, P., Heidinger, A. K., and Comstock, J. M.: Effects of ice particle size vertical inhomogeneity on the passive remote sensing of ice clouds, Journal of Geophysical Research: Atmospheres, 115, doi:10.1029/2010JD013835, https://agupubs.onlinelibrary.wiley.com/doi/abs/10.1029/2010JD013835, 2010.